DYSTROGLYCANOPATHY-TYPE MUSCULAR DYSTROPHY: EVALUATION OF PATHOPHYSIOLOGY AND THERAPEUTIC TARGETING IN A MOUSE MODEL OF FUKUTIN DEFICIENCY

by

STEVEN JAMES FOLTZ

(Under the Direction of Aaron M. Beedle)

ABSTRACT

Muscular dystrophies are a group of genetic disorders characterized by muscle necrosis, atrophy, and progressive weakness. Several of these diseases are caused by defects in the dystrophin-glycoprotein complex, an integral membrane complex linking the extracellular matrix to the subcellular actin cytoskeleton in skeletal muscle. The central factors in this linkage are extracellular α-dystroglycan, which interacts with laminin and other matrix receptors via the presence of a unique *O*-mannose glycan structure, transmembrane β-dystroglycan, and intracellular dystrophin, which binds β-dystroglycan near its C-terminus and actin at its N-terminus. Mutations in genes processing α-dystroglycan disrupt its attachment to laminin and cause a subset of muscular dystrophy termed secondary dystroglycanopathy. Patient phenotypes span a broad spectrum that includes, on one end, congenital muscular dystrophy along with severe brain and eye abnormalities, and, on the other, mild, adult-onset muscle disease.

Although dystroglycanopathies are fatal, they are currently without effective treatment or cure.

A challenge to the development of therapeutic agents for muscular dystrophies is the identification of druggable targets. Because the primary biochemical defect in dystroglycanopathies (as well as other dystrophin-glycoprotein related muscular dystrophies) lies within a structural complex, one approach has been to upregulate compensatory or homologous protein complexes or to modulate certain physiological properties of muscles so that they are less vulnerable to contraction induced damage. While this strategy has yielded a number of promising results, it has primarily utilized genetic approaches that are technically infeasible for use in human patients. Thus, identification of small-molecule interventions that ameliorate dystrophic features is of great interest.

We employ a novel *Fktn*-deficient mouse model of dystroglycanopathy to probe pathological features of disease, including abnormal muscle regeneration and fibrosis which are key determinants of disease progression. Furthermore, we identify abnormal activation of the mammalian target of rapamycin (mTOR) signaling pathway and show that it can be targeted to improve histological and functional parameters of dystroglycanopathy muscle. Our results set the stage for preclinical evaluation of mTORC1 inhibition as a novel therapeutic approach for muscular dystrophy.

INDEX WORDS: skeletal muscle, muscular dystrophy, dystroglycan, fukutin, muscle differentiation, muscle fiber-type, mammalian target of rapamycin (mTOR), rapamycin

DYSTROGLYCANOPATHY-TYPE MUSCULAR DYSTROPHY: EVALUATION OF PATHOPHYSIOLOGY AND THERAPEUTIC TARGETING IN A MOUSE MODEL OF FUKUTIN DEFICIENCY

by

STEVEN JAMES FOLTZ

B.S., The University of Delaware, 2011

B.A., The University of Delaware, 2011

A Dissertation Submitted to the Graduate Faculty of The University of Georgia in Partial Fulfillment of the Requirements for the Degree

DOCTOR OF PHILOSOPHY

ATHENS, GEORGIA

2016

DYSTROGLYCANOPATHY-TYPE MUSCULAR DYSTROPHY: EVALUATION OF PATHOPHYSIOLOGY AND THERAPEUTIC TARGETING IN A MOUSE MODEL OF FUKUTIN DEFICIENCY

by

STEVEN JAMES FOLTZ

Major Professor:	Aaron M. Beedle
Committee:	Brian S. Cummings
	Mandi M. Murph
	Han-Rong Weng
	Lance Wells

Electronic Version Approved:

Suzanne Barbour
Dean of the Graduate School
The University of Georgia
August 2016

DEDICATION

To my parents

ACKNOWLEDGMENTS

To everyone who helped me through this experience: thank you. I am grateful for the guidance of my graduate committee and the kind assistance I've received from College of Pharmacy staff. I'd most especially like to thank my advisor Aaron Beedle: it's been a pleasure. You've been an outstanding mentor and have offered me nothing but thoughtful advice. Lastly, a warm hello to my brother, Brian, and my girlfriend, Emily, who have been with me through good times and bad. Thanks for keeping me sane.

TABLE OF CONTENTS

Page

LIST OF TABLES

Page

LIST OF FIGURES

Page

CHAPTER 1

INTRODUCTION AND LITERATURE REVIEW

Muscular dystrophies are a diverse group of genetic diseases characterized by progressive muscle weakness. While the age of onset and clinical manifestations vary considerably between and even within different types of dystrophy, all share the common feature of muscle fiber necrosis followed by regeneration. Muscle possesses robust regenerative capacity, but this ability is inevitably compromised following several degenerative cycles. Because of this, functional muscle fibers in dystrophic tissue are replaced over time with non-functional depositions of extracellular matrix proteins or adipocytes. In cases with involvement of the respiratory or cardiac muscles, this process ultimately results in premature death. Despite the significant threat to human health, these diseases remain without a cure. However, recent advances in our understanding of disease progression have opened up a number of avenues for therapeutic development and extended hope to the patient community. This introduction will review patient phenotypes and the current understanding of underlying disease mechanisms particularly in muscular dystrophies arising from defects in the essential muscle cell membrane-stabilizing dystrophin-glycoprotein complex. Included in these diseases are Duchenne muscular dystrophy, the most common form of muscular dystrophy in children, and several lethal congenital muscular dystrophies. Due to their prevalence and severity, substantial effort is directed toward the study and treatment of dystrophin glycoprotein complex-related muscular dystrophies. Herein follows a review and discussion of the

current literature regarding muscular dystrophies arising from defects in the dystrophin glycoprotein complex. Special attention will be paid to the primary and secondary aspects of disease, along with recent advances and their implications for therapeutic development.

The Dystrophin-Glycoprotein Complex

Duchenne muscular dystrophy , the most common form of muscular dystrophy in children, is an X-linked recessive disorder affecting approximately 1 in 3600 -6000 males (1,2). The genetic locus affected in Duchenne muscular dystrophy was identified through linkage analysis of the X-chromosome in the early 1980s, and the discovery of its protein product, dystrophin, followed a few years later (3-5). Despite the elucidation of the primary biochemical defect in Duchenne muscular dystrophy, the functional significance of dystrophin remained unclear. The first clues to its role came from immunochemical localization studies that demonstrated that dystrophin was present at the sarcolemma of normal, but not Duchenne muscular dystrophy, muscle (6). Shortly thereafter, it was determined that intracellular dystrophin linked to a transmembrane glycoprotein (7). Cosedimentation experiments first established a potential relationship between dystrophin and actin, and dissociation of cytoskeletal proteins from the sarcolemma concomitantly interrupted the dystrophin/glycoprotein interaction, leading to the hypothesis that dystrophin is purposed as a bridge between the muscle membrane and the underlying structural network (8). Furthermore, direct binding of costameric actin to isolated sarcolemma was confirmed in membranes isolated from dystrophin-expressing wildtype muscle fibers, but not those from dystrophin-deficient fibers, illustrating a bona fide

interaction between dystrophin and actin *in situ* (8-10). However, this model describes only a piece of a larger system.

The transmembrane glycoprotein that binds on its intracellular surface to dystrophin is β-dystroglycan, which is transcribed from an mRNA that also encodes α-dystroglycan (from which it is post-translationally cleaved) (11-13). α-Dystroglycan dimerizes with β-dystroglycan and binds several extracellular matrix proteins. Dystrophin and dystroglycan therefore provide a critical link between the extracellular matrix and the intracellular cytoskeleton and form the backbone of the dystrophin-glycoprotein complex, an integral membrane complex also containing the sarcoglycans, syntrophins, sarcospan, and α-dystrobrevin (8,11,14,15) (Figure 1.1). Work on α-dystroglycan's function as an extracellular matrix receptor first utilized overlay experiments to demonstrate that α-dystroglycan binds specifically to laminin and not to a number of other extracellular matrix proteins in muscle. Several basic residues within the laminin G 4-5 domains of laminin were found to be required for this interaction; the early observation that dystroglycan glycosylation was also required hinted that negatively charged sugars on dystroglycan associate ionically with laminin. Importantly, this raised the possibility that α-dystroglycan might serve as a receptor for a number of other laminin G domain-containing proteins. Indeed, α-dystroglycan binds agrin and perlecan at the neuromuscular junction, pikachurin in the eye, and neurexin in the brain, all with important implications for tissue function (16-22). Mutations in genes encoding proteins of the dystrophin glycoprotein complex can disrupt its function as a stabilizer of the sarcolemma, but the extent of pathogenesis is crucially dependent on the specific nature of the mutation and the extent to which the coded protein is altered.

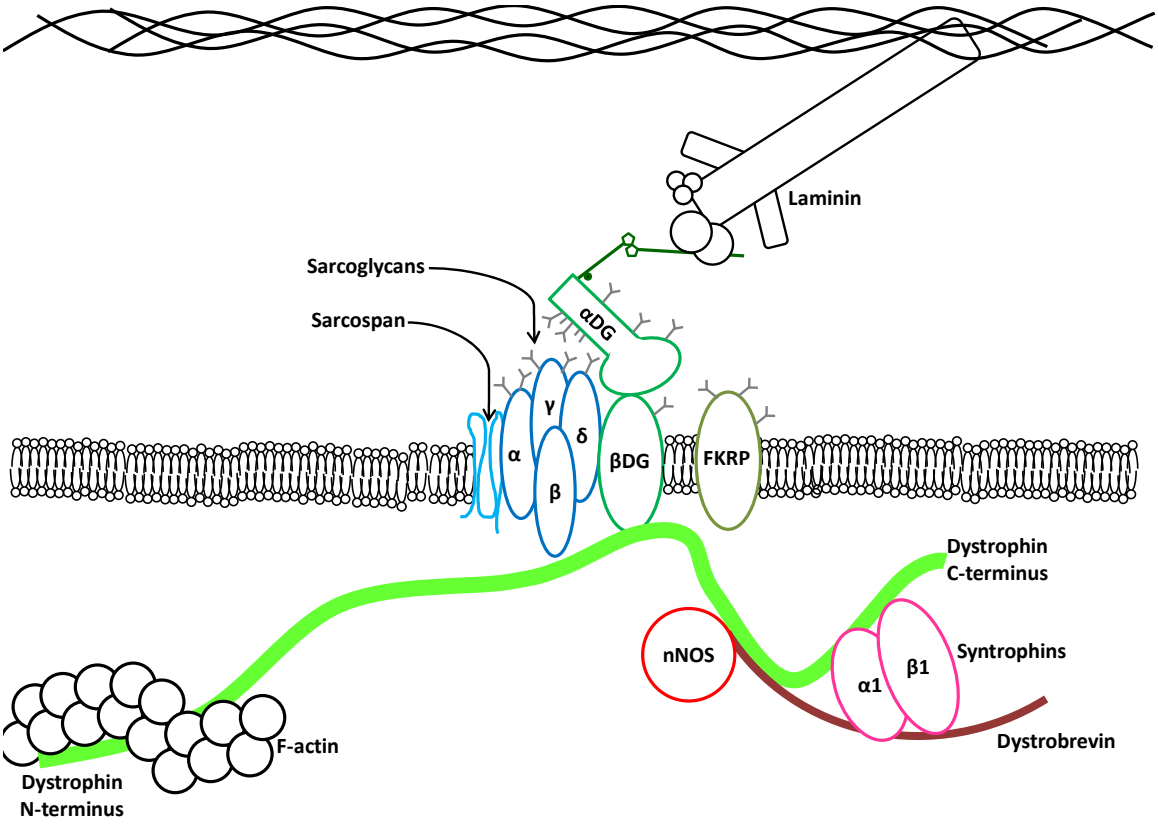

Figure 1.1 The dystrophin-glycoprotein complex. The basal lamina/extracellular matrix and the intracellular cytoskeleton are connected, glycosylation-dependently, by linkages from α-dystroglycan, β-dystroglycan, and dystrophin. The supportive sarcospan/sarcoglycan subcomplex and dystrophin-associated signaling adapter proteins are also shown.

The Duchenne muscular dystrophy gene is the largest in the human genome with an approximate length of 2400 kilo-base pairs (kb). The full-length dystrophin mRNA, spanning 79 exons, is approximately 14 kb in length and encodes a protein of 427 kilo-Daltons (kDa). As such, it is relatively vulnerable to pathogenic mutations, although a number of these are clustered at specific "hot spots" (e.g. exons 2-20 and 45-53) (23,24). While defects in dystrophin are responsible for Duchenne muscular dystrophy, an allelic variant of dystrophinopathy known as Becker muscular dystrophy has also been described. Typically, Becker muscular dystrophy mutations consist of in-frame deletions that result in a truncated but partially functional dystrophin, leading to a subdued phenotype in patients (24,25). Importantly, a number of other dystrophin isoforms exist with specific tissue and sub-tissue localizations, and it is likely that dystrophin mutations that disrupt the function of relatively fewer of these isoforms, result in milder patient phenotypes (26-31). Along with dystrophin, there are six sarcoglycans (α-, β-, γ-, δ-, ε-, ζ-sarcoglycan), the first four of which form a tetrameric subcomplex within the skeletal muscle dystrophin glycoprotein complex; mutations in α-, β-, γ-, or δ-sarcoglycan are associated with a milder form of muscular dystrophy known as limb-girdle muscular dystrophy 2C-2F (32,33). In contrast, loss of other dystrophin glycoprotein complex proteins, including the syntrophins, which are adaptor molecules that facilitate the localization of certain signaling molecules to the dystrophin glycoprotein complex, does not result specifically in a muscle phenotype. However, the entire dystrophin glycoprotein complex is absent from the sarcolemma in DMD and the loss of syntrophin function, at least in muscle, is thus contained within the Duchenne phenotype (34-36). Dystrobrevin deficiency is a general feature of both DMD and the sarcoglycan-associated

limb-girdle muscular dystrophies, and although α-dystrobrevin null mice do have a mild muscle phenotype, no pathogenic mutations of α-dystrobrevin have been reported in humans (37-39). Interestingly, a group of patients with inherited myopathy had reduced sarcolemmal dystrobrevin and/or syntrophins, but apparently normal levels of most dystrophin glycoprotein complex proteins (dystrophin, sarcoglycans, and β-dystroglycan). However, an underlying genetic abnormality was not determined in any of these cases (35). While sarcospan is also lost from the muscle membrane in dystrophinopathy, sarcospan-KO mice have apparently normal muscle and its function within the dystrophin glycoprotein complex remains largely unexplained (40). Interestingly, a detailed evaluation of sarcospan-deficient mice has revealed a concomitant reduction in dystrophin glycoprotein complex and related utrophin-glycoprotein complex abundance at the sarcolemma, suggesting that it may stabilize dystrophin or utrophin expression; furthermore, transgenic overexpression of sarcospan appears to reduce dystrophic pathology in dystrophin-mutant mice through upregulation of homologous utrophin (41,42).

Unlike dystrophin and the sarcoglycans, mutations in *DAG1*, encoding dystroglycan, are exceedingly rare in humans. In fact, there have been only two confirmed instances of primary dystroglycanopathy described to date (43,44). α-Dystroglycan is a heavily glycosylated protein with a unique *O*-mannose glycan structure that serves to bind to extracellular matrix proteins; α-dystroglycan containing this modification is termed "functionally glycosylated" because it is only through the presence of this glycan structure that it is able to act as a receptor for extracellular matrix proteins. Defects in glycosyltransferases or glycan-modifying enzymes responsible for

the synthesis of this structure cause a set of disorders termed secondary dystroglycanopathy-type muscular dystrophies. These diseases span a broad phenotypic spectrum and include severe congenital muscular dystrophies that most often result in death within the first 10 years of life. Currently, 10 glycosyltransferases are known to directly participate in the extension of this unique glycan: protein *O*-mannosyl-transferase 1 and 2 (POMT1/2), protein *O*-linked mannose N-acetylglucosaminyltransferase 2 (POMGNT2), β-3 *N*-acetylgalactosaminyltransferase 2 (B3GALNT2), protein *O*-mannose kinase (POMK), fukutin, fukutin-related protein (FKRP), transmembrane protein 5 (TMEM5), β-4 glucuronyl transferase 1 (B4GAT1), and like-acetylglucosaminyl transferase (LARGE). Interestingly, at least one of the primary mutations in *DAG1* disrupts the ability of LARGE to bind to the N-terminal domain of α-dystroglycan, resulting in hypoglycosylation reminiscent of secondary dystroglycanopathy (reviewed in(45)).

Over the past several years, significant progress has been made towards understanding the functional glycan structure on α-dystroglycan; in fact, a link spanning entirety of a linear chain from α-dystroglycan through the terminal sugars that bind laminin has now been described (Figure 1.2). POMT1/2 form a complex to catalyze the addition of mannose to one of two threonine residues (Thr 317/319) in the heavily glycosylated mucin-domain of α-dystroglycan (46-48). POMGNT2 and B3GALNT2 add a β-4 linked GlcNAc and β-3 linked GalNAc, respectively, to complete the so-called core M3 foundation of the functional *O*-mannose glycan. Next, POMK phosphorylates the 6 position of mannose with unclear consequences for dystroglycan function (49). Until recently it was believed that this phosphorylation event was the first step in functional

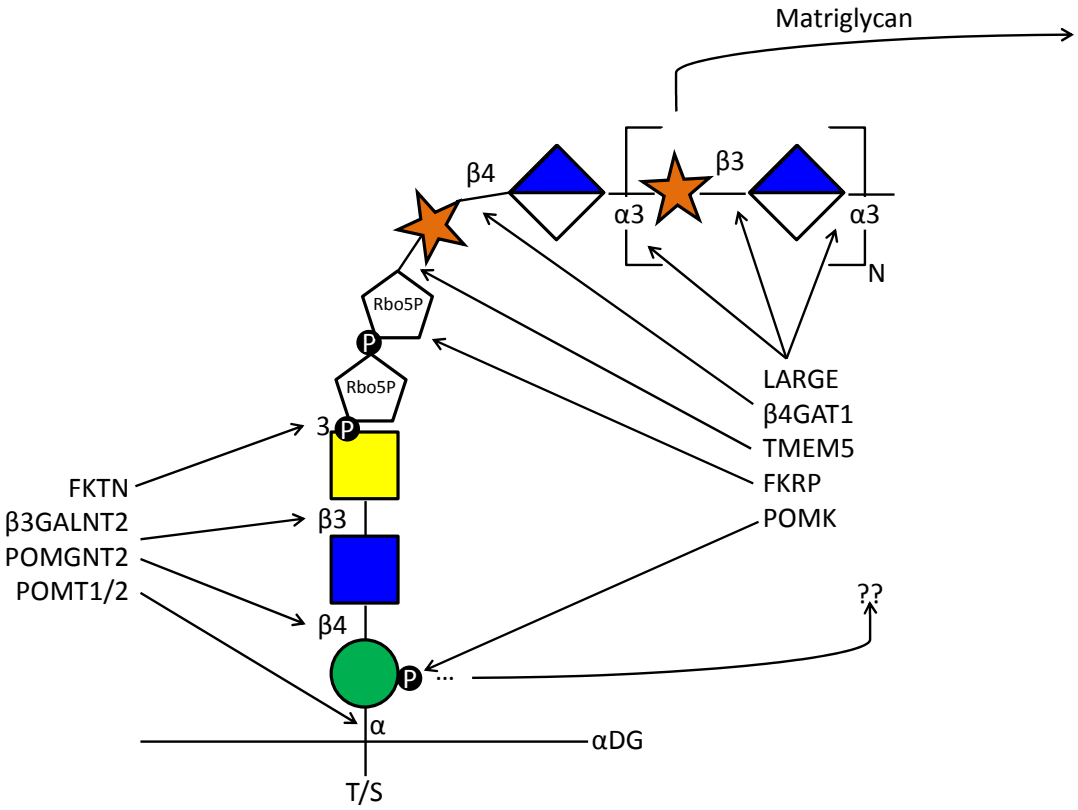

Figure 1.2 Functional *O*-mannose glycan of α-dystroglycan. Cartoon depiction of sugars comprising the extracellular matrix binding glycan structure, beginning with *O*-mannose attachment in α-linkage to α-dystroglycan. 10 known enzymes catalyze the elaboration of this structure, which terminates in LARGE-synthesized tandem repeats of xylose and glucuronic acid recently coined "matriglycan." Note: Ribitol-5P (Rbo5P), is a linear alcohol shown here as a pentagon for convenience. The contact points between adjacent sugars (and/or alcohols) are not meant to reflect the linkage position. See Table 1.1 below for a complete list of dystroglycanopathy genes. Abbreviations: LARGE, like-acetylglucosaminyl transferase; β4GAT1, β-4 glucuronyl transferase 1; TMEM5, transmembrane protein 5; FKRP, fukutin-related protein; POMK, protein *O*-mannose kinase; FKTN, fukutin; β3GALNT2, β-3 *N*-acetylgalactosaminyl transferase 2; POMGNT2, protein *O*-mannose *N*-acetylglucosaminyl transferase 2; POMT1, protein-*O*-mannosyl transferase 1; POMT2, protein-*O*-mannosyl transferase 2.

glycan branching and that the laminin-interacting sugar moiety lay downstream. Furthermore, it was hypothesized that the dystroglycanopathy genes *FKTN* and *FKRP* (encoding fukutin, and fukutin-related protein, respectively), acted immediately downstream of the phosphate added by POMK (50,51). However, it was discovered that fukutin catalyzes the addition of ribitol-5-phosphate (Rbo5P) to the 3-position of GalNAc, which is followed by successive addition of Rbo5P at C1 of the first Rbo5P by FKRP, and that the rest of the functional glycan extends downstream of these modifications (52). The result is a unique tandem Rbo5P structure, never before observed in mammals, extending from the core M3 base. This is followed by the transfer of xylose to the 1-position of the 2nd Rbo5P and then β-4 addition of glucuronic acid to xylose (53-55). Ultimately, this process creates a glycan structure primed for terminal action by LARGE, which functions as both an α-3 xylosyl- and β-3 glucuronyltransferase (56). In fact, several (at least 13) repeats of this [-3-xylose-α1, 3-glucuronic acid-β1-] appear required for the interaction between α-dystroglycan and its extracellular matrix targets (52,57). Because of its unique structure and its role in binding matrix proteins, this disaccharide repeat has been coined "matriglycan" (45).

In addition to genes synthesizing the functional *O*-mannose structure on α-dystroglycan, a number of enzymes are responsible for synthesizing sugar-donor substrates required for its extension. Loss of function mutations in these genes result in "tertiary dystroglycanopathy." In several cases, proteins other than α-dystroglycan are modified with sugars also required for the functional O-mannose glycan (i.e. *O*-mannosylated); in such instances, tertiary dystroglycanopathies and the congenital disorders of glycosylation converge. However, among the genes causative for tertiary

dystroglycanopathy, at least one, isoprenoid synthase domain-containing (*ISPD*), which catalyzes the formation of CDP-ribitol, seems to be linked exclusively to dystroglycan because a ribitol modification has not been observed on any other protein in mammals (52). Mutations in at least 4 other genes (GDP-mannose pyrophosphorylase β [*GMPPB*], dolichyl-phosphate mannosyltransferase polypeptides 1, 2, 3 [*DPM1*, *DPM2*, *DPM3*]), involved in the formation of GDP-mannose, have also been described as causative for dystroglycanopathy-like congenital or limb-girdle muscular dystrophies (58-64). There is one known dystroglycanopathy gene which appears not to modify the functional O-mannose structure at all: protein *O*-mannose beta-1,2-N-acetylglucosaminyl transferase (*POMGNT1*). POMGNT1 participates in the synthesis of a linear sialylated *O*-mannose tetrasaccharide on α-dystroglycan but loss of this structure via enzymatic deglycosylation does not abolish laminin binding activity (65). It remains unclear why defects in POMGnT1 cause a dystroglycanopathy phenotype, but in some patients POMGnT1 mutations result in mislocalization of the enzyme, which is normally Golgi-resident, to the endoplasmic reticulum, where it may be able to compete with POMGNT2 for extension of *O*-mannose glycans (45,66,67). However, complete genetic ablation of *Pomgnt1* in mice results in a substantial reduction of the laminin-binding activity of α-dystroglycan, suggesting that it is somehow required for the formation of the functional glycan structure (68). This is supported by analysis of muscle from a subset of POMGnT1 patients with a heterogeneous population of α-dystroglycan, some of which is able to function as an extracellular matrix receptor (66,69). It has also been suggested that an interaction between POMGnT1 and fukutin facilitates localization of these enzymes to the Golgi apparatus, where they are catalytically active. This indicates that

POMGnT1 may also function to modulate α-dystroglycan glycosylation independently of its glycosyltransferase activity (70). The original classification of severe congenital muscular dystrophies now known to be dystroglycanopathies categorized patients into three groups: Walker-Warburg syndrome, muscle-eye-brain disease, and Fukuyama congenital muscular dystrophy. Walker-Warburg syndrome was associated with the most severe phenotypes and was initially distinguished from the similar muscle-eye-brain disease based on the extent of neurological involvement in the disease (greater in Walker-Warburg syndrome) (71,72). Fukuyama congenital muscular dystrophy was distinguished by lacking or mild ocular abnormalities and its prevalence in Japan, where it was discovered (73). Fukuyama congenital muscular dystrophy and muscle-eye-brain disease genes were mapped prior to the discovery of the "Walker-Warburg syndrome locus" and attributed to the genes *FKTN* and *POMGNT1*, respectively (74); later, a study in 30 Walker-Warburg syndrome patients identified 3 distinct genetic loci, giving the first hint that these diseases have at least some degree of genetic heterogeneity (75). Today, secondary dystroglycanopathies are seen as occupying space on a spectrum, with relatively greater disruption of dystroglycan modification causing worse phenotypes. Cases of Walker-Warburg syndrome might now be termed severe congenital muscular dystrophy, congenital muscular dystrophy with mental retardation is an intermediate disease that maintains a neurological phenotype, congenital muscular dystrophy without mental retardation is relatively milder, and limb-girdle muscular dystrophy comprises the mildest muscle phenotype and may or may not include neurological defects, with onset in the late teen years in some cases. Although causative genes have been ascribed to each of the aforementioned classifications, it is now recognized that dystroglycanopathies are

allelic in nature; mutations in a "Walker-Warburg syndrome gene" might give rise to limb-girdle muscular dystrophy if functional disruption of the encoded protein is modest. In recognition of this, a new nomenclature system has been devised which classifies muscular dystrophy, dystroglycanopathy-type (MDDG) into three categories: MDDGA, severe muscular dystrophy with brain and eye involvement; MDDGB, congenital muscular dystrophy without mental retardation; MDDGC, limb-girdle phenotype (76). Dystroglycanopathy patients have now been identified with mutations in *POMT1* (46), *POMT2* (47), *POMGNT1* (75), *FKTN* (74), *FKRP* (77), *GTDC2/POMGNT2* (78), *LARGE* (79), *TMEM5* (58), *B3GALNT2* (80), *B3GNT1*/*B4GAT1* (81), *POMK* (82,83), *ISPD* (58,59), and enzymes responsible for the generation of dolichol-phosphate mannose, the sugar-nucleotide donor that serves as a substrate for protein mannosylation: *GMPPB* (64), *DOLK* (84), *DPM1* (63), *DPM2* (62), and *DPM3* (61) (Table 1.1).

The dystroglycanopathies frequently present with muscular dystrophy, but the degree of involvement and pathology in other organs, including the brain, varies considerably between patients. The most commonly described neurological phenotype is cobblestone lissencephaly, which refers to the smooth cerebrum found in some patients. Neuronal migration during development is clearly affected following the loss of α-dystroglycan glycosylation and leads to disorganization of the cortical laminae. In severe cases, cerebellar atrophy is common and leads to an apparent "rounding" of the brain. Cognitive impairment is a feature of many dystroglycanopathies, and is moderate to severe (in order) in Fukuyama congenital muscular dystrophy, muscle-eye-brain disease, and Walker-Warburg syndrome. Eye abnormalities include atrophy of the optic nerve or

Table 1.1 Dystroglycanopathy Genes

Gene	OMIM Accession #	Product	Known Function(s)	Phenotype: Old	Phenotype: New
DAG1	128239	Dystroglycan, α and β subunits	ECM receptor	WWS, MEB, LGMD with cognitive impairment, asymptomatic hyperCKemia	MDDGA9 MDDGC9
POMT1	607423	Protein *O*-Mannosyl Transferase 1	Ser/Thr α-mannosylation	WWS, MEB, congenital muscular dystrophy with mental retardation, LGMD2K	MDDGA1 MDDGB1 MDDGC1
POMT2	607439	Protein *O*-Mannosyl Transferase 2	Ser/Thr α-mannosylation	WWS, MEB, congenital muscular dystrophy with mental retardation, LGMD2N	MDDGA2 MDDGB2 MDDGC2
POMGNT1	606822	Protein *O*-Mannose β2-*N*-Acetylglucosaminyltransferase 1	Transfers β2 *N*-acetylglucosamine to mannose	WWS, MEB, congenital muscular dystrophy with mental retardation, LGMD2O	MDDGA3 MDDGB3 MDDGC3
POMGNT2 (Formerly *GTDC2*)	614828	Protein *O*-Mannose *N*-Acetylglucosaminyltransferase 2	Transfers β4 *N*-acetylglucosamine to mannose	WWS	MDDGA8
B3GALNT2	610194	β3-*N*-Acetylgalactosaminyltransferase 2	Transfers β3 *N*-acetylgalactosamine to β4-linked *N*-acetylglucosamine	WWS/MEB	MDDGA11
FKTN	607440	Fukutin	Ribitol-5P transferase to 3-position of *N*-acetylgalactosamine	WWS, MEB, FCMD, congenital muscular dystrophy with mental retardation, LGMD2M	MDDGA4 MDDGB4 MMDGC4
FKRP	606596	Fukutin-related protein	Ribitol-5P transferase to ribitol-5P	WWS, MEB, MDC1C congenital muscular dystrophy with mental retardation, LGMD2I	MDDGA5 MDDGB5 MDDGC5
TMEM5	605862	Transmembrane protein 5	Xylosyltransferase (to ribitol)	WWS/MEB	MDDGA10
B4GAT1 (Formerly *B3GNT1*)	605517	β4-glucuronyltransferase 1	β4-Glucuronyltransferase	WWS	MDDGA13
LARGE	603590	Like-acetylglucosaminyltransferase	α3-xylosyltransferase/ β3-glucuronyltransferase	WWS, MEB, MDC1D	MDDGA6 MDDGB6
POMK	615247	Protein *O*-Mannose Kinase	*O*-mannose phosphorylation at 6 position	WWS, LGMD	MDDGA12 MDDGC12
GMMPB	615320	GDP-Mannose pyrophosphorylase B	Catalyzes formation of GDP-mannose from mannose-1P and GTP	MEB, congenital muscular dystrophy without mental retardation, LGMD	MDDGA14 MDDGB14 MDDGC14
DOLK	610746	Dolichol Kinase	Phosphorylation of dolichol	CDG1M	Congenital Disorder of Glycosylation, Type Im
DPM1	603503	Dolichol-phosphate mannosyltransferase polypeptide 1	Formation of Dol-P-mannose from GDP-mannose and Dolichol-P		Congenital Disorder of Glycosylation, Type Ie
DPM2	603564	Dolichol-phosphate mannosyltransferase polypeptide 2	Formation of Dol-P-mannose from GDP-mannose and Dolichol-P		Congenital Disorder of Glycosylation, Type Iu
DPM3	605951	Dolichol-phosphate mannosyltransferase polypeptide 3	Formation of Dol-P-mannose from GDP-mannose and Dolichol-P		Congenital Disorder of Glycosylation, Type Io
ISPD	614631	Isoprenoid synthase domain-containing	Formation of CDP-ribitol from CTP and ribitol-5P	WWS/MEB	MDDGA7 MDDGB7 MDDGC7

glaucoma, corneal clouding or congenital cataracts, and retinal dysplasia or hypoplasia (e.g. (46,47,71,72,75)). Muscle phenotypes vary widely from "floppy babies" without the ability to sit up (Walker-Warburg syndrome), to adult onset (limb-girdle muscular dystrophy) in which muscle defects are often identified as difficulties completing mildly or moderately strenuous physical activities (e.g. stair climbing, running). Diagnostic criteria may include genetic testing/screening along with a review of family medical history and physical and neurological examinations. Results may be functionally verified by serum creatine kinase test (a generic marker of muscle damage), a tissue biopsy evaluated for histopathology, and muscle/brain MRIs (85). Histological hallmarks of muscular dystrophy include centrally located myonuclei, muscle fiber size variation, accumulation of extracellular matrix scar tissue (fibrosis), and fatty infiltration. Biopsies are also routinely evaluated for the presence of functionally glycosylated α-dystroglycan at the sarcolemma. Furthermore, with the recent elucidation of the laminin binding O-mannose glycan and the discovery of several new dystroglycanopathy genes, identification of specific dystroglycanopathy-causing mutations is more likely than it was even a few years ago.

Life expectancy is significantly shortened in the three severe congenital muscular dystrophies, and patients typically die within the first decade of life; in Walker-Warburg syndrome, patients have a median survival of about 10 months and do not live past 3 years, due largely to skeletal muscle dysfunction. Because brain and eye pathologies result mainly from developmental defects, post-natal correction is not feasible. Therefore, therapies directed towards skeletal or cardiac muscle currently stand as the most likely treatments to improve patient quality of life (by introducing or prolonging

independent locomotion) and extend lifespan. This, along with the primary muscle phenotypes in DMD, Becker muscular dystrophy, and sarcoglycan-deficient limb-girdle muscular dystrophies, has led to intense focus on skeletal muscle disease in dystrophin glycoprotein complex-related pathologies. Animal models have been central to this work and will be reviewed in detail in the next section.

Animals models of dystrophin glycoprotein complex-defects and their phenotypes

Defects in dystrophin, dystroglycan, and the sarcoglycans all result in muscular dystrophy; this is also the case in animals, and there are a number of animal models of defects in each of those dystrophin glycoprotein complex components. However, KO models of other dystrophin glycoprotein complex components have also been made and have revealed surprising roles for proteins assumed to participate minimally in dystrophic pathology of dystrophin glycoprotein complex-related muscular dystrophy. One example of this is the α-dystrobrevin (*adbn*$^{-/-}$) KO mouse, which actually has a mild myopathy on its own, and which, when crossed into a dystrophin-deficient lineage exacerbates muscular dystrophy and significantly decreases lifespan. The muscle pathology in *adbn*$^{-/-}$ mice is at least partially attributable to a loss of neuronal nitric oxide synthase (nNOS) signaling; nNOS localizes to the dystrophin glycoprotein complex where it catalyzes the synthesis of vasodilating nitric oxide, improving blood supply following mechanical stimulation in muscle. However, this requires α-dystrobrevin for proper sarcolemmal targeting (37,86-88). Loss of nNOS signaling is also seen in Duchenne muscular dystrophy and contributes to fatigue in patients, consistent with the loss of all sarcolemmal dystrophin glycoprotein complex in the disease (89). Exacerbation of dystrophin-deficient muscular dystrophy by loss of dystrobrevin must therefore be

nNOS-independent; indeed, α-dystrobrevin appears necessary for stabilization and maturation of the neuromuscular junction, which is typically intact in muscle lacking dystrophin. In similar fashion, α1-syntrophin, a signaling molecule recruited to the dystrophin glycoprotein complex through interaction with dystrobrevin, is also required for nNOS signaling and NMJ maintenance. However, it remains unclear whether other signaling functions of the dystrophin glycoprotein complex are disrupted by loss of dystrobrevin or the syntrophins and contribute to pathology of dystrophin glycoprotein complex-related muscular dystrophies (39,90).

Mouse models mutated for α-, β-, γ-, and δ-sarcoglycan have been made and all show a progressive muscle phenotype. Interestingly, δsarcoglycan-, but not αsarcoglycan-deficient mice lost the sarcoglycan complex (and sarcospan) in vascular smooth muscle and developed cardiomyopathy. βsarcoglycan and γsarcoglycan KO mice also develop muscular dystrophy with loss of the entire sarcoglycan/sarcospan complex. Interestingly, the rest of the dystrophin glycoprotein complex shows proper sarcolemmal localization in the absence of sarcoglycans, and the link between intracellular actin and extracellular laminin is preserved (91-94). Sarcoglycan-null mice show muscle membrane fragility but do not have increased susceptibility to contraction induced damage (95). The sarcoglycans associate directly with the C-terminal domain of dystrophin, and therefore may provide structural reinforcement of the dystrophin glycoprotein complex near the actin-binding site (96). The relatively mild limb-girdle phenotype seen in sarcoglycan KO mice and human patients further suggests that at least some of the functions of the dystrophin glycoprotein complex are maintained in the absence of the sarcoglycan complex. By comparison, the entire dystrophin glycoprotein

complex is absent from the sarcolemma in dystrophin-deficient muscle, which typically coincides with a more significant pathological involvement of the tissue.

The dystrophin deficient *mdx* mouse, which has a nonsense point mutation in exon 23 of dystrophin, is the most commonly used animal model of dystrophinopathy. As in human patients, the entire dystrophin glycoprotein complex is lost from the sarcolemma in these mice; however, their muscles, with the exception of the diaphragm, show a relatively low level of disease involvement (5,97). Lifespan studies have shown that while *mdx* mice do have a reduced life expectancy compared to strain-matched wild-type controls, they reach ages exceeding 20 months (98). The precise reasons for the mild phenotype observed in these animals are unclear, but it appears that upregulation of the dystrophin homologue utrophin may be a mitigating factor in disease. Normally enriched post-synaptically at the neuromuscular junction, utrophin has been noted to decorate the sarcolemma of regenerating fibers in *mdx* muscle, where it forms part of the utrophin-glycoprotein complex (UGC) which is able to function similarly to the dystrophin glycoprotein complex. Furthermore, transgenic overexpression of utrophin in *mdx* mice drastically improved the dystrophic pathology in the more severely afflicted diaphragm muscle. This observation led to the generation of *mdx*/*utrn*$^{-/-}$ double knockout mice that lack both dystrophin and utrophin; these mice show a substantial muscle phenotype and often die by 20 weeks of age (99-102). Because the severe dystrophy observed in *mdx*/*utrn*$^{-/-}$ double-knockouts more closely resembles the human Duchenne muscular dystrophy phenotype, it is considered in many ways to be a superior model for the study of Duchenne muscular dystrophy disease and therapy. In addition to the dystrophin/utrophin double-deficient mouse, a number of *mdx* variants, with different

dystrophin mutations and degrees of muscle pathology, have also seen application as dystrophinopathy models (103,104). Interestingly, available evidence suggests that the manifestation of a phenotype in *mdx* muscle is highly dependent on the host strain. When the original *mdx* exon 23 mutation is bred into the DBA-2 background, muscle health is dramatically diminished when compared to what is observed in *mdx*/B10 mice (the strain in which the mutation initially arose) (105,106).

Non-rodent models of dystrophinopathy are also available and are widely used in preclinical testing of therapies. Zebrafish, dog, and, most recently, pig models of dystrophinopathy have been described (107-114). Of these, the Golden Retriever muscular dystrophy dog is the best characterized and represents the closest animal model to human disease presently available. A major advantage of this model is that affected dogs are more similar in size to pediatric patients, and challenges of dose delivery can therefore be better approximated than in smaller animals (115). Furthermore, Golden Retriever muscular dystrophy dogs have been used to test new technologies (e.g. magnetic resonance imaging (MRI)) for use as tools to evaluate disease pathology (116,117). Recently, a pair of aphenotypic dystrophin-mutated dogs from a Golden Retriever muscular dystrophy pedigree was reported. This discovery, along with that of an increased dystrophic phenotype depending on genetic strain, strongly suggests the presence of modifier genes that modulate the severity of dystrophic disease (118,119).

In stark contrast to the mild *mdx* dystrophin mutant, complete loss of *Dag1* (dystroglycan) is embryonic lethal in the mouse. However, it appears that disruption of the functional O-mannose structure on α-dystroglycan is sufficient to cause the observed lethality. Mice null for dystroglycan-processing genes, including *Pomt1*, *Pomt2, Fktn*,

and *Fkrp* all die between embryonic day 8.5 and 12.5 (E8.5-12.5) (50,120-123). Underlying this is the failure to form Reichert's membrane, which separates trophoblasts and parietal endoderm cells in murine embryonic development (124). To circumvent this problem, a LoxP flanked ("floxed") *Dag1* allele was generated, which allows for analyses of tissue and timing specific consequences of dystroglycan loss. In the presence of a Cre recombinase enzyme, LoxP sites are recombined to excise the floxed sequence; therefore, Cre transgenes under a number of cell- or tissue-specific gene promoters have been generated (125). Dystroglycan KO mice conditional for mature muscle (muscle creatine kinase, MCK-cre), whole CNS (glial fibrillary acidic protein, GFAP-cre), epiblasts (Mox2-cre, MORE mice), and Schwann cells (P0-cre) have revealed roles for dystroglycan developmentally and post-developmentally in multiple organ systems and have confirmed the role of dystroglycan in a number of patient phenotypes (126-129). While these novel dystroglycan KO mice have been useful in studying the impacts of dystroglycan loss they do not recapitulate the primary molecular defect in humans, where α-dystroglycan glycosylation, but not protein, is lost.

A mouse harboring a spontaneous *Large* mutation, known as the myodystrophy mouse (herein, Large^{myd}) is frequently used as a model of secondary dystroglycanopathy; however, the first description of this mutant vastly preceded the discoveries that dystroglycan-hypoglycosylation results in muscular dystrophy and that LARGE is required for functional dystroglycan glycosylation (130-132). Demonstration that Large^{myd} mice are deficient for dystroglycan glycosylation and that this is causative for their dystrophic phenotype established this line as a standard model for dystroglycanopathy. However, simultaneous loss of *Large* in all tissues confounds the

relative contributions of functional dystroglycan glycosylation in different disease-afflicted compartments. Specifically, it is challenging to sort muscle-intrinsic, nervous system-intrinsic, and combined or synergistic phenotypes of both the muscle and the nervous system. An interesting example of nerve/muscle ambiguity, although it has been resolved, is that Large^{myd} mice have morphologically abnormal neuromuscular junctions and reduced expression of the nicotinic acetylcholine receptor, likely due to a role for agrin/perlecan-αdystroglycan complexes in facilitating nicotinic acetylcholine receptor clustering (19,133-136). As a consequence, miniature endplate potentials, which represent the depolarization of the post-synaptic (muscle) end of the NMJ due to a single vesicle of neurotransmitter, are significantly lower in Large^{myd} muscle even though quantal content (which measures the amount of neurotransmitter contained within in a single vesicle) is significantly higher. This suggests that a number of endplates in *myd* mice are improperly innervated but a subset of properly innervated endplates may compensate (133). The post-synaptic defect in muscle was confirmed by a study demonstrating that muscle-specific transgenic Large expression in Large^{myd} mice restores NMJ structure and function (137). However, deletion of dystroglycan specifically in the CNS had no effect on pre-synaptic neurotransmission but reduced high-frequency stimulated long-term potentiation of neurons. In agreement with this observation, Large^{myd} mice have an apparent memory deficit (126,138). Thus, the cognitive impact of α-dystroglycan hypoglycosylation complicates analysis of muscle function in widely used assays that rely to some extent to the behavior or motivation of the animal (e.g. forelimb grip strength, treadmill run or open field activity, rotorod).

Aside from the Large^{myd} mouse, there has also been some interest in developing mouse models of secondary dystroglycanopathy that incorporate known patient mutations. In particular, founder mutations identified in *FKTN* and *FKRP* have high incidences within certain populations and are therefore reasonable choices for development of "knock-in" models (74,139). However, mice carrying these human mutations have subclinical phenotypes (140-142). Although this result is disappointing on first take, it has provided a central insight to our understanding of secondary dystroglycanopathies: mutations in α-dystroglycan processing genes may generate proteins with residual function sufficient to protect affected tissues. In the case of *Fktn* human patient knock-ins, mice homozygous for the human insertion retained a significant amount of high molecular-weight α-dystroglycan (indicating the presence of functional glycosylation). Generation of heterozygous patient/null (*Fktn*$^{HP/-}$) compound *Fktn* mutants substantially reduced, but did not abolish, glycosylated dystroglycan. Comparison of *Fktn*$^{HP/-}$ and *myd* mice demonstrated laminin binding activity in skeletal muscle protein prepared from Fktn but not Large mutants (140). It is currently hypothesized that congenital muscular dystrophy phenotypes require at least 70% loss of α-dystroglycan functional glycosylation, and it is predicted that more severe patient phenotypes should correspond to mutations that more significantly inhibit the activity of their respective gene products, although genotype-phenotype correlations for *FKTN* and *FKRP* have not been successful in predicting disease severity (143-145). Mice with human *FKRP* mutation knock-ins also fail to exhibit a distinct dystrophic phenotype, including those with mutations causing severe congenital muscular dystrophy in patients; however, inclusion of the resistance cassette used in selection during model development

substantially disrupts protein function and is therefore maintained rather than excised (122,142). Together, these results demonstrate that knock-in models are unsuitable for the study of secondary dystroglycanopathy and suggest that a KO approach is likely preferable. Because loss of α-dystroglycan functional O-mannosylation is embryonic lethal in mice, conditional knockout of dystroglycan processing genes is required for the generation of a viable colony. To date, this has been accomplished only for *Pomt2* and *Fktn* (50,121,146). As with floxed *Dag1* mice, these models are versatile because gene knockout is accomplished through the use of specific Cre recombinase transgenes. However, only *Fktn* has been knocked out specifically in skeletal muscle, via Myf5-driven cre (Myf5/Fktn KO mice). Furthermore, a whole-body tamoxifen-inducible *Fktn* KO mouse has been described which enables the assessment of fukutin loss in all tissues without the developmental and behavioral consequences observed in *myd* mice (50). These models are powerful when used together because they make it possible to investigate muscle-intrinsic and –extrinsic functions of fukutin. Altogether, three types of models are most commonly used for the study of congenital dystroglycanopathy-type muscular dystrophy: Myf5/Fktn KO mice, *FKRP* patient knock-in mice, and Large^{myd} mice. Of these, only the Myf5/Fktn KO mouse has disruption of α-dystroglycan glycosylation specifically in muscle. While Large^{myd} mice represent the lone spontaneous dystroglycanopathy model, affected animals can die at ages as early as 5 weeks, representing a significant challenge to their experimental use. Ultimately, all animal models of disease have distinct strengths and weaknesses, but due to its versatility and ability to generate disease-relevant phenotypes, the work described here utilizes the floxed *Fktn* mouse.

Muscle development and mechanisms of disease in dystrophin glycoprotein complex-related muscular dystrophy

Skeletal muscle specification is largely a function of four transcription factors termed myogenic regulatory factors: myogenic factor 5 (Myf5), myoblast determination protein (MyoD), myogenin, and muscle-specific regulatory factor 4 (MRF4 or Myf6). The myogenic regulatory factors are expressed at different times during developmental and post-developmental myogenesis, and their forced expression in non-muscle cell types induces the muscle program (147). Myf5 and MyoD control the maturation of satellite cells, the resident stem cells of muscle, to myoblasts, mono-nucleated progenitors committed to the muscle lineage. Myogenin is expressed as myoblasts fuse to form a nascent multi-nucleated muscle fiber, while MRF4, at least in adult muscle, appears to regulate terminal differentiation of myotubes (148,149). Mice with targeted KO of MyoD are viable and have no overt phenotype while mice deficient in Myf5 die shortly after birth due to malformation of the rib cage, but have apparently normal skeletal muscle (150,151). Because neither Myf5 nor MyoD KO mice are deficient in skeletal muscle, it was hypothesized that they either function redundantly or compensatorily in myoblast determination. This was demonstrated by the generation of Myf5/MyoD double KO mice, which were born but died minutes thereafter due to an inability to breathe independently (152). The presence of muscle specific mRNAs, including those encoding contractile proteins or acetylcholine receptor, were undetectable in the Myf5/MyoD-null pups, and histological examination revealed a complete absence of skeletal muscle (152). In contrast, myogenin-null mice have myoblasts that align in preparation for myofiber formation and express acetylcholine receptor mRNA; however,

the myoblasts fail to fuse, resulting in a total loss of functional skeletal muscle and perinatal lethality (153,154). Myf5 is first expressed during murine development at embryonic day 8 (E8), while myogenin expression follows at E8.5. MyoD is observed from days 10-12 and MRF4 appears briefly at E9 and then again at E16 and is the most prevalent myogenic regulatory factor postnatally (147,155). The MRF4 gene is in close proximity to Myf5, and it appears that Myf5 cis-activates MRF4 expression. This discovery enabled the development of allelic Myf5 mutants containing insertions of varying length; while all of these mutants are Myf5-null, larger insertions in Myf5 correspond to a stronger disruption of MRF4 transcription. Crosses of these Myf5 mutants with MyoD null mice led to generation of Myf5/MyoD-mutant mice. Interestingly, mutants in which MRF4 expression is relatively unaffected (i.e. smaller insertions into the Myf5 locus) develop muscle, challenging the postulated role for MRF4 specifically as a regulator of differentiation (156). The specific expression patterns of the various myogenic regulatory factors are therefore clearly regulated spatiotemporally in the developing embryo and require tight control for the correct formation of skeletal muscle.

Adult muscle consists of mature, post-mitotic myofibers and associated progenitor cells (satellite cells), which reside at the surface of the muscle fiber beneath the basal lamina (network of laminins sandwiched between the sarcolemma and the rest of the extracellular matrix) (157). Satellite cells are normally quiescent and require activation signals to enter the cell cycle, which is the first step in the formation of new muscle in adults. In muscular dystrophy, satellite cell activation occurs in response to a local injury and is followed by proliferation, fusion and terminal differentiation. Myf5 and MyoD

both control the progression of satellite cells into myoblasts but it appears that, physiologically, Myf5 regulates myoblast proliferation rate while MyoD potentiates their ability to differentiate further (158,159). Satellite cells are marked by the expression of paired box protein 7 (Pax7), which is lost in transition to myoblasts. However, a subset of satellite cells will coexpress Pax7 and MyoD, and eventually lose myoblast character and return to quiescence (160). This asymmetric self-renewal of the satellite cell pool is critical to its maintenance in mature muscle. Whether a satellite cell renews or proceeds along the myogenic lineage seems to depend on the segregation of signaling factors in dividing cells, which regulate Pax7 or myogenic regulatory factor expression to determine cell fate (161,162). The ability of satellite cells to function properly is central to muscle health; this ability may become compromised in muscular dystrophy, potentially underlying regeneration deficits that contribute significantly to disease progression, as will be discussed later in this section.

Mature muscle fibers are distinguishable based on mature isoform expression of specific proteins, including actin and myosin, which confer distinct metabolic and contractile properties (163) (Table 1.2). For the purpose of simplicity, we will refer to muscle fiber types according to the expression of myosin heavy chain forms. In humans, the major fiber type classifications are type I, expressing *MYH7* (slow-twitch, oxidative metabolism), type IIA, expressing *MYH2* (fast-twitch, oxidative metabolism), and type IIX, expressing *MYH1* (fast-twitch, intermediate metabolism). Other mammals also have fast-twitch, glycolytic fibers (IIB) that expresses *MYH4*; while *MYH4* is present in the human genome, it is not expressed. Individual muscle fibers may express multiple

mature myosin isoforms or switch from one type to another in age- and use-dependent manners (164). The entirety of a given muscle shows mosaicism with respect to the myosin isoforms expressed in individual fibers, but the overall composition of the muscle determines its twitch and fatigue characteristics (165-167). At birth and in newly regenerated muscle fibers, the embryonic myosin heavy chain (eMHC) isoform predominates. Terminal differentiation of muscle involves fiber-type specification, whereby expression of eMHC falls as mature myosin isoforms rise. In newborns, this process is mediated by the maturation of the neuromuscular system and the loss of polyneuronal innervation, in particular. Motor neurons and neuronal stimulation profoundly affect fiber type, which is important for use/disuse adaptation (reviewed in (165)).

Abnormal fiber-type distributions have been described in muscular dystrophies and may contribute to disease pathology. Specifically, type I fibers are apparently more stable under disease conditions. The slow and/or oxidative myogenic programs are controlled at least in part by the expression of peroxisome proliferator-activated receptor γ coactivator 1-α (PGC-1α). Direct transgenic overexpression of PGC-1α or KO of an upstream repressor dramatically shifts muscle towards a slow, oxidative phenotype (168,169). Furthermore, expression of PGC-1α in the *mdx* mouse improves several disease parameters and significantly reduces fatigue (170,171). This agrees with the observation in the Large-deficient *myd* mouse that the soleus (primarily oxidative)

Table 1.2 Mammalian Skeletal Muscle Fiber Types

Type	Gene (Myosin Heavy Chain)	Contraction Speed	Metabolism
Neonatal	MYH8	N.D.	N.D.
Embryonic	MYH3	N.D.	N.D.
1	MYH7	Slow	Oxidative
2A	MYH2	Fast	Oxidative
2B	MYH4*	Very Fast	Glycolytic
2X	MYH1	Fast	Intermediate

*Not expressed in humans

muscle, but not the extensor digitorum longus (EDL, glycolytic), was resistant to fatigue (172). Together, these results indicate that fiber-type modulation is a potential means of preserving dystrophic muscle, but it should be noted that slow-twitch muscles generate significantly less force than their fast-twitch counterparts. When placed in the context of weak dystrophic muscles, forced expression of the slow, oxidative program might have undesirable consequences for overall muscle strength or function. Furthermore, a predominance of type I fibers has been observed in severely affected muscles of Duchenne muscular dystrophy patients, demonstrating that some slow muscles are still susceptible to disease (173,174). Ultimately, sampling difficulties challenge a detailed analysis of fiber types in human patients and limit our knowledge of the extent to which they influence pathology.

It is clear that muscle is a dynamic tissue with intricate biology under both normal and disease conditions; however, despite the nuances separating the diverse muscular dystrophies, all types are marked by myofiber necrosis/degeneration (reviewed in (175)). Different types of muscular dystrophy diverge with respect to the primary cause of muscle damage, and are frequently categorized according to specific classes of molecular defects. While the clinical aspects of dystrophin glycoprotein complex-related muscular dystrophies differ, they share myofiber susceptibility to contraction-induced damage resulting from a failure to connect the muscle cytoskeleton to the extracellular matrix (176). This was first demonstrated in the *mdx* mouse, where stress-induced damage was significantly higher than in control animals. Work in the *myd* mouse (130,131) showed that muscle fibers lacking glycosylated α-dystroglycan demonstrate had increased accumulation of a membrane-impermeant dye following laser-induced damage *in vitro*.

Furthermore, wild-type fibers detached from laminin show similar vulnerability to damage, providing robust evidence that functionally glycosylated α-dystroglycan stabilizes the sarcolemma through attachment to laminin (177,178). Cells have evolved mechanisms to survive minor cell membrane insults; in muscle, these "micro-tears" engage a Ca^{2+}-sensitive membrane-repair machinery. Interestingly, loss of dysferlin, a protein involved in sarcolemmal repair, also results in muscular dystrophy, indicating that minor perturbations of the membrane are present even in muscle with a functional dystrophin glycoprotein complex (179-181). However, in dystrophinopathy or dystroglycanopathy muscle it appears that damage exceeds the cell's capacity for local membrane self-repair and leads to myonecrosis, representing the earliest phase of the dystrophic process. Altogether, these observations underscore the requirement of an intact muscle cell membrane to maintain tissue health.

In addition to the primary biochemical lesion of muscular dystrophies caused by a defective dystrophin glycoprotein complex, a number of other, secondary defects are histologically identifiable and distinguish normal and dystrophic muscle (discussed with patient phenotypes above). Skeletal muscle possesses a remarkable potential for regeneration, and in the earliest periods of muscular dystrophy, centrally nucleated myofibers are the most obvious distinction between normal and dystrophic muscle. Progression of muscular dystrophy seems to depend critically on either failed or defective regeneration, which corresponds to development of fatty/fibrotic tissue phenotypes. The precise mechanisms that govern regeneration in dystrophic muscle are not fully understood; as such, they represent an area of active research within the field. It is unclear whether α-dystroglycan glycosylation is required for proper satellite cell function

after injury, but the MCK-cre/dystroglycan-null mouse, which retains the dystrophin glycoprotein complex throughout all stages of regeneration, has only a mild dystrophy, suggesting that the dystrophin glycoprotein complex contributes to successful myogenesis (127). In all, alterations in the satellite cell niche, including its biochemical organization and the presence of other cell types (e.g. immune cells, fibroblasts), or in the ability of satellite cells to interact with their niche, could influence regeneration in diseased muscle. Still, until relatively recently, it was unclear whether satellite cells from dystrophic muscle bore an intrinsic defect that limited their ability to generate new myofibers. Work in the myd mouse, which has hypoglycosylated α-dystroglycan, demonstrated that satellite cells on isolated muscle fibers proliferated at significantly lower rates compared to those on wild-type fibers. However, when removed from their native fibers and cultured *in vitro*, proliferation rates of myd satellite cells were equivalent to wild-type levels. Furthermore, analysis of the laminin network on isolated muscle fibers of *myd* mice revealed a disorganization and discontinuity in comparison to highly uniform arrangements of laminin on wild-type fibers. Satellite cells isolated from wild-type mice and expanded *in vitro* were able to contribute to new myofibers in engraftment experiments only when first grown on plates coated with laminin, suggesting that satellite cells interact with laminin in a way that is central to their function (182). This striking result emphasizes the unexpected ways in which secondary defects of muscular dystrophy contribute to pathogenesis of disease. It should be noted, however, that FKRP knock-down mice have fewer $Pax7^{+}$ satellite cells in late embryonic development (E15.5), and that these satellite cells appear to have lower myogenic capability *in vitro* (183). It is unclear, however, if this defect is FKRP-specific or if *myd*

satellite cells are somehow exceptional; additional work is therefore required to clarify common versus gene-specific regenerative deficiencies.

The local environment of satellite cells indeed differs substantially in dystrophic compared to normal muscle and in ways that extend beyond the irregular satellite cell niche. Regeneration requires the coordination of several events according to a strict time course, including an initial period of inflammation and phagocytosis of cellular debris from the damage site, activation, proliferation and maturation of satellite cells, followed by their fusion and differentiation into multi-nucleated myotubes (for review, see (184,185)). In normal muscle, injury events are relatively infrequent, enabling repair and regeneration to proceed uninterrupted; however, this is likely not the case in dystrophic muscle. Consider, for example, a single region within the muscle that adjoins several fibers. Damage to any of these adjacent fibers will initiate a regeneration process, with early myotube formation starting around 3 days- and peaking at 7 days-post injury. If another damage event occurs within this time frame, the microenvironment of progenitors involved in repair of the first injury is altered, with potential consequences for regeneration.

In the immediate aftermath of a necrotic event, an inflammatory response dominates the degenerated region. Pro-inflammatory cytokines are released from blood vessels supplying the damaged muscle and from "resident" macrophages, which are activated in response to local injury (186). Acute inflammation functions to remove damaged cellular material, and recruits alternative populations of immune cells to the tissue that facilitate the progression of regeneration. Macrophages are classified according to their activation and inflammation profiles, with the most general

categorization distinguishing them as M1 (classically activated) and M2. M1 macrophages are most commonly associated with a pro-inflammatory phenotype, while M2 macrophages are categorized into three subtypes: M2a (alternatively activated), M2b, and M2c, each with distinct roles (187). M2c macrophages are primarily considered "anti-inflammatory," and suppress the activity of M1 macrophages to enable tissue repair. Thus, M1 macrophages are associated with the earliest periods of muscle regeneration, while M2c macrophages appear later. Under normal conditions, M2a macrophages are associated with the final steps of regeneration and repair, including the formation of new blood vessels and extracellular matrix synthesis. However, tight regulation of the M2a population is required for the proper formation of new muscle cells (188). Recent work has shown that secreted factors from M1 macrophages promote migration of muscle progenitors (MPs) but inhibit their fusion and differentiation (189,190). This supports a requirement for distinct temporal regulation of macrophages during muscle regeneration. Over time, dystrophic muscle transitions from an acute to chronic inflammatory phenotype, which likely impairs regenerative processes (191). Furthermore, chronic inflammation in dystrophin-deficient muscle is associated with accumulation of alternatively activated macrophages, which seems to correspond to progressive fibrosis (192,193). Interestingly, it has also been argued that macrophages participate directly in the sarcolemmal lysis that precedes necrosis (194). Macrophage depletion in *mdx* muscle significantly reduced incorporation of a membrane impermeable dye into muscle fibers, representing an apparent stabilization of the cell membrane (195). While inflammation has long been known as a secondary aspect of dystrophic disease,

current evidence suggests that it has more than a passive role in the progression of muscular dystrophy.

One of the clearest indicators of disease status in dystrophic muscle is the level of fibrosis, which increases substantially over time. Mechanisms regulating fibrosis are of increasing interest because the myofibers and fibrotic content in muscular dystrophy are inversely related and it is therefore expected that a delay in the development of fibrosis might prolong muscle function. Increasingly, it is becoming clear that various abnormal phenotypes in dystrophic muscle are interrelated and combine to fully produce the presentations of patients. As mentioned above, impairment of muscle regeneration parallels a worsening phenotype in dystrophic muscle; furthermore, it is probable that factors modulating the microenvironment of muscle progenitors share at least partial responsibility for this impairment (192,196,197). Muscle is replaced by either deposition of extracellular matrix proteins, which are synthesized by fibroblasts, or adipose tissue, in a process termed fatty degeneration. Initially, it was hypothesized that satellite cells were multipotent and could be forced into fibrogenic or adipogenic lineages. However, this was abandoned following the discovery of a single non-myogenic progenitor cell type that could differentiate into both fibroblasts and adipocytes (termed fibro/adipogenic progenitors, FAPs) (198,199). Co-culture of muscle progenitors (MPs) with FAPs significantly reduces the expression of the quiescence markers Pax3 and Pax7, and increases expression of the myogenic regulatory transcription factors Myf5 and MyoD, signaling commitment of MPs to the myogenic lineage. Importantly, the adipogenic potential of these cells is potently inhibited in the presence of myotubes, consistent with

the observation in muscular dystrophy patients that fatty degeneration/infiltration occurs late in the disease process after muscle content in the tissue is largely depleted (198).

While myofibroblasts and adipocytes arise from a common progenitor cell in muscle, their presence in dystrophic muscle do not strictly overlap. Although this reflects, at least in part, the strong negative influence of myofibers on adipogenic differentiation of FAPs, it also likely reflects other aspects of the disease state *in vivo* as well. In particular, paracrine signaling of transforming growth factor β (TGFβ) strongly induces a fibrotic phenotype in exposed FAPs. TGFβ is upregulated in both Duchenne muscular dystrophy and dystroglycanopathy muscle and coincides with substantial levels of tissue fibrosis (200). When properly regulated, however, TGFβ is not pathogenic but is instead a critical mediator of muscle repair. Following damage, local extracellular matrix is broken down to allow the expansion of the satellite cell population and the formation of new muscle fibers; formation of new extracellular matrix surrounding nascent fibers is one of the final steps completing the regenerative cycle (201-204). Under physiological conditions, this is accomplished via secretion of TGFβ from M2a macrophages. However, continual degeneration in dystrophic tissues leads to a persistence and eventual accumulation of these macrophages, which in turn increases pro-fibrotic cytokines in the tissue and leads to fibrosis commonly seen in dystrophic muscle.

While gene therapies are emerging as an attractive technology for the treatment of genetic diseases, several challenges need to be addressed before they are used clinically for treatment of muscular dystrophies of the dystrophin glycoprotein complex. First, in the cases of both dystroglycanopathy and dystrophinopathy, a successful gene therapy would replace missing aspects of the dystrophin glycoprotein complex at the sarcolemma,

which may prove to be antigenic. Secondly, because skeletal muscle comprises a significant portion of total body mass, it is unclear what level of dosing would be required to reach all target muscles. Although it is theoretically possible to specifically target the muscles most essential to survival (e.g. heart, diaphragm), a major goal of therapeutic development for muscular dystrophy is to improve patient quality of life, which includes an extension of the ambulatory period in patients. Full replacement of the dystrophin gene is probably impossible due to its extraordinary size, although some efforts to circumvent through various methods have shown some promise. In the case of dystroglycanopathies, the high number of causative genes combined with the rarity of patient mutations in several of them makes gene therapy an impractical proposition. Ultimately, since these diseases share the common loss of a transmembrane link between actin and the extracellular matrix, it might be possible to take advantage of this shared defect to develop treatments that apply to many or most dystrophin glycoprotein complex-related muscular dystrophies. One approach to accomplish this would be to design therapies that target the dystrophic process; however, knowledge of the signals regulating the process is required in order to successfully identify strong candidate molecules for intervention.

Signaling pathways in muscular dystrophy

Although widely known as a structural complex, the unexpected discovery of dystrophin glycoprotein complex-localized signaling molecules revealed new functions for the dystrophin glycoprotein complex in muscle. In particular, it is hypothesized that the dystrophin glycoprotein complex senses mechanical stimulation through its attachment to laminin and that associated signaling molecules can be stretch-activated.

However, in order to function as a mechanically activated signaling complex, the dystrophin glycoprotein complex requires an intact extracellular connection. Abnormal signaling events in dystrophinopathy/dystroglycanopathy related directly to the dystrophin glycoprotein complex could be caused by any of the following: 1) stretch-independent gain or loss of function resulting directly from detachment from laminin; 2) loss of function of dystrophin glycoprotein complex-mediated mechanotransduction; 3) compensatory signaling activities of other laminin receptors (in muscle, α7β1 integrin) at the cell surface. Furthermore, in secondary dystroglycanopathies specifically, the entirety of the dystrophin glycoprotein complex is present at the sarcolemma but unattached to extracellular matrix receptors like laminin (132). In this case, the dystrophin glycoprotein complex may modulate the cytoplasmic concentration of signaling proteins by acting as a scaffold for binding of inactive molecules that are activated by stretch in normal muscle but merely sequestered at the sarcolemma in the absence of laminin binding. It is therefore possible that secondary signaling phenotypes may differ between dystrophin deficient- and dystroglycanopathy-muscle. In support of this hypothesis, it has been shown that β-dystroglycan interacts directly with signaling proteins including growth receptor bound protein 2 (Grb2) and Mitogen-activated kinase kinase 2 (MEK2) and that interruption of the α-dystroglycan-laminin link *in vitro* recruited an inactive Grb2/MEK complex to the cell membrane (205-207).

The dystrophin glycoprotein complex scaffold also regulates nNOS, which synthesizes nitric oxide (NO) in response to mechanical stimulation to dilate vasculature. Loss of nNOS at the sarcolemma reduces muscle endurance, and in combination with dystrophin deficiency produces a compound phenotype of dysfunction with aspects of

weakness and fatigue (89). Recently, it has been suggested that nNOS activation is dystrophin- but not sarcolemma localization-dependent. Furthermore, 5′-adenosine monophosphate activated kinase activates nNOS in a stretch-dependent fashion, but appears not to co-localize with the dystrophin glycoprotein complex; therefore, it is likely that an as yet unidentified signaling molecule associates with the dystrophin glycoprotein complex and effects mechanotransduction of nNOS (208).

Evidence for misregulated laminin-dependent signaling processes has been reported in both *in vitro* and *in vivo* models of sarcolemmal detachment from the extracellular matrix, implying that loss of α-dystroglycan glycosylation alters muscle signaling pathways. Indeed, one study found that loss of the dystroglycan-laminin interaction in cultured myotubes reduced phosphatidyl inositol 3-kinase (PI3K)/Akt survival signaling and increased apoptosis, suggesting the presence of an alternative mechanism of death in dystrophic muscle fibers not involving membrane fragility (209). In contrast, increased Akt signaling was observed in *mdx* diaphragm and was increased following the application of passive stretch to the muscle (210). This appears to be a downstream consequence of a concomitant increase in expression of the integrin complex, which also binds to laminin and propagates stretch signals. However, integrin levels were unchanged in young, pre-diseased *mdx* mice, which further suggests that the sarcolemma is remodeled to compensate for the reduction in laminin binding associated with loss of the dystrophin glycoprotein complex. Akt activation led to downstream survival signaling through nuclear factor-κB (NF-κB). Although NF-κB has cell survival roles, it is also a negative regulator of muscle mass and inhibits muscle regeneration. Therefore, given the necrotic phenotype of dystrophin-deficient muscle, it is likely that

NF-κB functions pathogenically in *mdx* muscle (210,211). Increased NF-κB levels have also been observed in biopsies from Duchenne muscular dystrophy patients, a finding which has stimulated interest in the use of NF-κB inhibitors as novel therapeutics (200).

Increases in the activation of Akt are also associated with muscle hypertrophy signaling through the control of protein synthesis/turnover dynamics. Akt stimulates mammalian target of rapamycin (mTOR), which is a central mediator of muscle hypertrophy and a key regulator of protein translation (212,213). Protein degradation proceeds through two primary mechanisms, the ubiquitin proteasome and autophagy. The proteasome typically recycles the majority of proteins in a cell, while the autophagy pathway handles long-lived proteins, protein networks and organelles (214-216). Akt negatively regulates both of these functions: the proteasome through inhibitory phosphorylation of forkhead box (FOXO) transcription factors that regulate the expression of proteosomal genes and autophagy through phosphorylation of Beclin-1, which prevents autophagosome formation (217-219). A marked dysregulation of protein translation/autophagy exacerbates dystrophy in dystrophin-deficient muscle with an associated imbalance of cellular energetics and an accumulation of damaged mitochondria. Metabolic modification through either a low protein diet or pharmacologic activation of 5′-adenosine monophosphate activated kinase, a major energy sensor and mTOR regulator in muscle, benefits *mdx* muscle structure and function (220-222).

While these results implicate muscle-intrinsic Akt signaling in the pathogenesis of dystrophinopathy, paradoxical findings have been reported in *mdx* mice with a constitutively active Akt transgene; these mice have a mild disease burden with reduced sarcolemmal fragility and increased muscle regeneration (223). Furthermore, micro-

RNA mediated increases in Akt activation are associated with substantial improvements in dystrophin-deficient muscle (224). Downstream signaling of Akt is also required for proper muscle maintenance: muscle-specific abrogation of mTOR signaling results in a moderate to severe myopathy (225,226). Interestingly, loss of mTOR complex 1 (mTORC1), an effector of Akt signaling, results in feedback Akt activation with a simultaneous increase in fast-twitch muscle fibers (225). Fast fiber types are more sensitive to autophagy defects, and it is possible that this underlies the relative stability of type I fibers in dystrophic muscle (227,228). However, in the case of miRNA modulation of Akt, pathological amelioration was observed in the absence of fiber type remodeling. It remains unclear why some studies posit beneficial effects of Akt signaling while others suggest it is deleterious, but strategies to target the pathway for therapy will need to consider that Akt likely plays multiple, potentially conflicting roles in dystrophic muscle (Figure 1.3).

One major challenge to cell signaling studies in muscular dystrophy is the gradual change in tissue composition associated with disease progression. Importantly, muscle fiber-intrinsic and -extrinsic cell signaling programs are likely different and reflect varying functions of different cell types in muscle. The overall muscle environment proceeds through regenerative, inflammatory, and fibrotic phases and each of these is associated with prominence of specialized cells. While it is theoretically possible to target the molecular processes underlying each of these stages, it is also likely that therapeutics directed towards this goal would show fleeting efficacy. However, modulation of pathways involved in a number of these disease processes may offer distinct advantages over monotherapies aimed at a single disease feature. Because of its

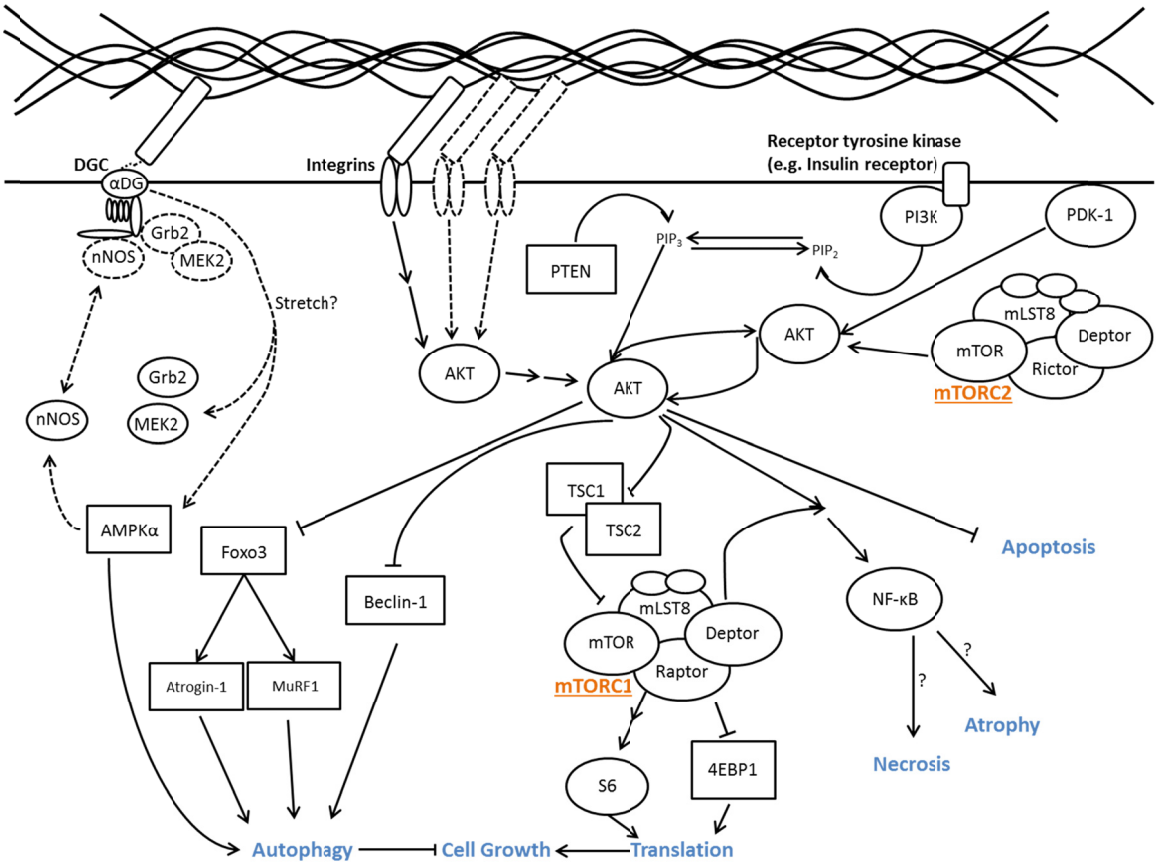

Figure 1.3 Diverse functions of Akt signaling in muscular dystrophy. Akt signals through stretch-dependent (integrins, dystrophin glycoprotein complex) and stretch-independent (receptor tyrosine kinases/growth factor receptors) mechanisms for a number of cellular outputs (blue), including cell growth and survival. Potential dystrophin glycoprotein complex or glycosylation dependent processes are shown with dotted lines. mTOR exists in two complexes (orange, underlined), one upstream (mTORC2) and one downstream (mTORC1) of Akt. Proteins positively coupled to Akt signaling are represented by ovals, while proteins opposed to Akt signaling are represented by rectangles.

widespread participation in physiological processes across diverse cell and tissue types, Akt/mTOR signaling has drawn some interest as a therapeutic target in muscular dystrophy. Interestingly, pharmacologic approaches to address the role of Akt and mTORC1 activities seem to demonstrate contrasting effects in dystrophic muscle; specifically, Akt activation and mTORC1 inhibition each seem to improve aspects of muscle pathology. In dystrophin-deficient muscle, activation of Akt with valproic acid reduced fibrosis and improved the integrity of the sarcolemma (229). Furthermore, inhibition of phosphoinositide 3-kinase (PI3K), an upstream activator of Akt, appears to be linked to decreased anti-apoptotic signaling of NF-κB in *mdx* mice (210). It is likely that divergent effects of Akt and mTORC1 regulation stem from mTORC1 independent functions of Akt, particularly with respect to its role in cell survival.

mTORC1 lies downstream of Akt and is known primarily as a regulator of protein translation, which it controls both directly, through phosphorylation of proteins associated with the translational machinery, and indirectly, through promotion of ribosome biogenesis (230). While normal muscle requires mTORC1 signaling for maintenance of muscle mass, activation in dystrophic muscle seems to have deleterious consequences, which include pathogenic inflammation and muscle fibrosis. The relative numbers of mono-nucleated non-muscle cells in dystrophic muscle is drastically increased compared to normal muscle. Since mTORC1 signaling may control protein synthesis in these abnormally prevalent cell types (e.g. fibroblasts, macrophages), it likely functions to exacerbate pathological features of muscular dystrophy. In support of this notion, use of rapamycin, an mTORC1 inhibitor, in *mdx* mice has been shown to reduce inflammation and fibrosis and improve muscle function (231,232). Additionally,

dystrophin- or collagen VI-deficient mice maintained on a low protein diet as a means of reducing mTORC1 activity demonstrate an improvement in histological parameters (221,233). However, these studies also implicate abnormal activation of Akt as a factor influencing muscle disease, contradicting results of Akt drug studies. While the results of rapamycin trials in dystrophic mice provide clearer results than attempts to probe the behavior of Akt, a number of questions, including the precise mechanism by which rapamycin improves muscular dystrophy, remain. It is unknown whether the findings in the *mdx* mouse will extend to other animal models of muscular dystrophy, an, in particular, those stemming from defects in the dystrophin glycoprotein complex. Furthermore, it is unclear to what extent mTORC1 should be inhibited to provide therapeutic benefit, especially in light of genetic experiments demonstrating the essential role of mTORC1 in normal muscle function (225,226). Rapamycin is by far the most widely used mTOR inhibitor for research purposes and is indicated for immunosuppression (i.e. graft rejection). Therefore, the use of rapamycin in basic and preclinical investigations of mTORC1 disruption makes some sense, especially in diseases with notable inflammatory phenotypes like the muscular dystrophies. However, its poor bioavailability mandates further study using drugs with improved pharmacological parameters like everolimus, which is formulated for oral use. Lastly, evaluation of mTORC1 inhibition as a treatment for muscular dystrophy will ultimately benefit from demonstrations of its performance in additional disease models outside of the mild *mdx* mouse.

Conclusion

As long as repairing the primary defect in a given muscular dystrophy is infeasible, alternative therapeutics capable of targeting common features of the various dystrophic processes are the most desirable. The ability to correctly identify targets and successfully modulate them pharmacologically is of paramount importance to the patient community. While the past several years have seen a number of substantive advances in our understanding of dystrophin glycoprotein complex-related pathologies as well as α-dystroglycan glycosylation and function, therapeutic development is still limited. Additional insights into different disease processes and the ways in which they combine to produce the complex dystrophic phenotype are needed in order to direct drug discovery and therapeutic development. However, there is still an urgent need to provide patients with treatment options, especially in congenital muscular dystrophies where patients are likely to die within the first decade of life. The following chapters will describe work to determine novel disease mechanisms and treatment strategies in animal models of secondary dystroglycanopathy.

CHAPTER 2

ABNORMAL SKELETAL MUSCLE REGENERATION PLUS MILD ALTERATIONS IN MATURE FIBER TYPE SPECIFICATION IN *FKTN*-DEFICIENT MUSCULAR DYSTROPHY MICE[1]

[1]Foltz SJ, Modi JN, Melick GA, Abousaud MI, Luan J, Fortunato MJ, and Beedle AM. (2016) Abnormal Skeletal Muscle Regeneration plus Mild Alterations in Mature Fiber Type Specification in *Fktn*-Deficient Dystroglycanopathy Muscular Dystrophy Mice. *PLoS One* 11(1): e0147049, Reprinted here with permission of the publisher, July 19, 2016

Abstract

Glycosylated α-dystroglycan provides an essential link between extracellular matrix proteins, like laminin, and the cellular cytoskeleton via the dystrophin-glycoprotein complex. In secondary dystroglycanopathy muscular dystrophy, glycosylation abnormalities disrupt a complex *O*-mannose glycan necessary for muscle structural integrity and signaling. *Fktn*-deficient dystroglycanopathy mice develop moderate to severe muscular dystrophy with skeletal muscle developmental and/or regeneration defects. To gain insight into the role of glycosylated α-dystroglycan in these processes, we performed muscle fiber typing in young (2, 4 and 8 week old) and regenerated muscle. In mice with *Fktn* disruption during skeletal muscle specification (Myf5/*Fktn* KO), newly regenerated fibers (embryonic myosin heavy chain positive) peaked at 4 weeks old, while total regenerated fibers (centrally nucleated) were highest at 8 weeks old in tibialis anterior (TA) and iliopsoas, indicating peak degeneration/regeneration activity around 4 weeks of age. In contrast, mature fiber type specification at 2, 4 and 8 weeks old was relatively unchanged. Fourteen days after necrotic toxin-induced injury, there was a divergence in muscle fiber types between Myf5/*Fktn* KO (skeletal-muscle specific) and whole animal knockout induced with tamoxifen post-development (Tam/*Fktn* KO) despite equivalent time after gene deletion. Notably, Tam/*Fktn* KO retained higher levels of embryonic myosin heavy chain expression after injury, suggesting a delay or abnormality in differentiation programs. In mature fiber type specification post-injury, there were significant interactions between genotype and toxin parameters for type 1, 2a, and 2x fibers, and a difference between Myf5/*Fktn* and Tam/*Fktn* study groups in type 2b fibers. These data suggest that

functionally glycosylated α-dystroglycan has a unique role in muscle regeneration and may influence fiber type specification post-injury.

Introduction

The dystrophin-glycoprotein complex (DGC), including dystrophin, dystroglycan, sarcoglycans, sarcospan and additional intracellular scaffold and signaling molecules, provides an important connection from the intracellular actin cytoskeleton to the extracellular matrix in skeletal muscle and other tissues (11,12,234). Extracellular α- and transmembrane β-dystroglycan (αDG, βDG) are crucial to this link as unique *O*-mannose glycan structures on αDG bind directly to laminin, agrin, neurexin, and perlecan in the basement membrane, conveying structural and signaling integrity through αDG to βDG and dystrophin (8,16,17,20,235-238). Functional loss of this axis causes various forms of muscular dystrophy including X-linked Duchenne and Becker muscular dystrophies (dystrophin), and a number of autosomal recessive congenital and limb girdle muscular dystrophies (239). Secondary dystroglycanopathy, a disease with normal dystroglycan and DGC protein expression but abnormal αDG glycosylation, is emerging as a large and diverse class of autosomal recessive muscular dystrophies caused by mutations in one of 16 known genes involved in the *O*-mannose glycosylation of αDG [for review, see (240)]. This class of muscular dystrophies encompasses a broader range of phenotypes (severe congenital to mild late onset) than other DGC-related diseases, the varied pathomechanisms downstream of the loss of αDG-matrix binding are poorly delineated, and there are no validated therapies for patients.

Recent work by our group and others demonstrates a role for contraction-induced sarcolemmal damage in the dystrophic progression of dystroglycanopathy, but also indicates a role for αDG in skeletal muscle development and/or regeneration processes in

more severe disease phenotypes (50,57,82,146,178). Both developmental and regeneration processes influence the distribution of muscle fiber types as marked by the expression of various myosin heavy chain proteins. Type 1 fibers (expressing *MYH7*) confer a slow, fatigue-resistant muscle profile, while type 2 fibers are fast with variable fatigue: type 2a (*MYH2*), type 2x (*MYH1*), and type 2b (*MYH4*) isoforms have fast/oxidative, fast/intermediate and fast/glycolytic profiles, respectively, although humans do not express the type 2b isoform [for review see (165)]. Postnatally, immature isoforms are lost and fast isoforms emerge due to a combination of signals including increased load on the muscle, maturation of the neuromuscular junction, and a rise in thyroid hormone (165). Slow muscle fiber types may persist from the embryo or arise from a conversion of type 2a fibers to type 1 around 4 weeks of age (241).

Fiber death after a necrotic incident stimulates activation and proliferation of muscle resident stem cells, "satellite cells" [for review, see (242)]. Resulting myoblasts (expressing embryonic heavy chain) can fuse to one another and remaining mature fibers to repopulate the muscle compartment. Post-regeneration fusion typically leads to fiber type specification that is dependent on the stimulation frequency from the innervating motor neuron with low frequency stimulation driving type 1 differentiation and high frequency or aneural fibers becoming fast (165). Transition between fiber types is a common event in skeletal muscle and often reflects an adaptive response of muscles to use or disuse; because myosin protein turnover is slow, muscles experiencing fiber type transformation frequently harbor hybrid fibers with mixed myosin isotypes (e.g. 2a/x, 2b/x)(165). As the expression profile of distinct skeletal muscle fiber types convey specific contractile, metabolic, and fatigue properties, variation in fiber type specification

during development or regeneration in muscular dystrophy influences patient phenotype. In fact, variation in fiber type proportions and/or fiber type selective susceptibility to disease has been reported in a number of muscular dystrophies, including Duchenne muscular dystrophy (DMD), myotonic dystrophy, facioscapulohumeral and oculopharyngeal muscular dystrophies [e.g. (174,243-245)]. While fiber types have not been analyzed in any dystroglycanopathy model, muscle force measurements from the extensor digitorum longus (EDL) and soleus of *Large*$^{myd/myd}$ mice suggested an increased susceptibility of type 2 fibers to contraction-induced injury in dystroglycanopathy muscle (172).

To better understand the abnormal processes during skeletal muscle development and regeneration in dystroglycanopathy muscular dystrophy, we performed fiber isotype analysis in two mouse models with conditional knockout of dystroglycanopathy gene *Fktn*. In the Myf5-cre/*Fktn* knockout (Myf5/*Fktn* KO), gene disruption at embryonic day 8 initiates a dystroglycan glycosylation defect during skeletal muscle development, affecting downstream satellite cells and muscle fibers (50). In the whole animal inducible knockout, Cre-ER is expressed in all cells, but only translocates to the nucleus for gene excision when tamoxifen is present (tamoxifen-cre/*Fktn* KO mice, Tam/*Fktn* KO). In these Tam/*Fktn* KO inducible mice, *Fktn* gene knockout was induced in skeletal muscle (and all other tissue types) post-development (15). Our data indicate changes in the regeneration process and mild changes to fiber type differentiation post-injury, suggesting that functional αDG plays a role in these processes that may contribute to disease progression and phenotype.

Materials and Methods

Ethics Statement

All mouse procedures were approved by the University of Georgia Institutional Animal Care and Use Committee (AUP A2010 08-163, A2013 07-016). All efforts were made to minimize animal suffering.

Mice

Mice were maintained on a 12:12 light:dark cycle with standard husbandry and a supplement of wet food pellets on the cage floor 2 to 4 times per week. Myf5-cre/*Fktn* and whole animal inducible Tam-cre/*Fktn* conditional exon 2 knockout mice have been described previously, were a kind gift from Dr. Kevin Campbell (U. Iowa) and correspond to Jackson Laboratory strains #007893, #004682, and #019097 (50). Myf5-cre/*Fktn* knockouts (Myf5/*Fktn* KO; $Myf5^{+/cre}$;$Fktn^{L/L}$) were bred from $Myf5^{+/cre}$;$Fktn^{L/+}$ x $Myf5^{+/+}$;$Fktn^{L/L}$ or $Myf5^{+/cre}$;$Fktn^{L/+}$ x $Myf5^{+/+}$;$Fktn^{L/+}$ pairs. Whole animal CAG-creERT2 (Cre-ER) tamoxifen inducible *Fktn* knockout mice ($Tg^{+/Cre-ER}$;$Fktn^{L/-}$; Tam/*Fktn* KO) were bred from $Tg^{+/Cre-ER}$;$Fktn^{+/-}$ x $Fktn^{L/L}$ pairs so induction of Cre recombination was only necessary at one allele to induce homozygous exon 2 deletion. To induce recombination for gene knockout in Tam/*Fktn* KO mice, tamoxifen (Tam; Sigma, St. Louis, MO; or Cayman Chemical, Ann Arbor, MI) was dissolved in ethanol and diluted with sunflower oil (Sigma) to 100 mg/ml for delivery by oral gavage at 0.4 mg/g. Mice received the first round of Tam-treatment on two non-consecutive days (day 1 and 3) at 6 to 8 weeks of age and a second round of Tam-treatment 8 weeks later at 1 day pre- and 1 day post-toxin treatment. All littermate control mice were Tam-treated at the same time as their inducible KO littermates; all of the following genotypes were used for Tam/Fktn

LC mice as we previously demonstrated that heterozygotes and *Fktn* floxed mice have no phenotype: $Tg^{+/Cre\text{-}ER}$,$Fktn^{L/+}$; $Tg^{+/+}$, $Fktn^{L/-}$ or $Tg^{+/+}$, $Fktn^{L/+}$ [15].

A total of 26 animals were used in the analysis of 2, 4, and 8 week old (wko) iliopsoas and TA muscles: 2 wko Myf5/*Fktn* KO and LC, n = 4 each; 4 wko Myf5/*Fktn* KO and LC, n = 4 each; (except Myf5/*Fktn* LC iliopsoas, n = 3); 8 wko Myf5/*Fktn* KO and LC, n = 5 each. 27 mice were used for the Myf5/*Fktn* and Tam/*Fktn* regeneration study, and the CTX-treated and contralateral saline-treated muscles were collected from each mouse: Myf5/*Fktn* LC, n = 5; Myf5/*Fktn* KO, n = 7; Tam/*Fktn* LC, n =7; Tam/*Fktn* KO, n = 8.

Cardiotoxin-induced regeneration

On the day of cardiotoxin injection, mice were anesthetized by isoflurane, lower hindlimbs were shaved, and mice were given an analgesic dose of meloxicam 1 mg/kg (VWR, Radnor, PA) by subcutaneous injection. Cardiotoxin (Sigma), at 10 μM in 0.9% sterile saline, was delivered in 25 μL intramuscular injections longitudinal into the tibialis anterior (TA, with potential involvement of the extensor digitorum longus, EDL). Identical injection of sterile 0.9% NaCl was completed for the left hindlimb (saline vehicle control). All toxin injections were performed by the same experimenter (AMB) for consistency across the dataset. Mice were euthanized 14 days post-injection and muscles were dissected for cryopreservation according to standard protocols (50,246). Note, for this study, the TA and EDL were dissected out and analyzed as a single unit.

Immunofluorescence and microscopy

The iliopsoas or TA/EDL were cryosectioned to a depth of 1 mm from the proximal side, then 7 μm sections were cut and mounted on glass slides for histological and fiber type analysis. Sections analyzed were derived from a comparable 300 μm zone of Ilio or TA,

respectively, across all samples, accounting for minor variations in muscle dissection and a subset of samples that required re-sectioning. Immunofluorescent staining for myosin isoforms was performed using mouse monoclonal myosin heavy chain antibodies F1.652 (embryonic), BF-35 (all but 2x), BF-F3 (type 2b), SC-71 (type 2a), and BA-D5 (type 1) (Developmental Studies Hybridoma Bank, University of Iowa, Iowa City, IA) at 1:20 – 1:40 dilution. Samples were co-stained for nuclei (DAPI; Life Technologies, Grand Island, NY) and membrane/basement membrane counterstain by perlecan (heparin sulfate proteoglycan; EMD Millipore, Darmstadt, Germany) or αDGct rabbit monoclonal 5-2 (247) or related hybridomas 29-10 or 45-4, not previously reported. Neuromuscular junctions were analyzed using rabbit monoclonal antibody D35E4 against presynaptic marker synaptophysin (Cell Signaling Technology, Danvers, MA) and Alexa 488-coupled bungarotoxin for detection of nicotinic acetylcholine receptors at the postsynaptic endplate (Life Technologies). Muscle sections were blocked in 5% donkey serum in PBS for 30 min, incubated in primary antibody in 5% donkey serum at 4°C overnight, washed 3 x 5 min, incubated in secondary antibody (AlexaFluor A546 anti-mouse IgG1, IgG2b, or IgM and AlexaFluor A488 anti-rabbit or rat IgG; Life Technologies) with or without A488-bungarotoxin at 1:500 in 5% donkey serum for 30 min at room temperature, washed 3 x 5 min and mounted with PermaFluor (ThermoScientific, Waltham, MA). Detection of glycosylated αDG by indirect immunofluorescence with IIH6 antibody has been described previously (50). Tissues were viewed by 20X objective on an inverted epifluorescent microscope (Olympus, Center Valley, PA) and images were captured using a DP-72 camera and CellSens software (Olympus).

For image analyses, a series of overlapping images crossing the entire muscle section were taken and compiled into a section map in Photoshop (Adobe). Compiled maps were analyzed by blinded observers in Image Pro Express (Media Cybernetics, Rockville, MD) for fiber counts and whole section area; a subset (all knockouts at 14 d post-CTX) was also analyzed for single fiber area of embryonic myosin heavy chain-positive (eMHC) fibers. Whole section areas from compiled maps were compared for serial sections of the same muscle and the most representative section map for each muscle was selected for total fiber counting. Mean Ilio section areas were: Myf5/*Fktn* 2 wko LC 0.72 ± 0.21 mm^2; KO 0.56 ± 0.18 mm^2; 4 wko LC 1.08 ± 0.20 mm^2; KO 0.96 ± 0.13 mm^2; 8 wko LC 1.73 ± 0.35 mm^2; KO 1.21 ± 0.29 mm^2; two-way ANOVA age, $p < 0.05$. Mean TA/EDL section areas were: Myf5/*Fktn* 2 wko LC 1.20 ± 0.05 mm^2; KO 1.89 ± 0.29 mm^2; 4 wko LC 2.72 ± 0.39 mm^2; KO 1.95 ± 0.12 mm^2; 8 wko LC 5.13 ± 0.64 mm^2; KO 3.25 ± 0.46 mm^2; two-way ANOVA genotype*age, $p < 0.05$; age, $p < 0.0001$. Any serial section that deviated by ≥ 15% from the counted map was also counted separately for total fibers. Total fiber counts ranged from 246 to 1716 in the iliopsoas and from 920 to 3795 in the TA of 2, 4, and 8 wko Myf5/*Fktn* mice; total fibers ranged from 1157 to 7483 in TAs of Myf5/*Fktn* or Tam/*Fktn* mice enrolled in the CTX study. Positive fibers (centrally nucleated [CN], eMHC) were counted by manual tag and divided by the number of total fibers in the section map x 100. Proportions of mature fiber types (MHC type 1, 2a, or 2b) were analyzed as the percentage of a given fiber type per total mature fibers (total fibers within a muscle section less eMHC expressing fibers) for each sample. Proportions of MHC type 2x fibers were determined as the percentage

of fibers not stained by the MHC "all but 2X" antibody, which detects all MHC isoforms except type 2x, per total mature fibers for each sample.

Graphs and Statistics

Fiber-type and central nucleation data are plotted as scatterplots with each data point representing analysis from one study animal; mean and standard error are shown. In text data references are also reported as mean with standard error. Data are analyzed by two-way ANOVA with Bonferroni's post-test, which compares each row by all columns and each column by all rows (Prism 5, GraphPad, La Jolla, CA). Because separate littermate and knockout data are used from the two strains (Myf5/*Fktn* and Tam/*Fktn*) in fiber typing post-injury, we performed two-way ANOVA across all genotypes to facilitate comparisons between the two different types of knockout mice (e.g. Myf5/Fktn KO injured vs Tam/Fktn KO injured). Post-tests from this analysis of all genotype groups are denoted on figures using asterisks. We also performed two-way ANOVA on each strain group independently for the toxin-induced regeneration experiments (Myf5/*Fktn* only and Tam/*Fktn* only) to enable further interpretation of significance detected in the "all genotypes" analysis. Two-way ANOVA interaction (Genotype*Toxin or Genotype*Age) p values are reported on each figure; individual group effects (Genotype, Age, or Toxin) are only reported if the interaction p value is not significant. eMHC-positive areas are plotted as proportion of fibers within a given size range (bin) per total number of eMHC-expressing fibers. Optimal bin sizes for eMHC-positive fiber areas were determined previously (50). Fiber-size distributions were non-normal (D'agostino & Pearson omnibus normality test failed), so data were analyzed by a two-tailed Mann-Whitney test (Prism 5, GraphPad, La Jolla, CA). $p < 0.05$ is considered statistically significant in all tests. *, $p < 0.05$; **, $p < 0.01$; ***, $p < 0.001$.

Results

Dystrophy progressively increases in Fktn-deficient muscle

Sarcolemmal attachment to the extracellular matrix through specific glycan structures on αDG is critical for muscle protection against contraction-induced damage (178). Accordingly, loss of *Fktn* or other genes involved in processing the *O*-Mannose glycan on αDG renders the sarcolemma vulnerable to contraction-induced damage and myonecrosis (50,146,172,248,249). To determine postnatal disease onset, we evaluated muscle regeneration in Myf5/*Fktn* KO muscle by the percentage of eMHC-expressing and centrally nucleated (CN) fibers in the iliopsoas and TA (with EDL) at 2, 4, and 8 weeks old (wko). CN was significantly increased in both iliopsoas and TA muscles of Myf5/*Fktn* KO mice, with a significant interaction between genotype and age in the TA, but not the iliopsoas (Figure 2.1A, B left). Post-tests identified elevated CN, a long-term marker of muscle regeneration, in 8 wko Myf5/*Fktn* KO TA (8 wko KO CN = 32.6 ± 4.1%) and iliopsoas (8 wko KO CN = 20.0 ± 4.8%), but a clear age-dependent increase in knockout muscle CN was only present for the TA muscle, due to an earlier onset of pathology in iliopsoas of some KO mice. In contrast, the proportion of eMHC-expressing fibers in both muscles was highly variable. However, there was a significant interaction between genotype and age (genotype*age) in the TA only; with increased eMHC-positive fibers in Myf5/*Fktn* KOs at 4 and 8 wko, reaching maximum at 4 weeks (4 wko KO eMHC = 12.8 ± 3.3%; Figure 2.1A, B right). In the Ilio, eMHC regenerating fibers were increased in Myf5/*Fktn* KO mice, with post-test significance at 4 weeks (4 wko KO eMHC = 15.0 ± 5.0%). Because eMHC is only temporarily expressed in regenerating muscle, it represents a "snapshot" of current regeneration at the time of analysis. Consequently, proportions of eMHC-expressing fibers are more variable and do

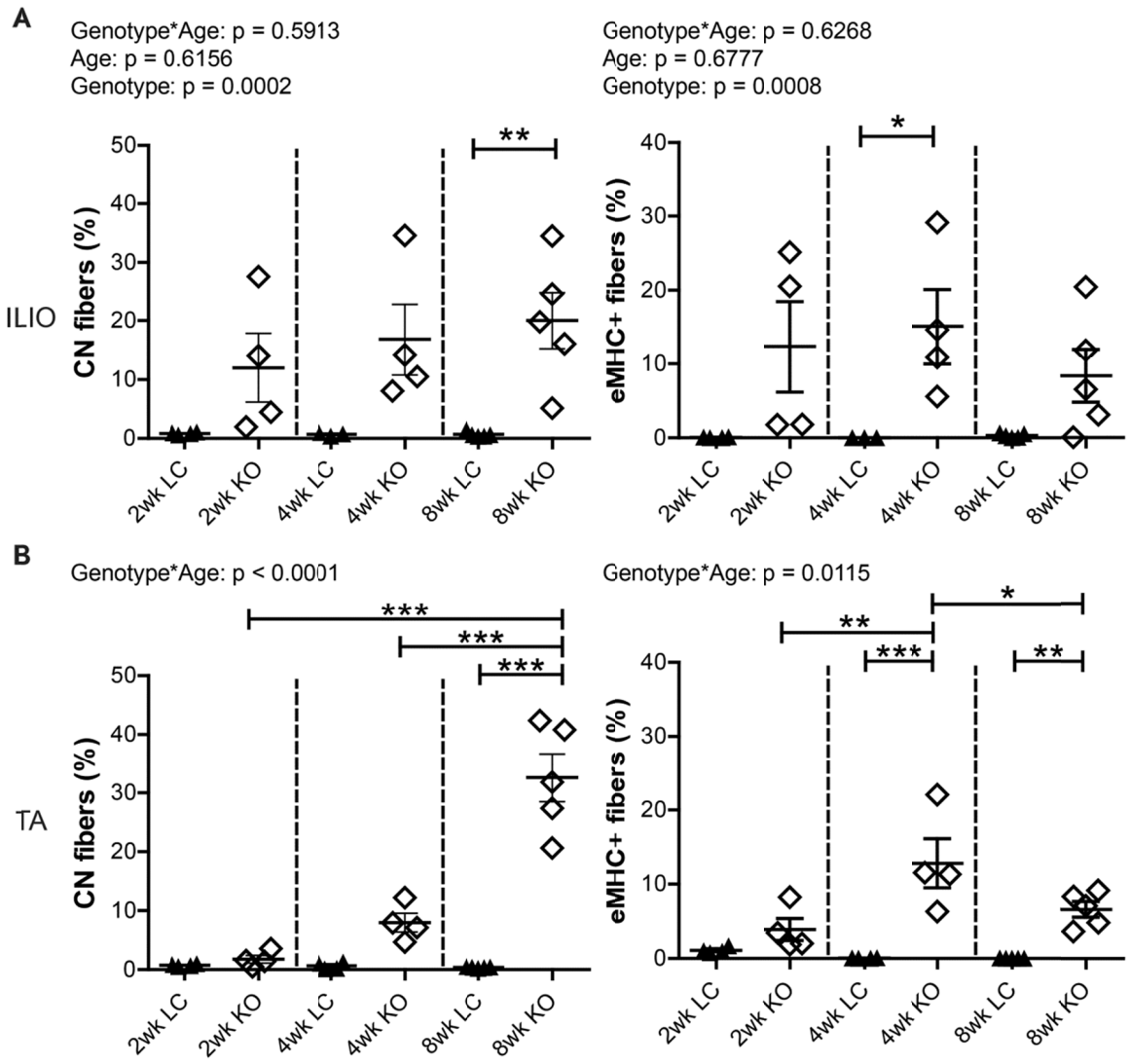

Figure 2.1 Dystrophy is prevalent and progressive in Myf5/Fktn KO muscle. Muscle regeneration after fiber necrosis as measured historically by central nucleation (CN, left) or transiently by embryonic myosin heavy chain expression (eMHC, right) in (A) iliopsoas or (B) TA muscle of 2, 4, and 8 wko Myf5/Fktn-deficient (KO) or control (LC) mice. *, $p<0.05$; **, $p<0.01$; ***, $p<0.001$. Two-way ANOVA with Bonferroni's post-test. TA, n = 4 mice per 2 and 4 wko group, n =5 per 8 wko group; Ilio, n=3-4 per 2 and 4 wko group, n=5 per 8 wko group.

not necessarily increase over time; CN, however, may persist for several months following a regeneration event, making it a suitable tool for examining the progression of disease. Thus, these data indicate that, on average, 20 – 30% of all muscle fibers have regenerated by 8 wko, confirming the development and progression of dystrophy in *Fktn*-deficient muscle and indicating a period of highly active muscle degeneration/regeneration peaking at 4 weeks and subsiding at 8 weeks.

Fiber type specification shows age-dependent differences

To assess whether *Fktn* loss alters muscle fiber differentiation, iliopsoas and TA muscles from 2, 4, and 8 wko Myf5/*Fktn* KO and LC mice were analyzed for expression of mature myosin heavy chain isoforms, indicative of different muscle fiber types. The iliopsoas was chosen because it is a smaller, proximal muscle that is more severely affected in Myf5/*Fktn* KO mice, while the TA is widely used in physiological assessment of muscle. In order to account for differences in the numbers of fibers in muscles across the sample set, data were analyzed as the proportion of isotype positive fibers per total mature fibers counted (presented here as percentages). By this measurement, there was no interaction between genotype and age (genotype*age) and no genotype effect for either iliopsoas or TA in type 1 (oxidative, slow-twitch) fibers, but there was a significant age effect in both muscles with fewer type 1 fibers in older mice compared to younger mice (Figure 2.2). In post-test analysis, type 1 fibers significantly decreased in iliopsoas of Myf5/*Fktn* KO from 4 to 8 weeks (Figure 2.2A, C), whereas in the TA, type 1 fibers were significantly decreased in all mice from 2 to 8 wko and in Myf5/*Fktn* KO mice from 4 to 8 wko, indicating that postnatal depletion of the type 1 fiber pool may proceed more slowly in Myf5/*Fktn* KO mice (Figure 2.2B, D). Neither type 2a (fast oxidative) nor type 2b (fast glycolytic) fibers were changed in the iliopsoas or TA muscles of Myf5/*Fktn*

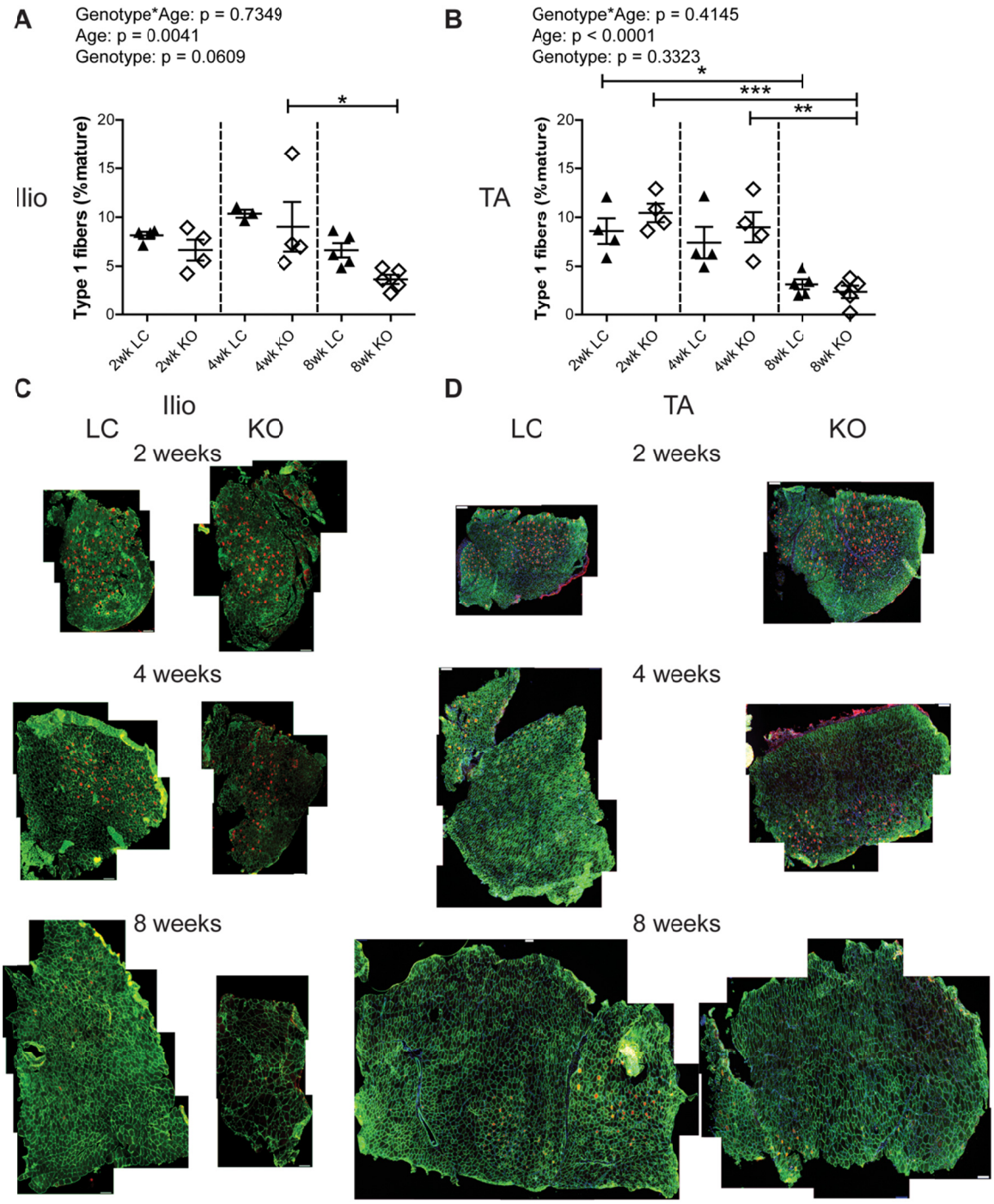

Figure 2.2 Frequency of type 1 oxidative fibers decreases with age in iliopsoas and TA. Oxidative type 1 fibers in (A) iliopsoas and (B) TA of 2, 4, and 8 wko Myf5/Fktn-deficient (KO) and control (LC) mice. *, $p<0.05$; **, $p<0.01$; ***, $p<0.001$, two-way ANOVA with Bonferroni's post-test. Whole tissue (C) iliopsoas and (D) TA maps of sections stained with anti-myosin heavy chain type 1 antibody (red), with basement membrane perlecan or sarcolemmal αDG core protein (green) and nuclear (blue) counterstains. Scale bar = 100 μm. n = 4 for all 2 and 4 wko measurements (except Ilio LC, n=3); n=5 for all 8 wko measurements.

KOs compared to LCs at any time points examined, although type 2a fibers were reduced in 8 wko compared to 4 wko KO mice (Figure 2.3). The proportion of type 2x (intermediate glycolytic) fibers was significantly affected by age, but not genotype nor genotype*age interaction (Figure 2.4). Type 2x were not yet developed in 2 wko mice but progressively increased through 8 weeks of age in iliopsoas and TA muscles. In post-test analysis, both 4 and 8 wko mice had more type 2x fibers in the iliopsoas compared to 2 wko mice, while in the TA, Myf5/*Fktn* LC had increased type 2x fibers at 4 and 8 weeks, but KO mice type 2x fibers were only elevated at 8 weeks (Figure 2.4). Thus, the transition timing to widespread type 2x fiber specification in TA may be minimally affected in *Fktn*-deficient muscle. Altogether these data demonstrate that postnatal mature fiber type specification is primarily age-dependent, with minimal or no affect due to *Fktn*-deficiency.

Muscle fiber differentiation is altered following induced regeneration in post-development, whole-body compared to developmental, muscle-specific Fktn KO mice

To understand the role of functionally glycosylated αDG in fiber type specification of regenerated fibers, we used cardiotoxin (CTX) to induce widespread, synchronized regeneration in two different *Fktn*-deficient mouse models: developmental, skeletal muscle-specific Myf5/*Fktn* KO (as above) and whole animal, Cre-ER *Fktn* mice, in which *Fktn* deletion is induced by tamoxifen-mediated translocation of Cre-ER to the nucleus for gene excision (Tam/*Fktn* KO are Tam-treated $Tg^{+/Cre\text{-}ER}$,$Fktn^{L/-}$; and Tam/*Fktn* LC mice are Tam-treated $Tg^{+/Cre\text{-}ER}$,$Fktn^{L/+}$, $Tg^{+/+}$,$Fktn^{L/-}$, or $Tg^{+/+}$,$Fktn^{L/+}$) (50). The tibialis anterior (TA) was chosen for analysis because it is the smallest muscle that is easily accessible for intramuscular CTX delivery, ensuring that a greater proportion of the muscle compartment is toxin affected. Myf5/*Fktn* mice were toxin injected at 6 wko

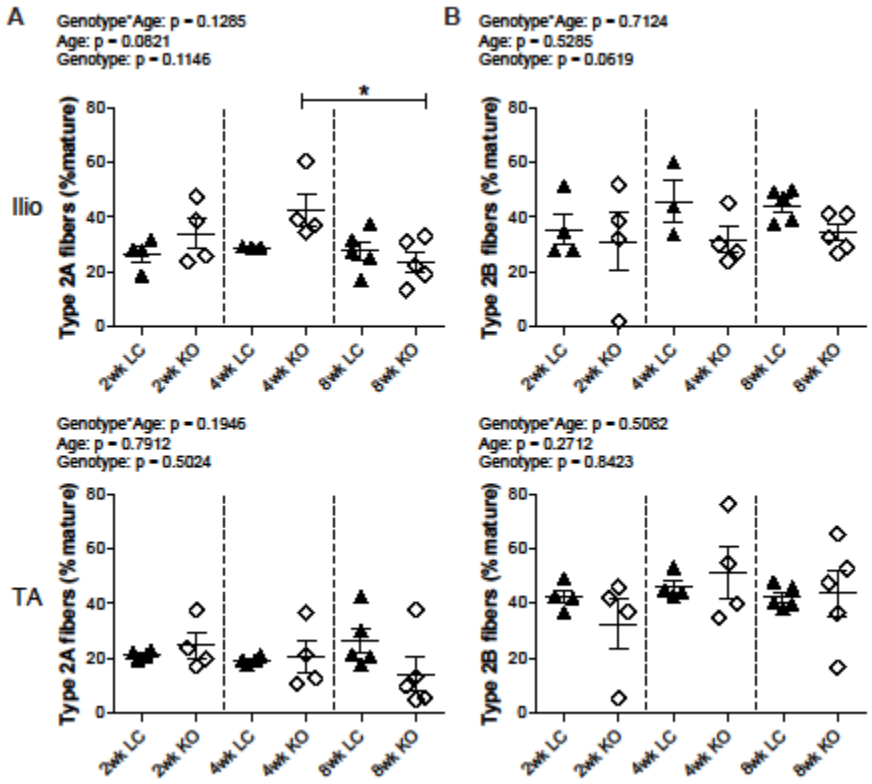

Figure 2.3 Frequencies of type 2a oxidative and type 2b glycolytic fast-twitch fibers are unchanged in iliopsoas and TA between Myf5/Fktn KO and LC mice. (A) Oxidative type 2a fibers in iliopsoas (top) and TA (bottom) of 2, 4, and 8 wko Myf5/Fktn-deficient (KO) and control (LC) mice. (B) Glycolytic type 2b fibers in iliopsoas (top) and TA (bottom) of 2, 4, and 8 wko Myf5/Fktn-deficient (KO) and control (LC) mice. *, $p<0.05$; two-way ANOVA with Bonferroni's post-test. n = 4 for all 2 and 4 wko experimental groups (except Ilio 4 wko LC, n = 3); n = 5 per 8 wko group.

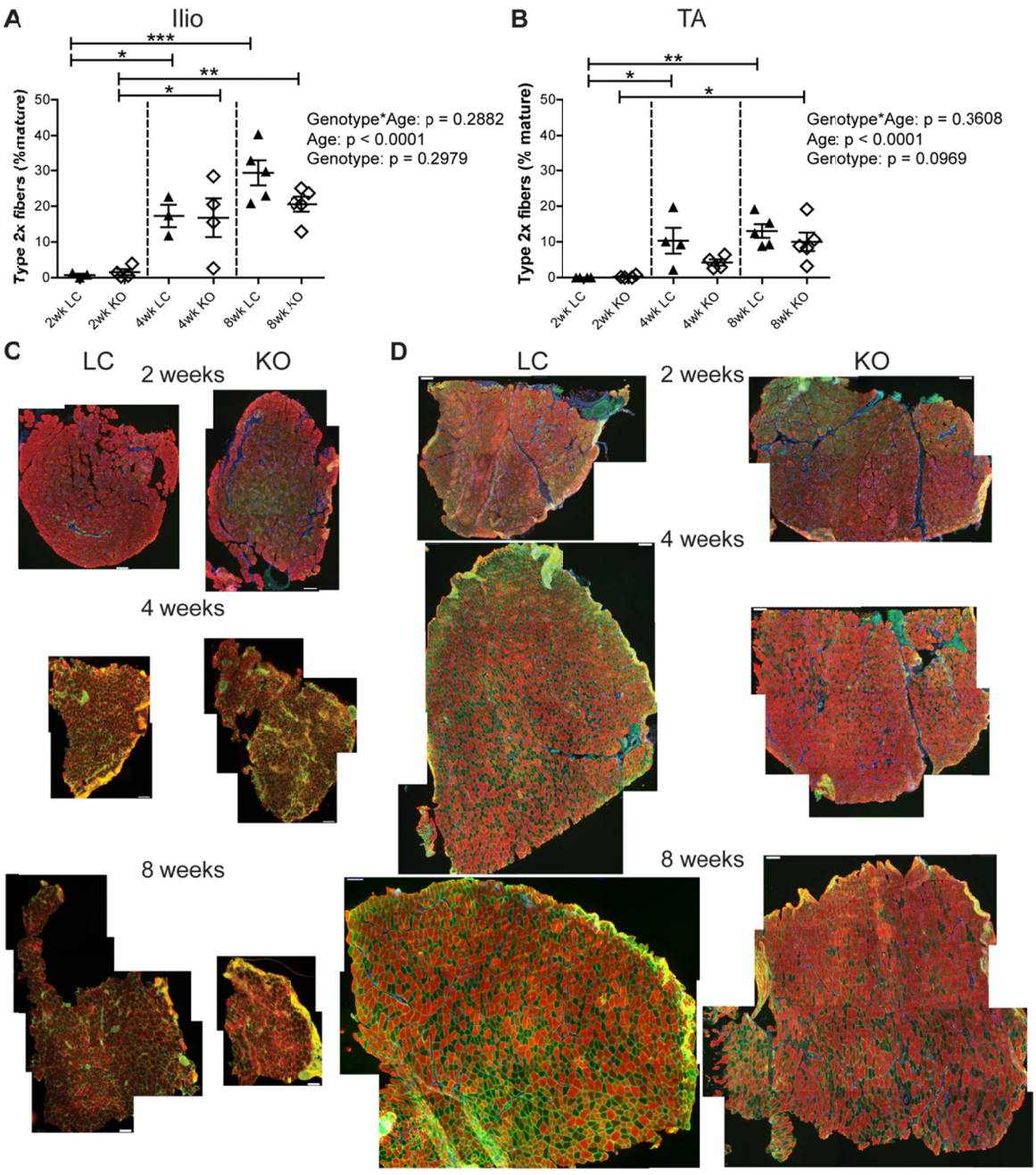

Figure 2.4 Minor delay in progression of glycolytic type 2x fiber switching in TA of Myf5/Fktn KO mice normalizes by 8 weeks. Glycolytic intermediate-twitch 2x fibers in Myf5/Fktn-deficient (KO) and control (LC) (A) iliopsoas and (B) TA muscles. *, $p<0.05$; **, $p<0.01$; ***, $p<0.001$, two-way ANOVA with Bonferroni's post-test. Whole tissue (C) iliopsoas and (D) TA maps of sections stained with antibody detecting all myosin isoforms except type 2x (red), with basement membrane perlecan or sarcolemmal αDG core protein (green) and nuclear (blue) counterstains. Unstained (negative) fibers were counted to measure type 2x. Scale bar = 100µm. n = 4 for all 2 and 4 wko measurements (except Ilio 4wko LC, n=3); n = 5 per 8 wko group.

and muscle was collected 2 weeks after injury at 8 wko. As Myf5 expression begins at embryonic day 8 (250,251), mouse gestation is ~19 days, and tissue was collected at 8 wko, the Myf5/*Fktn* KO muscle is approximately 10 weeks post-*Fktn* deletion. Therefore, Tam/*Fktn* mice were sacrificed 10 weeks following tamoxifen induction of *Fktn* deletion so that the length of *Fktn*-deficiency was comparable between Tam/*Fktn* and Myf5/*Fktn* KO animals. Loss of *Fktn* function was confirmed by staining TA sections with the αDG functional glycan specific antibody IIH6. In saline injected TA, the vast majority of fibers in both Myf5/*Fktn* and Tam/*Fktn* KOs were negative for glycosylated αDG; however, Tam/*Fktn* KOs had significantly higher residual IIH6 levels than their Myf5/*Fktn* counterparts (Figure 2.5). As the efficiency of gene knockout in muscle satellite cells of Tam/*Fktn* KOs has not been previously addressed and because Myf5/*Fktn* KOs exhibit minor fiber populations with residual αDG glycosylation, we also examined IIH6 staining in Myf5/*Fktn* and Tam/*Fktn* KOs 14 days after toxin injection. We observed no differences in the proportions of IIH6-positive fibers between saline- and toxin-injected TAs in either mouse strain (n=6), indicating that regenerated fibers are not disproportionately arising from cell populations that may have escaped *Fktn* gene excision (Figure 2.5).

In analysis of regeneration 14 days post-toxin injury, there was a significant interaction between genotype and toxin (genotype*toxin) for CN and eMHC measures of skeletal muscle regeneration (Figure 2.6). In post-hoc analysis, all CTX-treated groups had higher CN compared to saline (contralateral) controls (Figure 2.6A; saline-treated CN means range 2.3 ± 0.3% [Tam LC] to 27.8 ± 3.3% [Myf5 KO] vs. toxin-treated CN means range 23.2 ± 2.7% [Tam KO] to 54.4 ± 4.3% [Myf5 LC]). CN was also elevated

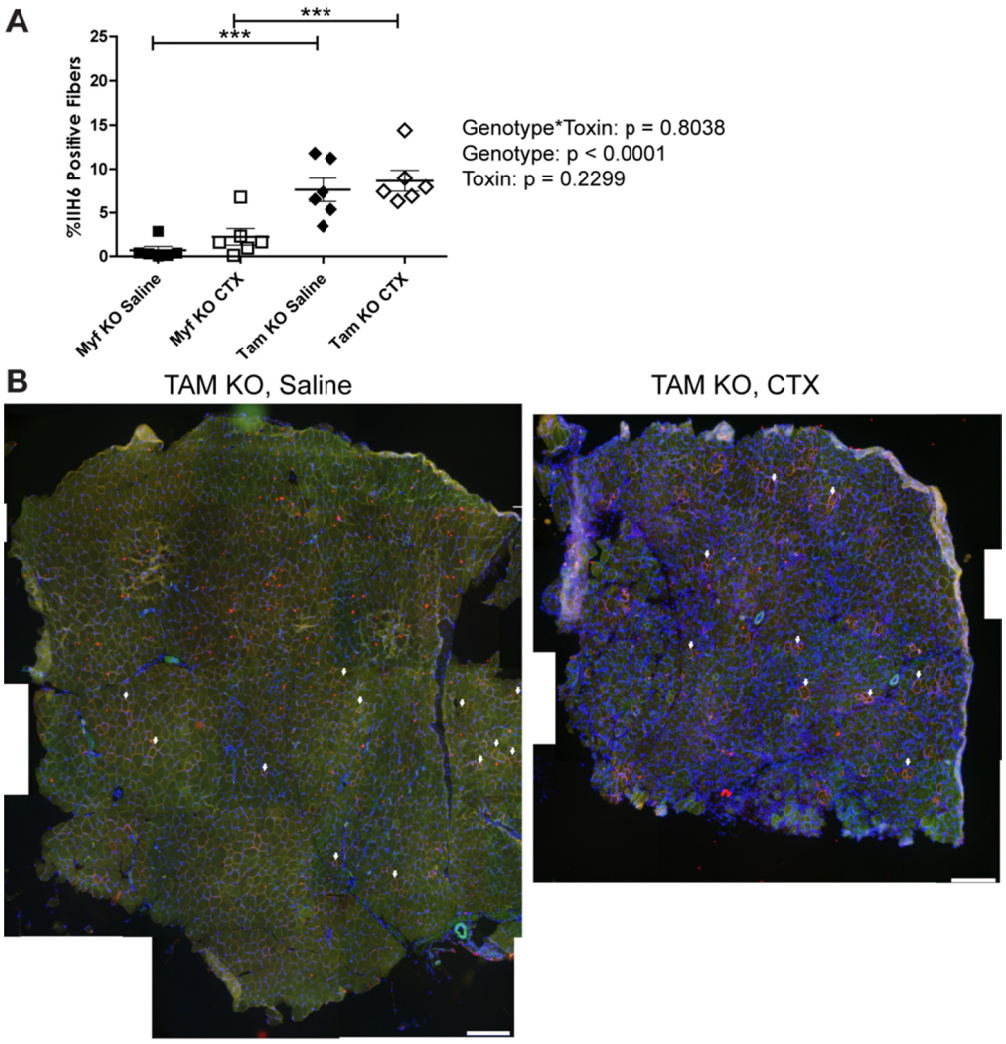

Figure 2.5 Injury does not induce revertant expression of α-DG glycosylation in Tam/Fktn KO mice. (A) Quantification of fibers with glycosylated α-DG in TAs of Myf5/Fktn or Tam/Fktn mice. ***, $p<0.001$, two-way ANOVA with Bonferroni's post-test. (B) TA muscle sections showing glycosylated αDG (antibody IIH6, red) and core αDG protein (antibody 5–2, green) with DAPI nuclear counterstain 14 days post-saline or cardiotoxin (CTX). Scale bar, 200μm. White arrows mark some representative fibers with glycosylated αDG. Note, red punctate staining is background from mouse IgM-A546 secondary antibody.

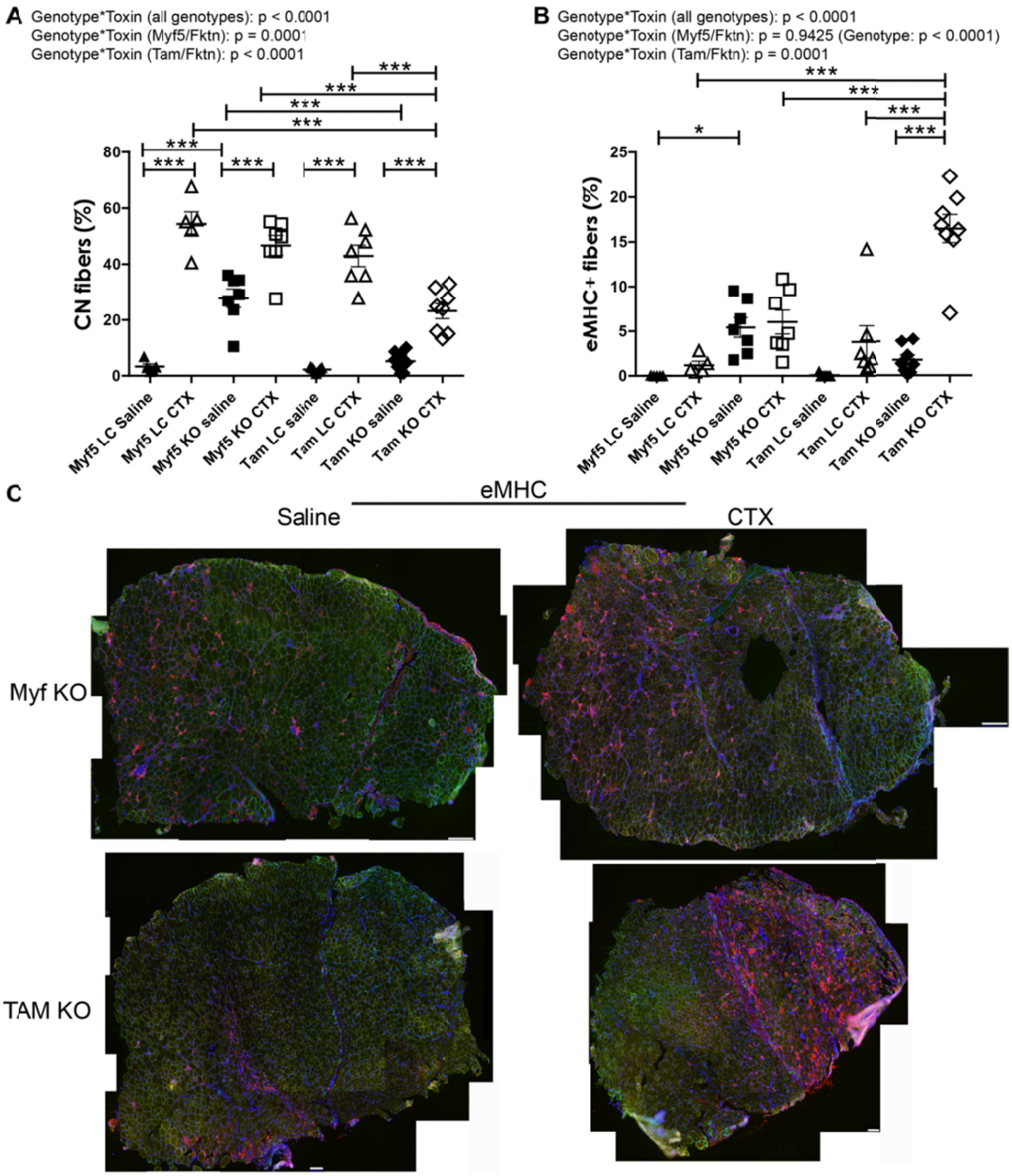

Figure 2.6 Differentiation is delayed in whole-body Tam/Fktn KO mice following cardiotoxin (CTX) induced regeneration. Muscle regeneration measured by long- (CN, (A)) or short-term (eMHC, (B)) markers in muscle specific (Myf5) and whole-body (Tam) Fktn KO and LC mice following intramuscular injection with saline or CTX. *, $p<0.05$; **, $p<0.01$; ***, $p<0.001$; two-way ANOVA with Bonferroni's post-test (all genotypes combined) depicted on figures; two-way ANOVA per strain (Myf5/Fktn or Tam/Fktn) are also reported. (C) Whole tissue maps of tibialis anterior (TA) muscles from Myf5/Fktn or Tam/Fktn KO muscle injected with saline or CTX stained with anti-eMHC antibody (red), with sarcolemmal αDG core protein (green) and nuclear (blue) counterstains. Scale bar = 100 μm. n = 5, Myf5 LC; n = 7, Myf5 KO and Tam LC; n = 8, Tam KO.

in saline Myf5/*Fktn* KO compared to saline Myf5/*Fktn* LC TA muscle, similar to findings in naïve 8 wko TA and iliopsoas muscles (Figure 2.1; Figure 2.6A). In contrast, CN was not different between saline-injected Tam/*Fktn* KO and LC mice and was significantly lower in saline-injected Tam/*Fktn* KO than in Myf5/*Fktn* KO muscle (Figure 2.6A, C). Interestingly, proportions of CN fibers were significantly lower 14 days post-CTX in Tam/*Fktn* KO mice compared to all other CTX-treated groups, suggesting that a potential defect or delay in regeneration/differentiation accompanies whole-body *Fktn* excision (Figure 2.6A, C). This interpretation is supported by the unexpected finding that eMHC in Tam/*Fktn* KO CTX muscle was significantly increased relative to both Tam/*Fktn* KO saline muscle and all other CTX groups 14 days after treatment (Figure 2.6B, C; Tam KO eMHC = 16.5 ± 1.6%; all other groups, mean eMHCs range from 0.0 ± 0.0 to 6.0 ± 1.3%). We previously noted that eMHC positive fiber areas were much smaller in naïve 20 week old Myf5/*Fktn* KO compared to a milder, mature-muscle specific knockout MCK/*Fktn* KO mice and in Myf5/*Fktn* KO versus LC 7 days post toxin-injury (50); therefore, we analyzed the size of eMHC expressing fibers in the 14 day post-toxin Myf5/*Fktn* and Tam/*Fktn* KO mice here. At 14 days post-toxin, regenerating (eMHC+) fibers tended to be very small in both Myf5/*Fktn* and Tam/*Fktn* TAs. However, Myf5/*Fktn* KOs had substantially fewer transiently regenerating fibers at this time point (55-366 fibers, n=7) compared to their Tam/*Fktn* counterparts (337-1840 fibers, n=8) (Figure 2.7). Note, very small eMHC expressing fibers generally do not have central nuclei, so the reduction in Tam/*Fktn* KO CN can be explained, in part, but the high number of small eMHC remaining at 14 days post-toxin in this model. These data suggest that either αDG function in regeneration is dependent on its presence or absence

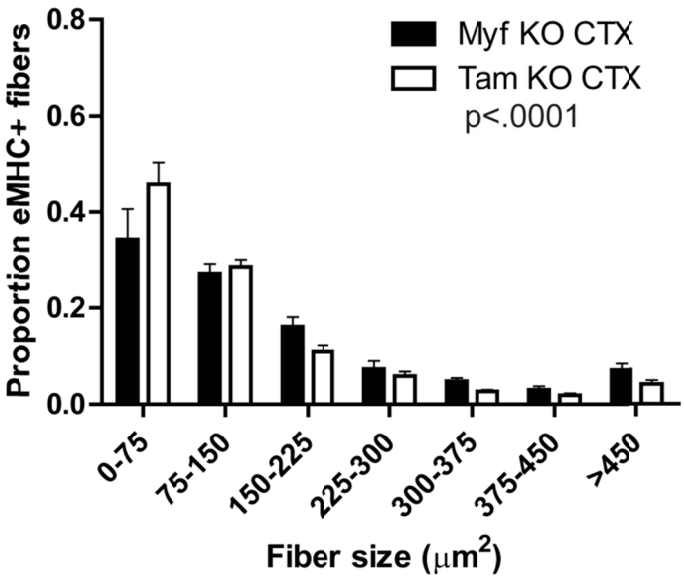

Figure 2.7 Regenerating myofibers are smaller in Tam/Fktn KO mice. Proportions of eMHC-expressing muscle fibers in TAs of Myf5/*Fktn* (black bars) or Tam/*Fktn*(white bars) KO mice 14 days after CTX injection grouped according to size. The number of eMHC-positive muscle fibers ranged from 55–366 in Myf5/*Fktn* (n = 7) and 337–1840 in Tam/*Fktn* KOs (n = 8). $p < .0001$, two-tailed Mann-Whitney test.

during development or that non-muscle αDG, such as brain or motor neuron αDG, is also critical for regeneration or the transition to terminal differentiation in muscle fibers post-injury.

In order to clarify the role of αDG glycosylation in muscle fiber type specification, we examined fiber type distributions in TA muscle of saline- or toxin-injected Tam/*Fktn* and Myf5/*Fktn* mice. There was a genotype*toxin interaction across all genotypes for proportions of type 1 (slow-oxidative) fibers due primarily to a genotype*toxin interaction in Tam/*Fktn* mice (Figure 2.8). Type 2a (fast-oxidative) fibers were subject to genotype*toxin interaction, primarily due to different toxin-induced regenerative responses between Myf5/*Fktn* KO and Tam/*Fktn* KO as detected by statistical post-tests. However, a genotype*toxin interaction and a genotype group effect were detected in independent analyses of Tam/*Fktn* and Myf5/*Fktn* strains, respectively (Figure 2.9), further indicating the possibility of abnormal differentiation of regenerated fibers in whole-body *Fktn* KOs.

Analysis of type 2b fibers revealed substantial variability in the prevalence of this fiber type across all groups; however, there was a significant genotype effect as all Tam/*Fktn* mice had lower means for type 2b than Myf5/*Fktn* mice (including littermates), which may reflect an age dependent type 2b fiber preference between the two strains in the study, with no effect of *Fktn* deficiency (Figure 2.10A). In contrast, a genotype*toxin interaction was detected for type 2x fibers. In post-test comparisons, regeneration after CTX injury decreased the relative frequency of type 2x fibers in all groups (Figure 2.10). The presence of a toxin-induced regeneration effect, but no interaction in independent analyses of Myf5/*Fktn* and Tam/*Fktn* strains, suggests that the overall genotype*toxin

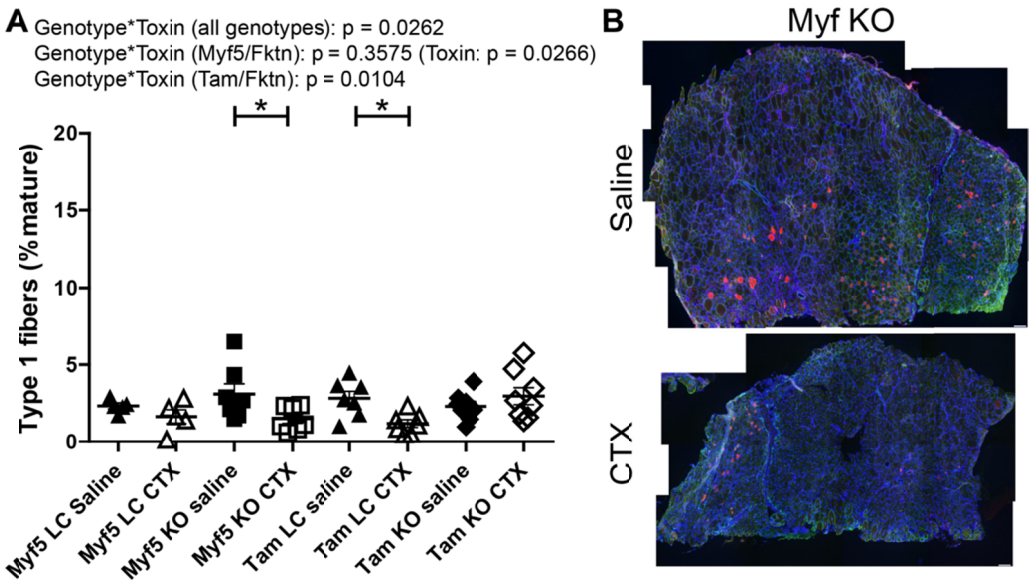

Figure 2.8 Slow oxidative fibers are decreased in Myf5/Fktn KO and Tam/Fktn LC mice following CTX injection. (A) Quantification of slow type 1 oxidative fibers in TA muscle of saline- or CTX-injected Myf5/Fktn and Tam/Fktn LC or KO mice. *, $p<0.05$; **, $p<0.01$; ***, $p<.001$; two-way ANOVA with Bonferroni's post-test (all genotypes combined) depicted on figures; two-way ANOVA per strain (Myf5/Fktn or Tam/Fktn) are also reported. (B) Whole tissue maps of CTX-injected TA muscle stained with anti-myosin heavy chain type 1 antibody (red), with sarcolemmal αDG core protein (green) and nuclear (blue) counterstains. Scale bar = 100 μm. n = 5, Myf5 LC; n = 7, Myf5 KO and Tam LC; n = 8, Tam KO.

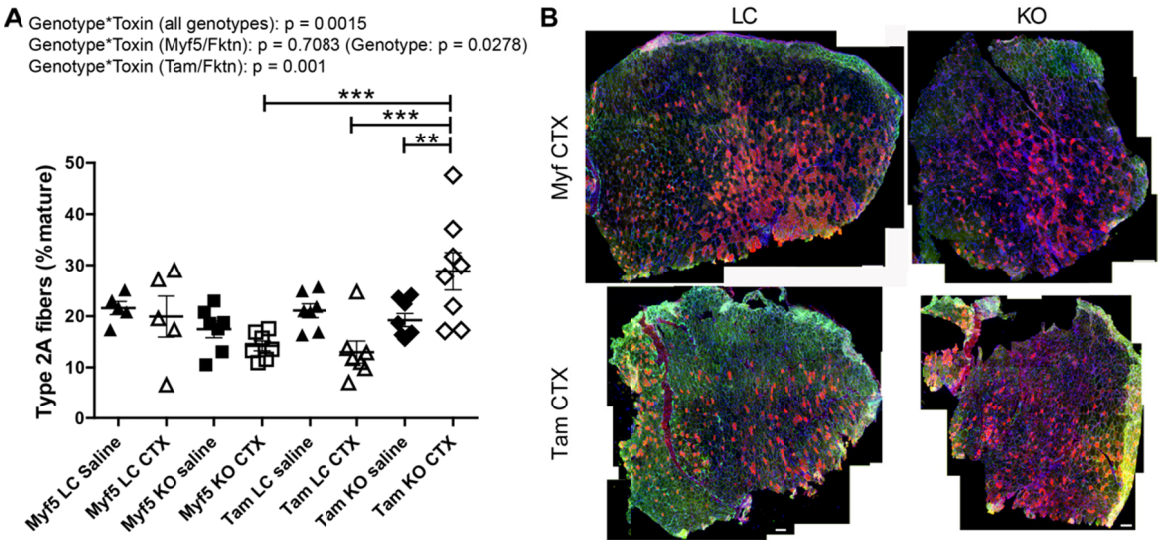

Figure 2.9. Fast oxidative fibers are increased in Tam/Fktn KO mice following CTX injection. (A) Quantification of fast type 2a oxidative fibers in TA muscle of saline- or CTX-injected Myf5/Fktn and Tam/Fktn LC or KO mice. *, $p<0.05$; **, $p<0.01$; ***, $p<.001$; two-way ANOVA with Bonferroni's post-test (all genotypes combined) depicted on figures; two-way ANOVA per strain (Myf5/Fktn or Tam/Fktn) are also reported. (B) Whole tissue maps of CTX-injected TA muscle stained with anti-myosin heavy chain type 2a antibody (red), with sarcolemmal αDG core protein (green) and nuclear (blue) counterstains. Scale bar = 200 μm. n = 5, Myf5 LC; n = 7, Myf5 KO and Tam LC; n = 8, Tam KO.

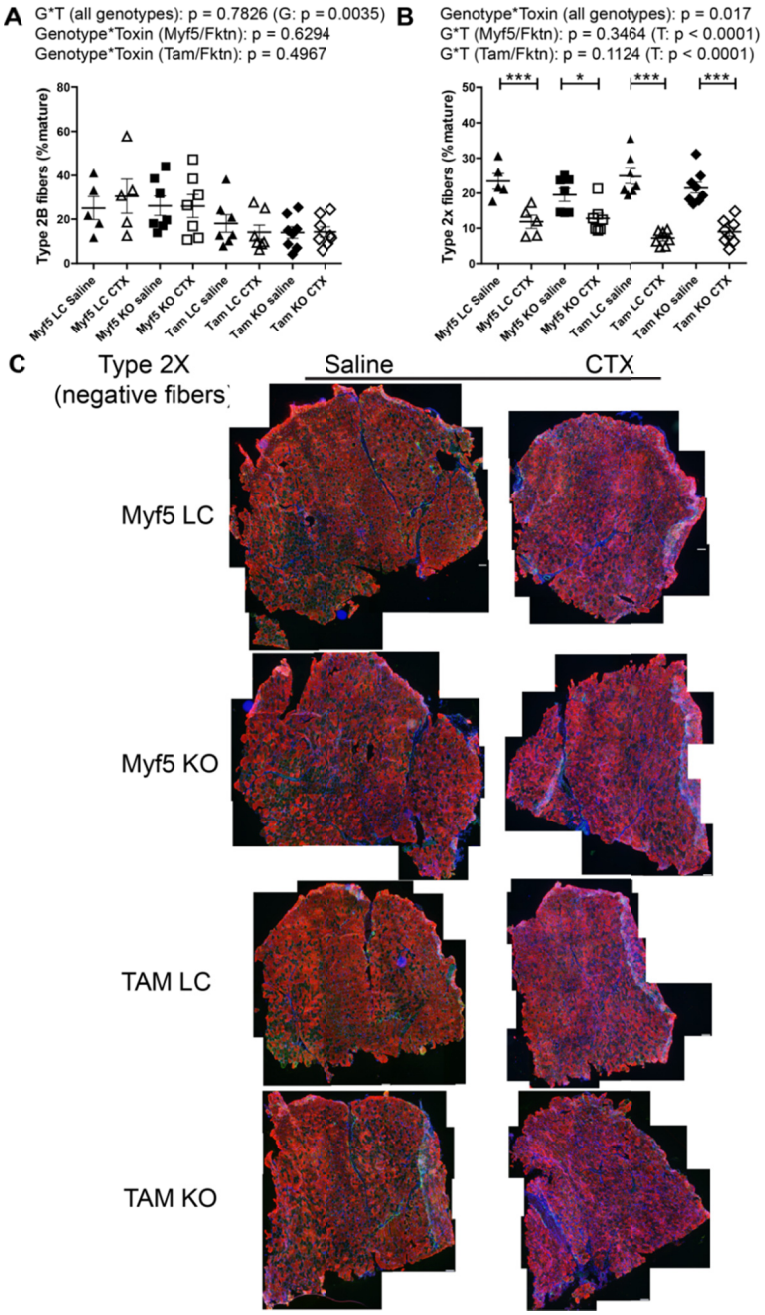

Figure 2.10 Glycolytic type 2x, but not type 2b, fibers decrease following muscle regeneration. Glycolytic type 2b (A) or type 2x (B) fiber proportions in muscle-specific (Myf5) or whole-body (Tam) Fktn¬ KO and LC muscle injected with saline or CTX. *, $p<0.05$; ***, $p<0.001$; two-way ANOVA with Bonferroni's post-test (all genotypes combined) depicted on figures; two-way ANOVA per strain (Myf5/Fktn or Tam/Fktn) are also reported. (C) Whole tissue maps of TA muscle from Myf5/Fktn or Tam/Fktn KO and LC muscle injected with saline or CTX and stained with an antibody detecting all myosin heavy chain isoforms except type 2x. Unstained (negative) fibers were counted to measure type 2x. Scale bar = 100 μm. n = 5, Myf5 LC; n = 7, Myf5 KO and Tam LC; n = 8, Tam KO.

effect (all genotypes) reflects the greater magnitude of type 2x fiber loss in the Tam/*Fktn* cohort compared to the Myf5/*Fktn* cohort, possibly an age rather than a knockout effect. In sum, these results indicate specific roles for functional αDG in the transition from eMHC and in the differentiation to type 1 and 2a fibers in regenerated skeletal muscle after injury; however, the contributions of αDG glycosylation in muscle development versus αDG glycosylation in non-muscle tissues are not fully clear. In particular, loss of *Fktn* in pre-synaptic motor neurons of the neuromuscular junction (NMJ) in Tam/*Fktn*, but not Myf5/*Fktn*, KO mice could affect muscle innervation and regeneration. Therefore, we probed sections from saline- or toxin-injected TAs of Myf5/*Fktn* and Tam/*Fktn* mice with synaptophysin (for detection of the pre-synaptic component of the NMJ) and α-bungarotoxin (BGTX, for detection of nicotinic acetylcholine receptors at the muscle endplate). While full elaboration of the neuromuscular junction morphology cannot be determined from muscle transverse sections, we did measure NMJ occupancy (colocalization of both presynaptic synaptophysin and postsynaptic BGTX). There was no difference in the innervation/occupancy status of NMJs according to genotype*toxin interaction or genotype, although there was a significant toxin effect, apparently due to increased variability and a reduced group mean in injured littermate mice (Figure 2.11).

Discussion

Skeletal muscles exhibit fiber type mosaicism, but myofibrillar phenotype varies considerably between muscles according to muscle use. A growing body of work has shown shifts in fiber type predomination of muscles in various dystrophic conditions, but the underlying mechanism of these changes is not fully understood (174,244,252-254). Decreased muscle function in dystrophic patients and mouse models often involves

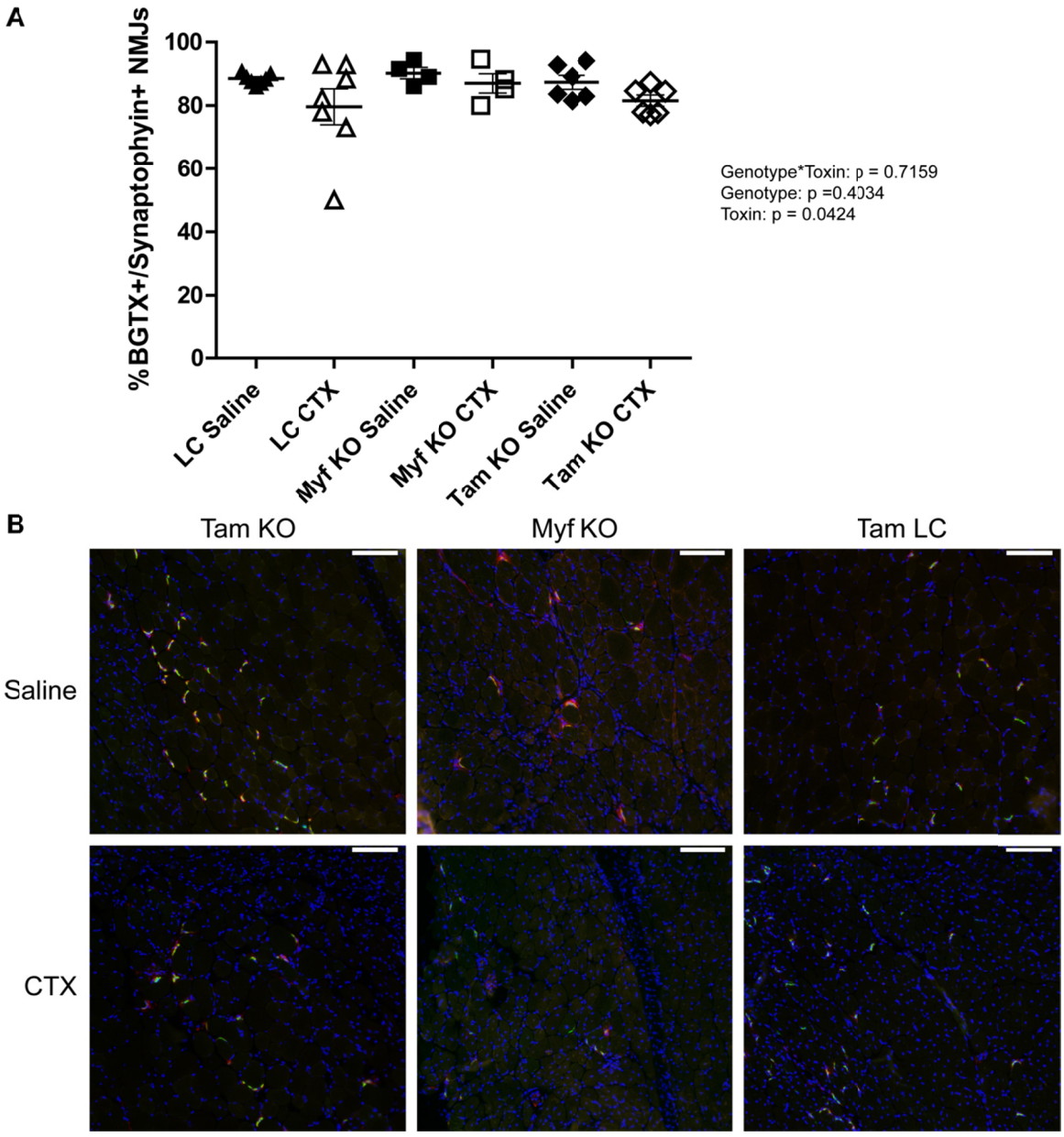

Figure 2.11 Both presynaptic and postsynaptic components are present at neuromuscular junctions in 14 d regenerated muscle of Myf5/Fktn and Tam/Fktn KOs. (A) Proportion of NMJs positive for synaptophysin and BGTX in saline- or CTX-injected TA of Myf5/Fktn and Tam/Fktn KOs or grouped Myf5/Tam LCs. (B) Representative images showing localization of NMJ pre-synaptic (synaptophysin, red) and post-synaptic markers (BGTX, green) in Myf5/Fktn KO and Tam/Fktn KO and LC TAs injected with saline or CTX. Nuclei stained with DAPI (blue). Scale bar = 100μm. n = 7, LC; n = 4, Myf5 KO; n = 6 Tam KO.

components of both muscle weakness and fatigue, so enhanced populations of low-endurance, fast-twitch fiber types may negatively affect performance in dystrophic tissues (255,256), suggesting a protective role for activation of the oxidative myogenic program. However, these observations do not extend to all muscles, as the vastus lateralis of both human DMD patients and GRMD dogs show a reduction of type 2 fibers, suggesting that enhancement oxidative program may actually be deleterious in some muscles (116,173,257).

Despite extensive examination of fiber types in dystrophin-deficient muscle, little work has been done in models of aberrant αDG glycosylation. Analysis of biopsies from rectus femoris or biceps brachii of Fukuyama-type congenital muscular dystrophy patients, whose muscles contain defective *Fktn*, revealed increased type 1 and decreased type 2b fibers in a subset of patients; however, differences in the ages of the patients sampled may have contributed to inter-patient variability with respect to muscle fiber types (258). A study in the *LARGE*$^{myd/myd}$ mouse, a spontaneous mutation model for dystroglycanopathy, found that while both the soleus and EDL muscles were weak in myd mice, the soleus was resistant to force loss following lengthening contraction (172). The soleus had increased β1 integrin, suggesting an increase in the frequency of the other major laminin-binding complex in muscle, α7β1 integrin. However, a clear relationship between fiber type and integrin expression has not been established and it is therefore unclear whether oxidative fiber types, increased integrin content, or a combination of the two protect the soleus from lengthening-contraction induced damage. The low proportion of type 1 fibers in the TA and iliopsoas analyzed here may not reflect fiber dynamics in muscles enriched for slow, oxidative contraction, like the soleus. Overall, it

remains unclear if the altered fiber phenotypes identified here help to drive the disease process or are simply biomarkers of underlying pathogenic or nonpathogenic differences due to altered αDG structural or signaling axis.

In spontaneous models of MD, it is difficult to distinguish the roles of the affected gene in developmental, regenerating, or muscle-extrinsic regulation of fiber type. In particular, dystrophic muscle undergoes cycles of early, highly active and later, slowly progressive disease states as the regenerative capacity of the muscle is exhausted (259,260). To more clearly determine the roles of αDG in muscle regeneration and fiber type specification, we induced widespread regeneration in both muscle-specific (Myf5) and whole body (Tam, inducible) *Fktn* KO muscle. We noted clear differences in the numbers of regenerated fibers (CN) between saline-treated Myf5/*Fktn* and Tam/*Fktn* KO muscle, suggesting that early loss of αDG glycosylation has developmental consequences that may enhance muscle susceptibility to damage. We previously showed that there were more eMHC-positive (regenerating) fibers in 20 week old Myf5/Fktn KO mice compared to a milder, mature muscle MCK/*Fktn* KO model, and that the eMHC-positive fibers were much smaller in both naïve Myf5/*Fktn* versus MCK/*Fktn* KO muscle and in 7 day post-toxin Myf5/*Fktn* KO versus LC muscle. As expected, the proportion of very small regenerating fibers (< 75μm^2) was lower at 14 days in this study versus 7 days post-toxin in Myf5/*Fktn* KOs (~35% 14 days post to ~55% 7 days post) previously reported (15), indicating further growth and maturation of the regenerated muscle fiber pool with the additional time post injury. However, we report the surprising finding that post-development, whole-body inducible Tam/*Fktn* KOs had significantly more eMHC-positive fibers compared to all other toxin injected groups; furthermore, regenerating

fibers in Tam/*Fktn* KOs were significantly smaller than those in Myf5/*Fktn* KOs. Notably, delayed muscle fiber maturation has also been reported in FCMD muscles (133). Thus, while developmental, muscle-specific *Fktn* ablation appears to increase vulnerability to damage, post-developmental, muscle-intrinsic and -extrinsic *Fktn* loss may also lead to defective and/or delayed regeneration. Specifically, differences between Myf5/*Fktn* and Tam/*Fktn* KO mice could be due to the presence/absence of glycosylated αDG in muscle development, the presence/absence of glycosylated αDG in motor neurons, and/or mouse age.

Motor neurons play a significant role in post-developmental fiber specification, but do not appear to dictate fiber type in developing muscle; furthermore, muscle innervation is at least partially responsible for the induction of the slow-fiber program, meaning that the developmental muscle-intrinsic fiber-specification pathway, under normal conditions, favors fast-type fibers (165,261,262). Interestingly, we found that CTX-induced regeneration promoted an increase in the oxidative phenotype in whole-body Tam/*Fktn* KO mice but no change or a decrease in the oxidative phenotype in early Myf5/*Fktn* KO mice. Together, these results suggest that functionally glycosylated αDG may be important in both the presynaptic motor neuron (muscle extrinsic) and postsynaptic muscle (muscle intrinsic) components of muscle regeneration and fiber type determination or that developmental loss of αDG processing impacts the determination of muscle regeneration and subsequent muscle fiber type post-development. Since muscle from both Myf5/*Fktn* and Tam/*Fktn* KO mice are *Fktn*-deficient in skeletal muscle myofibers and satellite cells, it is expected that the muscle intrinsic sensory signaling pathways controlling fiber specification should be comparable. Thus, *Fktn* loss in motor

neurons may affect myosin expression through altered activity, although NMJ occupancy was not different between LC and KO mice. However, there is also evidence that specific myoblast populations formed during development, may favor generation of different fiber types; specifically, satellite cell subpopulations tend to form muscle of predetermined fiber types (165,263,264). Since *Fktn* deletion is initiated at E8 in Myf5/*Fktn* KO mice, muscle progenitors in developing muscle are affected by hypoglycosylation of αDG, representing an alternative explanation for phenotypic differences between Myf5/*Fktn* and Tam/*Fktn* KO mice. It is likely that a combination of αDG-driven developmental and neuronal factors contribute to fiber type specification; however, additional work will be required to clarify such mechanisms.

CHAPTER 3

FOUR-WEEK RAPAMYCIN TREATMENT IMPROVES MUSCULAR DYSTROPHY IN A FUKUTIN-DEFICIENT MOUSE MODEL OF DYSTROGLYCANOPATHY [2]

[2]Foltz SJ, Luan J, Call JA, Patel A, Peissig KB, Fortunato MJ, and Beedle AM (2016) Four-week rapamycin treatment improves muscular dystrophy in a fukutin-deficient mouse model of dystroglycanopathy. *Skeletal Muscle* 6:20, Reprinted here with permission of the publisher, July 19, 2016

Abstract

Background: Secondary dystroglycanopathies are a subset of muscular dystrophy caused by abnormal glycosylation of α-dystroglycan (αDG). Loss of αDG functional glycosylation prevents it from binding to laminin and other extracellular matrix receptors, causing muscular dystrophy. Mutations in a number of genes, including *FKTN* (fukutin), disrupt αDG glycosylation.

Methods: We analyzed conditional *Fktn* knockout (*Fktn* KO) muscle for levels of mTOR signaling pathway proteins by western blot. Two cohorts of Myf5-cre/*Fktn* KO mice were treated with the mTOR inhibitor rapamycin (RAPA) for 4 weeks and evaluated for changes in functional and histopathological features.

Results: Muscle from 17-25 week old fukutin-deficient mice has activated mammalian target of rapamycin (mTOR) signaling. However, in tamoxifen-inducible *Fktn* KO mice, factors related to Akt/mTOR signaling were unchanged before the onset of dystrophic pathology, suggesting that Akt/mTOR signaling pathway abnormalities occur after the onset of disease pathology and are not causative in early dystroglycanopathy development. To determine any pharmacological benefit of targeting mTOR signaling, we administered RAPA daily for 4 weeks to Myf5/*Fktn* KO mice to inhibit mTORC1. RAPA treatment reduced fibrosis, inflammation, activity-induced damage, and central nucleation, and increased muscle fiber size in Myf5/*Fktn* KO mice compared to controls. RAPA-treated KO mice also produced significantly higher torque at the conclusion of dosing.

Conclusion: These findings validate a misregulation of mTOR signaling in dystrophic dystroglycanopathy skeletal muscle and suggest that such signaling molecules may be relevant targets to delay and/or reduce disease burden in dystrophic patients.

Background

The dystrophin-glycoprotein complex (DGC) provides a critical link between the extracellular matrix and the intracellular cytoskeleton to enhance cell membrane stability (8,11,178). α-Dystroglycan (αDG) is an extracellular protein within the DGC that acts as a receptor for laminin and other matrix proteins, but it requires the presence of a rare *O*-mannose glycan structure for this function (11,48,53,54,67,240). Disruption of αDG *O*-mannose glycosylation impairs its laminin binding activity causing a group of diseases known collectively as secondary dystroglycanopathies, which are characterized by progressive muscle pathology along with variable involvement of the brain and eyes (132). To date, mutations in at least 15 genes, including *FKTN*, encoding fukutin, have been identified as causative for secondary dystroglycanopathies (74,79,131,265). Recently, fukutin has been directly implicated in the modification of the core M3 *O*-mannose structure on α-DG as a ribitol-5-phosphate transferase that acts upstream of functional modification by like-acetylglucosaminyl transferase (LARGE) (52). Despite these advances, current therapeutic strategies for dystroglycanopathies are limited, and they remain without treatment or cure.

Disease pathology in DGC-related muscular dystrophies has been attributed to increased susceptibility of the sarcolemma to contraction-induced damage following disruption of αDG-laminin binding, leading to cycles of muscle degeneration and regeneration (178). Dystrophic muscles lose regenerative capacity over time and muscle

fibers are gradually replaced with fibrotic or fatty tissues (259,260,266). However, recent evidence suggests that loss of dystroglycan functional glycosylation induces developmental and regeneration-specific defects that may also contribute to disease severity (50,57,146,182,267).

To date, signaling studies in models of dystroglycanopathy have been limited; however, disruption of αDG-laminin interactions might result in downstream signaling consequences. Antibody-mediated laminin detachment has been shown to dysregulate the serine/threonine kinase Akt (protein kinase B), leading to increased apoptosis in cultured myotubes (209). While best known for its role in cell survival, Akt is also critical for a number of physiological processes in muscle and has been implicated in the progression of dystrophy in dystrophin-deficient mice (210,223,268). Akt is activated through phosphorylation at threonine 308 (T308) by phosphoinositide-dependent kinase 1 (PDK1) and at serine 473 by phosphoinositide-dependent kinase 2 (PDK2). More recently, the elusive PDK2 has been identified as a rapamycin insensitive complex of mammalian target of rapamycin (mTOR), known as mTOR complex 2 (mTORC2) (269). Activation of Akt leads to the downstream activation of mTOR complex 1 (mTORC1), which stimulates muscle growth and hypertrophy through increased protein synthesis (212,213). Interestingly, mTOR inhibition decreased muscle necrosis and effector T cell infiltration in the mdx mouse, a mild model of Duchenne and Becker muscular dystrophies (DMD/BMD) (231). Importantly, muscles from human dystroglycanopathy patients and animal models of disease demonstrate a marked variability in fiber size within a given tissue, often displaying abnormally high populations of both hypertrophic and atrophic cells (50,122). These findings suggest that abnormal regulation of cell

growth pathways may be a factor contributing to disease pathology. Altogether, manipulation of the molecular mechanisms controlling cell growth and viability might offer an avenue towards the amelioration of dystrophic pathology. Indeed, previous studies have indicated the therapeutic benefit of engaging cell survival signaling (224) or modulating cellular processes involved in cell size, including protein synthesis (through mTOR) and autophagy in other types of muscular dystrophy (232,270).

In the present study, we show that 17-25 week old (hereafter, "aged") *Fktn*-deficient dystroglycanopathy mice with later-stage muscular dystrophy have increased activation of mTOR. However, induction of *Fktn* loss post-development (in 6 week old mice) failed to change activation status of signaling proteins involved in the mTOR pathway prior to the onset of muscle pathology, indicating that mTOR activation may be a byproduct of the disease state. To better understand whether this change corresponds to pathogenic or compensatory processes in dystroglycanopathy muscle, we investigated the ability of the mTOR inhibitor rapamycin (RAPA) to alter dystrophic pathology. Daily oral dosing of RAPA from 8 to 12 weeks of age reduced histopathology, including proportions of centrally nucleated (CN) muscle fibers, and protected against increased serum creatine kinase (CK) levels following a damaging downhill treadmill run in Myf5/*Fktn* knockout (KO) mice. Ankle dorsiflexors [tibialis anterior (TA), extensor digitorum longus (EDL), extensor hallucis longus muscles] of RAPA-treated KO mice also produced significantly higher torque post- vs. pre-study, in contrast to untreated KO mice. Immunofluorescent analysis of iliopsoas after completion of the 4-week RAPA study demonstrated mTOR activation (determined by pS6 localization) in both muscle and non-muscle compartments of dystrophic tissue. However, pS6 levels correlated

closely with levels of fibrosis in VEH- but not RAPA-treated KO mice. Biochemical analysis revealed increased levels of proteins involved in autophagosome formation in untreated KO mice which were partially reduced following 4 weeks of RAPA treatment. Overall, our data suggest that manipulations in the mTOR pathway may have potential therapeutic benefit. Future studies will be important to define the best pharmacological agents and molecular targets in the mTOR pathway for skeletal muscle improvements in dystroglycanopathies.

Materials and Methods

Antibodies.

The following primary antibodies used in this study were purchased from commercial suppliers: Rabbit anti-Akt, p-Akt (S473 and T308), S6, p-S6 (S235/236), p-mTOR (S2448), mTOR, Beclin-1, LC3B, GAPDH and mouse anti-S6 from Cell Signaling (Cat# 4691, 4060, 2965, 2217, 4858 or 2211, 5536, 2983, 3738, 2775, 5174, 2317); rabbit anti-Vps15 (A302-571A) from Bethyl Laboratories; rat anti-perlecan from Millipore (MAB1948P); rat anti-CD11b from Fisher (BD Biosciences, BDB550282).; dystrophin (MANDYS16) and embryonic myosin heavy chain (eMHC, F1.652) from the Developmental Studies Hybridoma Bank (DSHB); rabbit anti-collagen VI (ColVI, 70R-CR009x) from Fitzgerald Industries. Antibodies detecting functionally glycosylated αDG (IIH6) and β-dystroglycan protein (βDG, 7D11) have been described previously (11,271) and were a gift from Dr. Kevin Campbell (U. Iowa) or purchased from DSHB. αDG-core antibodies (45-3, 5-2) were reported recently (247). Secondary antibodies conjugated to horseradish peroxidase, or Alexa Fluor® 488 or 546 were purchased from Millipore, Jackson ImmunoResearch, or Life Technologies.

Mice.

All mouse husbandry and experimental procedures were approved by the University of Georgia Institutional Animal Care and Usage Committee under Animal Use Protocols A2010 08-153 and A2013 07-016 (Beedle). Mice were maintained on a 12:12 hour light:dark cycle. Earclips were taken for identification and genotyping. Myf5/*Fktn* conditional KO and Tam/*Fktn* inducible KO mice have been described previously (50,267). Female mice homozygous for LoxP flanked (floxed) *Fktn* exon 2 ($Fktn^{L/L}$) were crossed to male mice heterozygous for the floxed *Fktn* allele and hemizygous for Myf5-driven Cre-recombinase ($Myf5^{Cre/+}$, $Fktn^{L/+}$) to generate developmental skeletal muscle knockout of *Fktn* ($Myf5^{Cre/+}$, $Fktn^{L/L}$, called Myf5/*Fktn* KO). Whole animal Tamoxifen inducible KO mice (driven by the CAGGCre-ER promoter, Jackson Laboratories strain #004682) were generated by crossing $Tg^{Cre\text{-}esr1/+}$, $Fktn^{+/-}$ and floxed *Fktn* ($Fktn^{L/L}$) mice to give $Tg^{Cre\text{-}esr1/+}$, $Fktn^{L/-}$ progeny (Tam iKO). Due to the incorporation of the null allele, tamoxifen-induced cre-recombination is required at only one allele to guarantee *Fktn* loss. Both female and male knockout and littermate mice were used for all studies with no preference or special consideration for sex. All study mice, except for the daily rapamycin dosing study with treadmill endpoint, were fasted for 12 hours (over the light cycle) prior to tissue collection. For mice in the daily rapamycin dosing study with muscle torque endpoint, the fast was started in the evening following muscle torque measurements for euthanization and tissue collection the following morning.

Tamoxifen Dosing.

Tamoxifen (Sigma or Cayman Chemical) was dissolved in 200 proof ethanol and diluted in sunflower seed oil (Sigma) heated to 70°C. Mice were given two 10 mg doses of tamoxifen by gavage two days apart at 6 weeks of age and one additional dose the week of tissue collection. A total of 18 mice were dosed for the study: 9 Tam iKO and 9 Tam littermate control (LC; $Tg^{+/+}$, $Fktn^{L/-}$; $Tg^{+/+}$, $Fktn^{L/+}$; or $Tg^{Cre\text{-}esr1}/^{+}$, $Fktn^{L/+}$).

mTOR Pathway Pharmacological Dosing.

10 mg/ml stock solutions of rapamycin (RAPA, Calbiochem or VWR Scientific) were made in DMSO (Sigma) and stored at -20°C. A working solution of 0.5 mg/ml was made by 1:20 dilution in 0.9% saline. 5% DMSO in 0.9% saline was dosed to vehicle control mice (VEH). Insulin (Sigma) was stored as a 7.5 mg/ml stock in 1% acetic acid and was diluted 1:10 in 0.9% saline to provide a working solution of 0.75 mg/ml (0.1% acetic acid in 0.9% saline was used as the vehicle control). For single dose studies, mice were fasted for a total of 12 hours and given vehicle or insulin by intraperitoneal injection at a dose of 0.1 U/g 30 minutes prior to sacrifice or given vehicle or RAPA (2 mg/kg) by gavage 6 hours prior to dissection. A total of 5 Myf5/*Fktn* KO mice were dosed with vehicle, 5 with rapamycin, and 6 with insulin. A total of 4 littermates were dosed with vehicle, 5 with rapamycin, and 6 with insulin.

Daily study mice were administered vehicle (VEH LC or KO) or 2 mg/kg RAPA (RAPA LC or KO) by oral gavage once a day for 4 weeks. In the first daily dosing study (with muscle torque endpoint), 5 mice were used in each group. In the second daily study (with treadmill endpoint), 8 and 7 Myf5/*Fktn* KO mice were dosed with RAPA and vehicle, respectively; and 6 RAPA-treated and 6 vehicle-treated littermate controls (LC;

Myf5$^{Cre/+}$,*Fktn*$^{L/+}$; *Myf5*$^{+/+}$,*Fktn*$^{L/L}$ or *Myf5*$^{+/+}$,*Fktn*$^{L/+}$) were used. One RAPA KO met statistical criterion for exclusion and was therefore not included in the final dataset (see statistics).

Physiological Measurements.

Mice in the daily rapamycin treatment study were analyzed for serum creatine kinase levels before and after a downhill exhaustion treadmill run. Mice were equilibrated to a 4-lane mouse treadmill (Accuscan) at a -10° angle for two 30 min session (25 min at 0m/min, 5 min at 3m/min) on days 1 and 2 after the last RAPA or VEH dose. Blood was collected from the ventral tail artery of study mice after the second equilibration session ("Pre-exhaustion bleed"). On the third day post-dosing, mice were run using the downhill exhaustion protocol (warm-up: 5 min at 3m/min; downhill exhaustion run: 5 min at 10m/min, 5 min at 15m/min, 5 min at 20m/min, and up to 15 min at 25m/min)(50). When mice remained on the shock pad for 10 consecutive seconds, exhaustion time was recorded and mice were removed from the treadmill. Treadmill run distances for Myf5/*Fktn* KO mice are reported as a normalized comparison to distances of cage- and/or age-matched LC mice running a simultaneous exhaustion protocol. Two hours after the run end, a post-treadmill blood sample was collected and mice were sacrificed for tissue collection. For creatine kinase measurements, serum was diluted 1:10 in ultrapure water and added to creatine kinase reagent (StanBio) according to manufacturer's protocol. The resulting mixture was assayed for CK activity using a Synergy 2 microplate reader (BioTek Instruments).

Torque was measured from the ankle dorsiflexors of mice as previously described (272,273). Mice were anesthetized with 1.5% isoflurane mixed oxygen, hair was

removed from the left lower hindlimb, and the foot was attached to a servomotor for torque measurement (Aurora Scientific, Aurora Canada). Muscle contraction was stimulated using Pt-Ir needle electrodes inserted percutaneously adjacent to the peroneal nerve using 1 to 2mA (stimulator Model 701C, Aurora Scientific). Isometric torque was measured in response to 20, 40, 60, 80, 100, 125, 150, and 200Hz of stimulation frequency. Each mouse in the RAPA daily study with muscle torque testing underwent two separate muscle torque exams, one prior to the onset of RAPA or VEH dosing (the "pre" test) and one on the day following the 28^{th} RAPA or VEH dose (the "post" test). Torque measurements were normalized to body mass (in kg) for each mouse to account for size differences between animals.

Kidney and Liver toxicity measurements.

Blood urea nitrogen (BUN) and serum alanine transaminase (ALT) were assayed using kits purchased from Arbor Assays and Cayman Chemicals, respectively. For BUN, serum was diluted 1:20 in ultrapure H_2O and analyzed by colorimetry according to manufacturer's protocol on a Spectramax microplate reader using Softmax Pro 5.3 software (Molecular devices). ALT was detected in serum diluted 1:10 in ultrapure H_2O via consumption of NADH in a coupled reaction. Absorbance measurements were taken at 340 nm (Synergy 2 microplate reader) every minute for 5 minutes and the average rate of change across a linear range was used to quantitate ALT.

Succinate dehydrogenase measurement.

TA muscles were homogenized on ice with a glass on glass dounce homogenizer in 2ml of 33mM PO_4^{3-} buffer. Samples were aliquoted and taken through three cycles of freezing and thawing before use. A method for spectrophotometric determination of

succinate dehydrogenase (274) was adapted for the microplate. Triplicate 4 or 8 µl volumes of tissue homogenate were incubated with 10 µl of 0.5 M sodium succinate for 2 minutes at 30°C. 10 µl of sodium cyanide was mixed into samples followed by 300 µl cytochrome C working reagent (0.1 M cytochrome C from equine heart in 0.17 M PO_4^{3-} buffer, 0.004 M $AlCl_3/CaCl_2$, and H_2O mixed 2.5:1:7.5) immediately prior to reading (Spectramax microplate reader). Reduction of cytochrome C was assessed by kinetic absorbance measurements at 550 nm. Data are presented as µmol cytochrome c reduced/minute/mg tissue mass.

Histology and Microscopy.

Seven-micron tissue cryosections were stained by hematoxylin and eosin (H&E) according to standard protocols. Sections were processed for secondary immunofluorescence (IF) as described previously (50,246,267). H&E or immunofluorescent stained skeletal muscle sections were imaged using an X71 inverted epifluorescent microscope with a Peltier element-cooled 12.8MP DP72 CCD camera and CellSens software (Olympus).

For analysis of eMHC, αDG glycosylation (IIH6) and central nucleation, tiled 20X images were taken across each entire muscle section and aligned to compile entire section maps in Photoshop (Adobe), then positive and negative fibers were counted manually using ImagePro Express (MediaCybernetics). Data are reported as percentages obtained by dividing the number of positive fibers by the total number of muscle fibers in an entire muscle section. Tissue maps from this analysis were also used for measurement of muscle fiber minimum diameter. Perimeters of individual muscle fibers were traced in a semi-automated fashion using a combination of manual segmentation (dark objects) and

manual polygon selection in ImagePro Premier v9.1 (Media Cybernetics), which calculated minimum diameter according to a reference distance (scale bar). Area values were sorted according to size, grouped into bins of 2.5μm (estimated from the formula $h = \frac{3.5\sigma}{n^{1/3}}$, where h is optimized bin size, σ is the standard deviation, and n is the number of observations), up to a maximum of 30 μm and plotted as a histogram. Analyses were performed blinded to experimental group and study design.

Sections incubated with anti-collagen VI, anti-CD11b, or anti-pS6 were imaged and mapped as above. Whole section maps were analyzed for fluorescent area using Fiji (Image J, (275)) software. Briefly, a region of interest was drawn to encircle the entire muscle section. The number of pixels/section was quantified and a color threshold was set. Pixels at brightness above the color threshold were considered positive for collagen VI, CD11b or pS6; these pixels were selected and counted. Data are expressed proportion of area, which is the number of positive pixels/total number of pixels in the section for each map.

Western Blotting.

Pooled hindlimb muscles (soleus, gastrocnemius, tibialis anterior [TA], hamstring, quadriceps, gluteus); or isolated quadriceps from individual mice were homogenized and solubilized in buffer containing 50 mM Tris (pH7.4), 150 mM NaCl, 1% Triton-X, and a homemade cocktail of phosphatase and protease inhibitors: pepstatin A, 0.6μg/ml; aprotinin, 0.5μg/ml; leupeptin, 0.5μg/ml; phenylmethanesufonylfluoride, 0.1mM; benzamidine, 0.75mM; calpain I inhibitor, 2μM; calpeptin, 2μM; NaF, 50mM; $NaPP_i$, 10mM; β-glycerophosphate, 10mM . Initial studies included $NaVO_4$ for inhibition of tyrosine and alkaline phosphatases. However, there was marked sample

precipitation over time, so $NaVO_4$ was excluded from all samples reported here. Insoluble material was pelleted at 142,000xg for removal and the resulting supernatant was filtered through cheesecloth. Protein concentrations were determined using a modified DC protein assay (Bio-Rad) with a SpectraMax microplate reader (Molecular Devices).

Solubilized skeletal muscle protein samples (500µg) were loaded onto 3-15% gradient gels for SDS-PAGE. Protein was transferred to PVDF (Millipore), blocked with 1% milk in Tris buffered saline with 0.1% Tween-20 (TBS-T), and probed with primary antibody overnight, as described previously (50,246). Secondary antibodies conjugated to horseradish peroxidase were used and blots were imaged with West Pico or West Dura chemiluminescent reagent (Pierce) and the Fluorchem HD2 digital imager (Protein Simple). All study mice (n=4-8 per group) from each group were tested by western blot with a minimum of two technical replicates. One sample (VEH LC) in the daily RAPA dosing study was unfit for analysis by western blot and was excluded from those data sets.

Cytokine/Chemokine Multiplex Assay.

Transforming growth factor-β (TGF-β, TGFBMAG-64K-01) or mouse cytokine/chemokine (MCYTOMAG-70k: interleukin-1β, monocyte chemotactic protein-1, and tumor necrosis factor-α) magnetic bead kits were purchased from Millipore for analysis via the Luminex xMAP platform. Solubilized protein (50µg) or diluted serum samples (1:30, TGF-β; 1:4 cytokine/chemokine multiplex) were loaded onto a pre-wet 96-well plate and incubated with antibody-conjugated magnetic beads overnight at 4°C. Beads were pelleted using a handheld magnet, samples were decanted, and pelleted beads

were resuspended in the presence of biotinylated detection antibodies. Finally, the beads were treated with streptavidin-conjugated phycoerythrin and imaged with the MAGPIX (Luminexcorp) using xPonent 4.2 software. Median fluorescent intensity (MFI) for each sample was normalized as fold increase over background MFI.

Graphing, Data Analysis, and Statistics.

Band densitometry for western blot was measured using AlphaView 3.0 software (Protein Simple). Band intensities of a given blot were set as a proportion of the maximum intensity (equal to 1), and these values for the protein of interest were normalized to the corresponding value of the total protein content for phospho-epitopes of signaling proteins or to loading control (GAPDH) for all others.

Data are plotted as scatter plots (each individual data point represents one study mouse) with the group mean and standard error of the mean using Prism 5 (GraphPad). As a number of plots contained possible outlier samples, a Dixon's q-test (276,277) was applied to every data set with a critical value of α=.05 to identify true outliers. A number of datasets contained an outlier in one of the study groups. For the most part, the individual outlier mouse was not consistently an outlier across datasets; therefore no action was taken in these cases. However, one mouse in the daily dosing study was a clear outlier in the majority of its datasets. Therefore, this mouse was excluded from reported data. Differences between study groups were determined by two-tailed Student's *t*-test or two-way analysis of variance (ANOVA) with Bonferroni's post-test in Prism 5. The interaction (e.g. Drug*Genotype) p-value from two-way ANOVA analysis is reported on all figures and individual main effects (e.g. Drug, Genotype) are reported only in the absence of a significant interaction between variables. Statistical significance

between groups is denoted by *, p<.05; **, p<.01; ***, p<.001. A significant difference between one group and two or more other groups is represented on plots by a line originating from the first group, with downward ticks indicating each group from which it differed. Asterisks above downward ticks indicate significance level. Fiber size distributions were compared by two-way ANOVA at each bin size (Prism 5, GraphPad). A significant interaction (Drug*Genotype $p<0.05$) is marked by * and a significant genotype ($p<0.05$) effect is marked by †. Correlations were determined by Pearson (Gaussian) or Spearman (non-parametric) tests.

Results

The Akt/mTOR signaling axis is altered in dystroglycanopathy muscle.

Abnormal intracellular signaling has been reported in various forms of muscular dystrophy, including other DGC-related diseases (reviewed in (278)), but not in dystroglycanopathy. To determine whether Akt/mTOR signaling is altered in dystroglycanopathy mice, we examined the activation status of pathway proteins in fasted Myf5/*Fktn* KO muscle from mice aged 17-25 weeks, an age range with substantive remodeling of the muscle compartment. Myf5/*Fktn* KO mice were selected for study because 1) *Fktn*-deficiency is the most common form of congenital dystroglycanopathy; 2) this conditional knockout model bypasses embryonic lethality associated with total *Fktn* loss; and 3) *Fktn* excision is initiated during muscle development causing moderate to severe dystroglycanopathy, similar to the phenotypic spectrum observed in human patients. As expected, Myf5/*Fktn* KO mice had significantly less functional αDG glycosylation in solubilized hindlimb skeletal muscle than age-matched LC mice (Figure 3.1A). Akt activation status was not different in Myf5/*Fktn* KO compared to LC mice

using either T308 or S473 normalized to total Akt protein (Figure 3.1 A, B). In contrast, the activated pool of mTOR, the kinase subunit of mTORC1 and mTORC2 was increased (phospho-S2448/total mTOR) (Figure 3.1A, B). mTOR serine 2448 is phosphorylated in a feedback loop by mTORC1 substrate S6 kinase 1 (279,280), indicating elevated mTORC1 activity in the skeletal muscle of Myf5/*Fktn* KO compared to LC. Despite this indication of elevated S6 kinase activity, phosphorylation of its downstream target, translation initiator ribosomal protein S6, was not significantly increased in Myf5/*Fktn* KO vs. LC mice relative to total S6 protein although total S6 protein was elevated (Figure 3.1A, B; Figure 3.2). The considerable variability in expression of Akt and S6 proteins in Myf5/*Fktn* KO mice (Figure 3.2) may reflect differences in the severity of muscular dystrophy within the aged knockout cohort. Therefore, the iliopsoas muscle was examined histologically for inter-individual disease pathology. The iliopsoas was chosen because it is a proximal muscle more severely affected in Myf5/*Fktn* KO mice and has a relatively small cross-sectional area with less intra-section variability in pathology. As expected, there was extensive fibrosis (increased collagen VI, ColVI) and variation in muscle fiber size in iliopsoas muscles of the aged Myf5/*Fktn* KO mice, but dystrophy in some mice was more severe than in others (Figure 3.1C, D). When total S6 protein expression was plotted versus ColVI fibrosis for individual Myf5/*Fktn* KO study mice, there was a significant positive correlation (Pearson r=.8147, Figure 3.1D). Therefore, some variation in cellular signaling pathways may be explained by a loss of muscle fibers and/or an increase in the fibrotic content of the muscle compartment in late-stage dystrophic Myf5/*Fktn* KO animals.

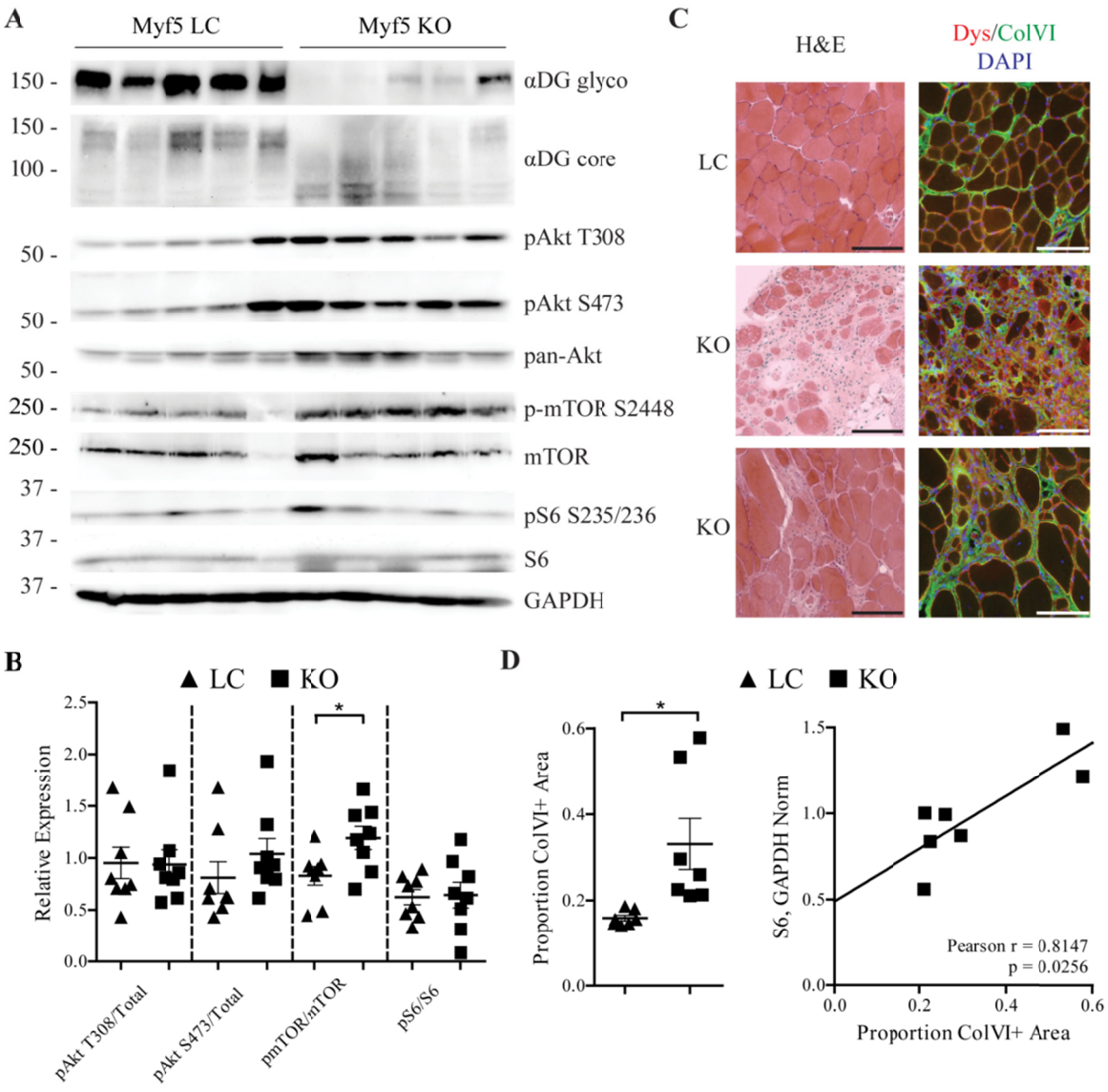

Figure 3.1 mTOR is activated in aged, fasted Myf5/*Fktn* KO muscle. (A) Western blot analysis of solubilized protein from hindlimb muscle of Myf5/*Fktn* LC and KO mice. (B) Quantification of Akt phosphorylation at T308 and S473, mTOR phosphorylation at S2448, S6 phosphorylation at S235/236, relative to total Akt, mTOR, and S6 protein, respectively, as a measure of protein activation. mTOR phosphorylation at S2448 normalized to total mTOR is significantly increased in KO muscle. Two-tailed Student's t-test; *, $p<0.05$. (C) Representative images of iliopsoas muscle from aged LC or KO mice. H&E staining and dystrophin (red), ColVI (green), DAPI (blue) immunofluorescence are shown. Scale bar =100μm. (D, Left) Quantification of ColVI in iliopsoas of aged mice reveals significantly increased collagen content in KO muscle. Two-tailed Student's t-test; *, $p<0.05$. (D, Right) Total S6 protein correlates with ColVI quantity in KO muscle (Pearson r=0.8147; p=0.0256). n=8 Myf5/*Fktn* LC and 8 Myf5/*Fktn* KO mice (n=7 per group for ColVI analysis due to tissue artifacts).

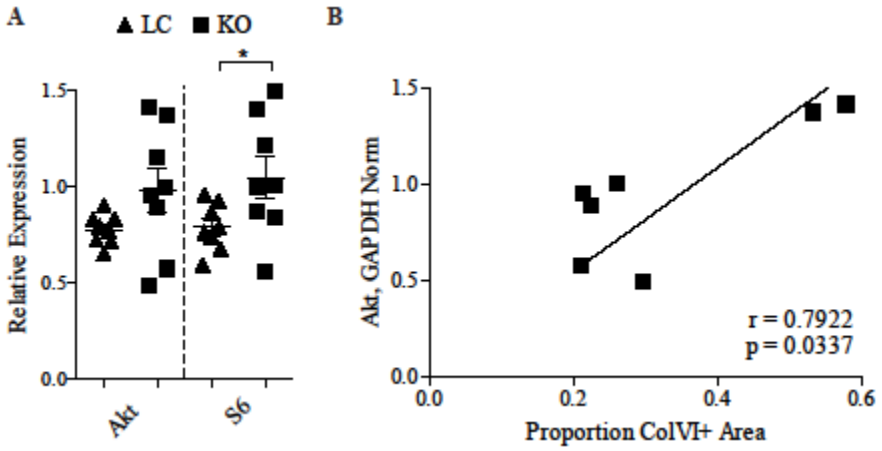

Figure 3.2 Akt/S6 protein expression in later-stage dystroglycanopathy muscle. (A) Quantification of Akt or S6 protein expression in 17-25 week old Myf5/*Fktn* LC and KO mice. Two-tailed Student's t-test. *, $p<0.05$. (B) Akt expression has a significant correlation with the proportion of ColVI+ area in KO muscle (Pearson $r = 0.7922$, $p=0.0337$). n=8 Myf5/*Fktn* LC and 8 Myf5/*Fktn* KO mice (n=7 per group for ColVI analysis due to tissue artifacts)

To determine whether abnormal activation of mTOR in KO muscle is due to a change in its ability to integrate input from external ligands, we probed the pathway by acute activation with insulin in Myf5/*Fktn* KO and LC mice. Twelve week old mice were chosen because muscle fibers populate a relatively larger proportion of the tissue compartment in Myf5/*Fktn* KO muscle at this time point. Animals were fasted for a total of 12 hours and treated with an insulin challenge or vehicle in the last 30 min. The dystroglycan glycosylation deficiency was confirmed in KO mice and S6 ribosomal protein activation was tested by western blot as a downstream readout of mTORC1 activity. Insulin significantly induced activation of S6, the target of mTORC1 substrate S6 kinase. Phosphorylation at S235/236 relative to S6 protein was increased in both LC (3.84±1.26-fold) and KO muscle (3.07±0.75-fold) (two-way ANOVA, drug effect p=0.0255). To assess basal levels of mTORC1 activity at this age, a separate cohort of mice was dosed with mTOR inhibitor rapamycin (RAPA) or vehicle 6 hours before muscle collection. RAPA reduced the ratio of S6 phosphorylation to S6 protein in fasted littermates (4.71 ± 2.40-fold) and Myf5/*Fktn* KO (7.24 ± 3.55-fold) compared to time-matched vehicle controls (two-way ANOVA drug p=0.0147). These results demonstrate that mTORC1 retains the capacity to respond to acute activation or inhibition in Myf5/*Fktn* KO mice.

mTOR activation is not coincident with loss of functional αDG glycosylation.

Although our results indicate misregulation of mTOR signaling in Myf5/*Fktn* KO mice, it is unclear whether this finding results directly from improper glycosylation of αDG or from the progressive dystrophic process. For example, changes in mTOR signaling could arise from any of these possibilities: first, loss of αDG binding to laminin

could change the activation status of signaling molecules to directly effect pathway changes identified here (e.g. (209)). Second, mTOR signaling could be initiated by disease processes contributing to the pathological progression, including muscle regeneration (223,268,281), differentiation and growth of replacement fibers (213,282-284), or fibrosis (285,286). Finally, mTOR pathway activation could be a compensatory adaptation by the muscle to mitigate damage burden on the tissue.

To address the first possibility, we employed the whole-body inducible *Fktn*-KO (iKO) mouse to induce *Fktn* exon 2 deletion and subsequent deficiency in αDG glycosylation post-development, a model we reported previously to have a reduction of αDG glycosylation as early as 2.5 weeks and evidence of muscle damage by 8 to 10 weeks post-tamoxifen (50). Adult mice were dosed with tamoxifen and euthanized (fasted) 5 weeks later to ensure that αDG glycosylation was disrupted, but dystrophic pathology was not yet present. Iliopsoas of tamoxifen-treated iKO mice (Tam iKO) were histologically normal but showed reduced immunoreactivity to IIH6 antibody against the glycosylated epitope of αDG (Figure 3.3A); furthermore, decreased αDG glycosylation and a shift to lower molecular weight αDG protein was confirmed by western blot (Figure 3.3B). Analysis of Akt, mTOR and S6 activation revealed no significant differences between Tam LC and Tam iKO mice (Figure 3.3B,C) suggesting that abnormal mTOR signaling is not a direct consequence of αDG hypoglycosylation.

4-Week daily mTORC1 inhibition improves disease features in dystroglycanopathy mice. These data indicate that mTOR activation in aged Myf5/*Fktn* KO is likely related to the dystrophic phenotype but do not distinguish between potential pathogenic or protective roles for this signal. Although previous studies have demonstrated the ability of

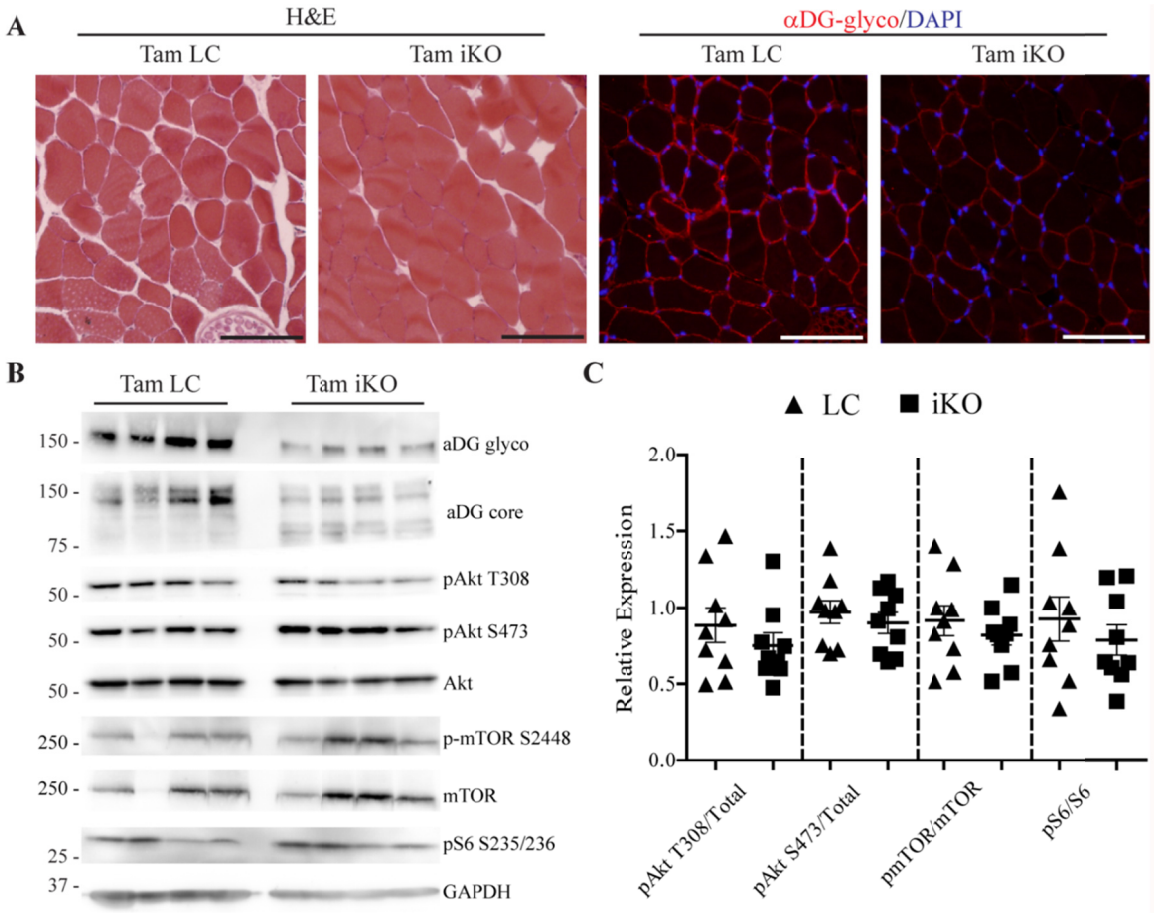

Figure 3.3 Akt/mTOR signaling is unchanged following loss of αDG glycosylation. (A) Representative images of littermate (Tam LC) or inducible knockout (Tam iKO) iliopsoas. H&E and αDG glyco images are shown. Scale bar = 100μm. (B) Western blot analysis of solubilized skeletal muscle from hindlimbs of Tam LC or Tam iKO mice. (C) Quantification of Akt phosphorylation at T308 and S473, mTOR phosphorylation at S2448, and S6 phosphorylation at S235/236 relative to total Akt, mTOR, and S6 protein, respectively, as a measure of protein activation. Data are presented as mean ± SEM. n=9 per group.

rapamycin to reduce the dystrophic phenotype in some models of muscular dystrophy, complete ablation of mTORC1 signaling through knockout of raptor, an obligate member of mTORC1, leads to a dystrophic phenotype in mice (225,231,232). This might indicate that mTORC1 signaling is necessary for the maintenance of normal skeletal muscle, but becomes pathogenic under disease conditions. To test whether mTORC1 signaling contributes to pathology in Myf5/*Fktn* KO mice, 8 week old KO and LC mice were dosed with 2 mg/kg RAPA or vehicle control (VEH) daily for 4 weeks by oral gavage. Although RAPA is approved for clinical use, adverse effects including nephrotoxicity and hepatotoxicity have been reported (287). To determine whether 4-week daily RAPA treatment induced damage to the kidneys or liver, we evaluated blood urea nitrogen (BUN) and serum alanine transaminase (ALT) levels in study mice during the final week of dosing. No effect of RAPA treatment was observed for either analyte: BUN (mg/dL) = 22.39±2.979, VEH LC; 20.37±2.698, RAPA LC; 17.50±3.70, VEH KO; 22.10±2.88, RAPA KO (two-way ANOVA, drug p=0.6812) and ALT (U/L) = 75.73±38.51, VEH LC; 66.30±21.52, RAPA LC; 86.84±36.78, VEH KO; 40.94±13.83, RAPA KO (two-way ANOVA, drug p=0.3552). Therefore, we have no evidence of treatment-related toxicity in the 4 week 2 mg/kg RAPA dosing regimen to dystroglycanopathy mice.

We employed 2 separate study designs to enable analysis of distinct functional outcomes: in the first study, we obtained *in vivo* torque measurements from ankle dorsiflexors prior to and at completion of the dosing regimen, and isolated single, fasted muscles for biochemical analysis. In the second study, tail vein blood was collected for determination of serum CK from study mice before and after a downhill treadmill run to exhaustion. Isometric torque measurements were taken across a spectrum of stimulation

frequencies (5, 10, 20, 40, 80, 100, 150, 200 Hz) in order to evaluate contractile ability while still simulating physiologic contraction, which occurs in rodents between 60 and 100 Hz (288). Data are plotted as a force-frequency curve to provide direct measurement of the frequency-dependence of tetanic contraction and the maximal torque, which is an indirect measure of maximal muscle force. Assessment of resultant force-frequency curves demonstrated an age-related improvement in dorsiflexor torque (Pre vs. Post) of VEH LC mice that was absent in VEH KO mice, indicating that Myf5/*Fktn* KO mice do not experience muscle strength improvements typical with maturation to adulthood (Figure 3.4A). In contrast, there was a significant interaction between frequency and time (Pre vs. Post) for both RAPA-treated LC and KO mice demonstrating robust gains in isometric torque at several stimulation frequencies (i.e., 150-200Hz in RAPA LC and 80-200Hz in RAPA KO) (Figure 3.4A). Maximal torque of LC and KO mice receiving RAPA improved by 14.02 ± 4.68 and 14.32 ± 3.66 N*mm/kg body mass, respectively, compared to a modest increase in VEH LC (7.92 ± 3.61) and highly variable changes in VEH KO mice (6.97 ± 12.10 S.E.M.). In the second cohort, 4-week RAPA treatment significantly increased treadmill run distances of Myf5/*Fktn* KO mice normalized to age- and trial-matched LC mice, corroborating the functional improvement seen via muscle force testing (Figure 3.4B).

CK values, indicating the presence of muscle damage, were also notably different between RAPA and VEH KO mice. First, basal serum CK (pre-treadmill) in VEH KO mice was not statistically different from LC mice (Figure 3.4C), a finding consistent with our previous work demonstrating elevated serum CK levels only in young Myf5/*Fktn* KO mice (50). This can be explained by the gradual replacement of CK-containing muscle

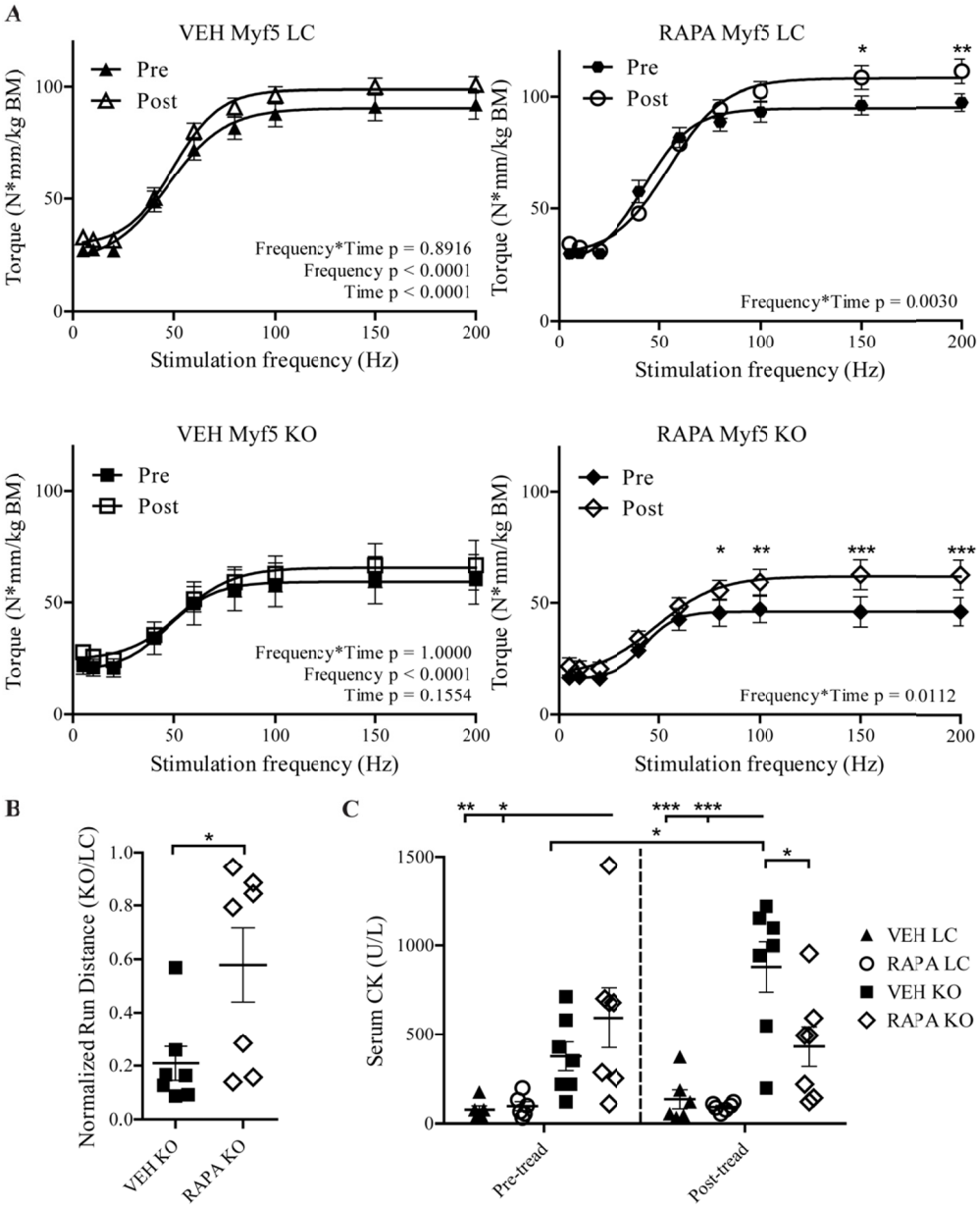

Figure 3.4 Four week daily RAPA treatment improves functional outcomes in Myf5/*Fktn* KO mice. (A) Force-frequency curves showing *in vivo* force measurements taken from tibialis anterior muscles of daily RAPA study mice prior to and at completion of RAPA or VEH dosing. Two-way repeated measures ANOVA with Bonferroni's post-test. *, $p<0.05$; **$p<0.01$; ***$p<0.001$. n=5 mice per group. (B) Comparison of downhill treadmill distances run by VEH and RAPA KO mice. Data are presented as the proportion of KO distance normalized to respective age- and treatment-matched LC mice from the same treadmill run. Two-tailed Student's t-test. *, $p<0.05$. n=7 mice per group. (C) Serum creatine kinase analysis of tail vein bleeds taken from daily RAPA study mice at the end of dosing (left, Pre-tread) or 2 hours after a downhill run to exhaustion (right, Post-tread). Two-way ANOVA with Bonferroni's post-test of all pairs. *, $p<0.05$; **, $p<0.01$; ***, $p<0.001$. n=6, VEH and RAPA LC; n=7, VEH and RAPA KO.

fibers with fibrotic tissue during disease progression, meaning that fewer muscle fibers are available to leak CK to the serum in older mice. However, basal serum CK was increased in RAPA KO mice (Figure 3.4C), suggesting a RAPA-induced delay in Myf5/*Fktn* KO pathology. Importantly, serum CK was significantly increased over basal levels by a downhill exhaustion run in VEH, but not RAPA, KO mice, suggesting that 4 week daily RAPA treatment was protective against muscle injury in Myf5/*Fktn* KO mice (Figure 3.4C).

If muscle injury were indeed reduced in RAPA KO mice, regenerative markers might likewise be decreased since regeneration in dystrophic muscle indicates prior degeneration. To evaluate cumulative regeneration across the timeline of the dosing study, we analyzed central nucleation (CN), which persists for several weeks to months following a regeneration event, in muscle fibers of the iliopsoas (289). RAPA KO mice had significantly fewer centrally nucleated fibers compared to VEH KO mice (Figure 3.5A, B). However, this could signify either that RAPA treatment reduces muscle damage or that it inhibits subsequent regeneration. To clarify this point, we assessed levels of embryonic myosin heavy chain (eMHC)-positive fibers, which transiently mark regeneration, in iliopsoas of RAPA-study mice. eMHC-positive fibers were unchanged between VEH and RAPA KO iliopsoas and were increased compared to drug-matched LC iliopsoas (two-way ANOVA, drug $p=0.9917$, genotype $p=0.0002$) (Figure 3.5A, B). Together, these results indicate that muscles in RAPA KO mice retain regenerative capacity in the short term, and support a myoprotective effect of RAPA treatment.

Fktn-deficient dystrophic muscle exhibits notable fiber size variability populated by an abundance of both small, atrophic fibers and larger, hypertrophic fibers. Since mTOR is

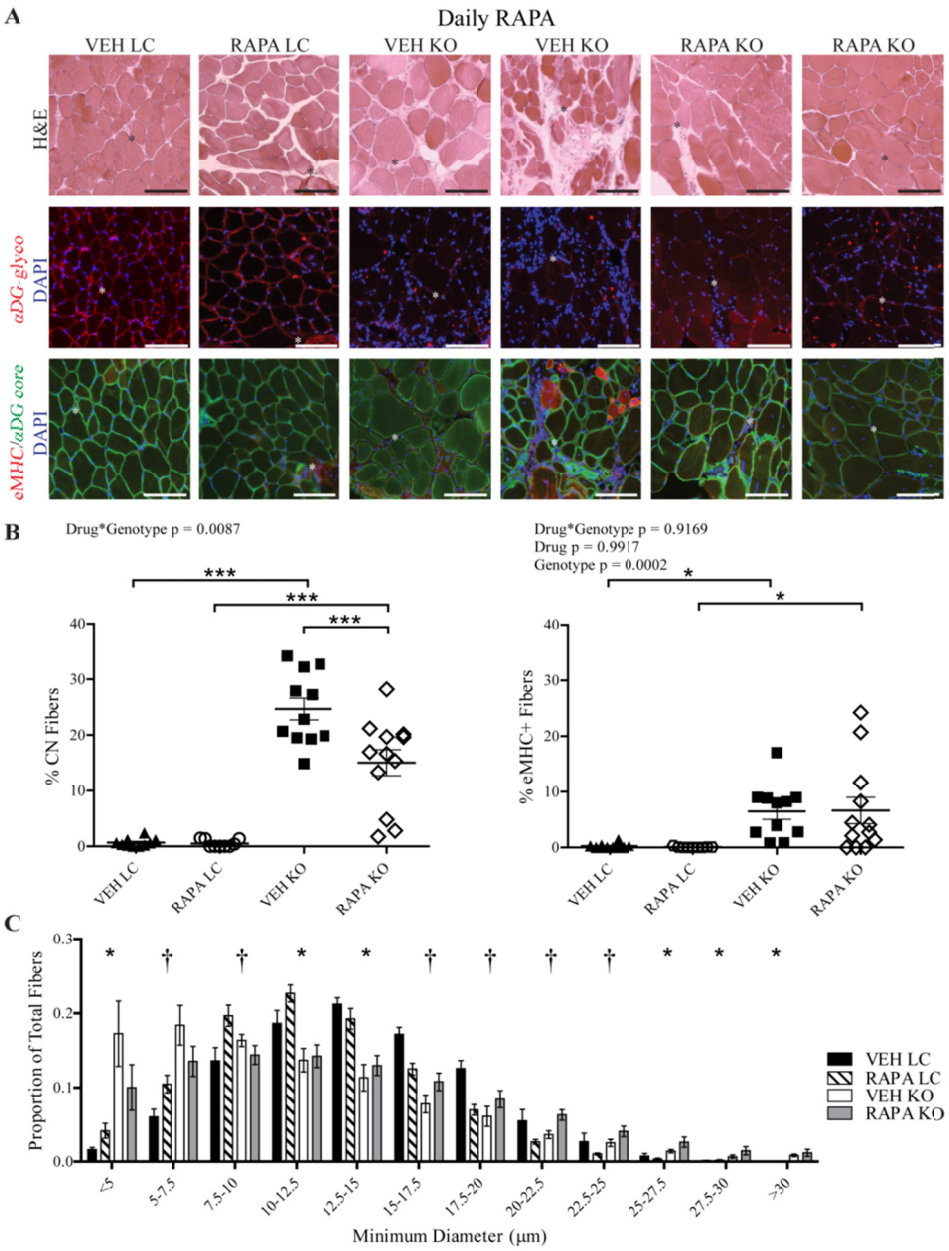

Figure 3.5 Daily RAPA reduces central nucleation and alters fiber size of Myf5/*Fktn* KO iliopsoas. (A) Images from iliopsoas muscles of VEH- or RAPA-treated LC and KO mice. H&E, functionally glycosylated αDG, and core αDG/embryonic myosin heavy chain (eMHC) are shown. Nuclear DAPI counterstain is shown in blue. Scale bar = 100μm. Asterisks denote identical tissue locations across images. Muscle fiber regeneration as measured historically by (B, left) central nucleation (CN) or acutely by (B, right) eMHC. Data are plotted as ((#positive fibers/total fibers)*100). Two-way ANOVA; *, $p<0.05$; ***$p<0.001$. n=10 VEH LC, n=9 RAPA LC, n=12 VEH KO, n=12 RAPA KO. (C) Distribution of muscle fiber minimum diameter from iliopsoas of VEH- and RAPA-treated LC and KO mice. Fibers are grouped into bins of 2.5μm. Two-way ANOVA performed for each bin. *, Drug*Genotype $p<0.05$; †, Genotype $p<0.05$. n=5 VEH LC (tissue artifact), n=5 RAPA LC (tissue artifact), n=7 VEH KO, n=7 RAPA KO.

a well-studied regulator of muscle fiber size, we hypothesized that RAPA treatment might alter this distribution in treated mice. Cross-sectional minimum fiber diameters were measured for all muscle fibers in the iliopsoas of RAPA-study mice. Littermate mice show more evenly distributed minimum fiber diameters, with few or no atrophic fibers. In contrast, fibers from both RAPA and VEH KO muscle had significantly higher proportions of small-sized fibers and an expanded proportion of fibers with minimum diameters greater than 25 μm (Figure 3.5C). In accordance with this, we observed a significant effect of genotype on fiber size at 6 of the 12 bin sizes. Furthermore, there was a significant Drug*Genotype interaction at the 5-7.5, 7.5-10, 15-17.5, 17.5-20, 20-22.5 and 22.5-25 μm minimum fiber diameter bins. To confirm that differences in fiber size between VEH and RAPA KO mice were not due simply to a reduction in small, regenerating fibers, we further analyzed distributions of regenerated (in KOs only) and non-regenerated muscle fibers separately. We found little difference between the fiber diameter distributions of all fibers compared to non-regenerated fibers only; furthermore, the proportions of regenerated fibers at each bin size were different only at the 20-22.5μm bin, indicating that changes in overall fiber size distributions are likely not attributable to differences in the pool of regenerating fibers (Figure 3.6). Thus, RAPA shifted fiber size towards larger values in KO muscle but relatively smaller values in LC muscle, further supporting the idea that *Fktn*-deficient muscle has some abnormal, RAPA-sensitive signaling activity.

Muscle damage is often followed by an inflammatory response involving macrophage infiltration that helps to mediate tissue repair. However, dystrophic muscle experiences repeated cycles of damage and repair with persistence of the inflammatory

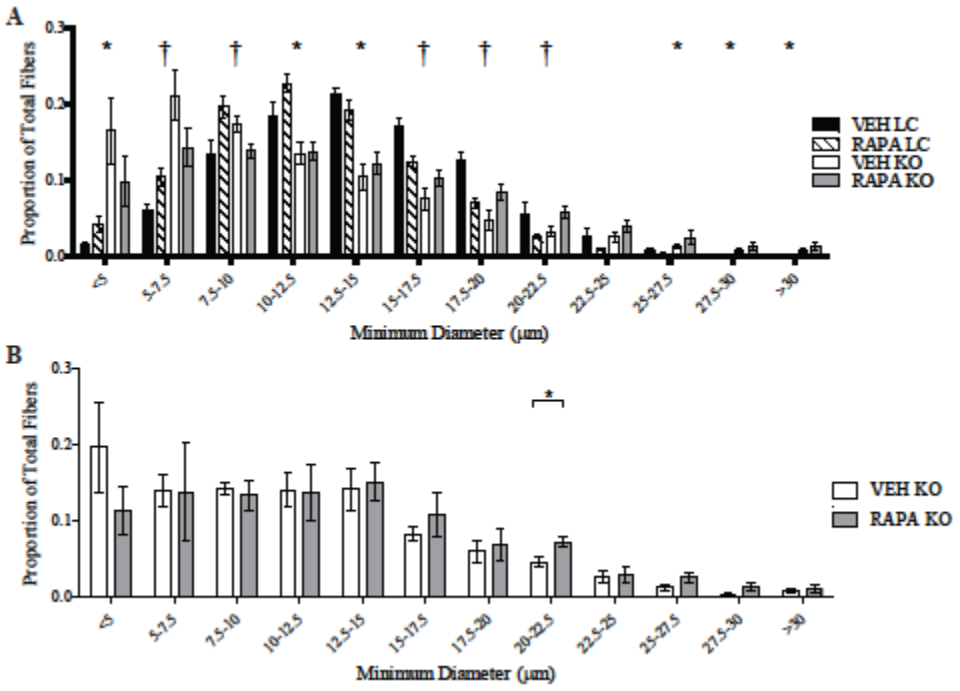

Figure 3.6 Distributions either non-regenerating or regenerating muscle fibers. (A) Distribution of muscle fiber minimum diameter from non-regenerated muscle fibers in iliopsoas of VEH- and RAPA-treated LC and KO mice. Fibers are grouped into bins of 2.5µm. Two-way ANOVA performed for each bin. *, Drug*Genotype $p<0.05$; †, Genotype $p<0.05$. n=5 VEH LC (tissue artifact), n=5 RAPA LC (tissue artifact), n=7 VEH KO, n=7 RAPA KO. (B) Distribution of muscle fiber minimum cross-sectional diameter from regenerated muscle fibers in iliopsoas of VEH- and RAPA-treated KO mice. Fibers are grouped into bins of 2.5µm. Regenerated fiber numbers range from 64-360 in VEH KO mice and 5-217 in RAPA KO mice. n=7 VEH KO, n=6 RAPA KO (mouse sample with only 5 regenerating fibers was excluded from fiber size bin analysis). Two-tailed Student's t-test; *, $p<0.05$.

phenotype (191,192). As RAPA treatment appears to offer protection against muscle damage, we hypothesized that localized tissue inflammation might be reduced in RAPA-treated Myf5/*Fktn* KO mice. We incubated iliopsoas muscle sections from study mice with an antibody detecting CD11b, a common marker for mature macrophages that may also be expressed by granulocytes, dendritic cells and NK cells (290). Tissues from both LC and KO mice were positive for isolated, "resident" immune cells; however, KO iliopsoas also displayed regions of intense staining likely marking major inflammatory invasion (Figure 3.7A). Importantly, RAPA KO mice had significantly less CD11b-positive fluorescence than VEH KO mice, indicating reduced inflammation with RAPA-treatment (Figure 3.7B). To determine if changes in tissue immune cell content corresponded to altered levels of cytokines in RAPA KO mice, we tested solubilized protein from the quadriceps muscle of study mice for the presence of pro-inflammatory (interleukin-1β, monocyte chemotactic protein-1, tumor necrosis factor α) cytokines in multiplex via MILLIPLEX Map assay. We observed a significant effect of genotype on IL-1β levels when normalized to assay background; however, we noted no differences in other pro-inflammatory cytokines tested (Figure 3.8A). Thus, IL-1β appears to be a RAPA-insensitive modulator of inflammation in dystroglycanopathy muscle.

Although muscle possesses considerable potential for regeneration, dystrophic muscle eventually loses regenerative capacity, due at least in part to chronic inflammatory conditions (192). Failed muscle regeneration frequently results in the replacement of functional muscle with fibrotic scar tissue, comprised largely of excess extracellular matrix proteins. Consistent with a fibrotic phenotype in *Fktn*-deficient muscle, transforming growth factor-β (TGF-β), a major fibrogenic cytokine, was

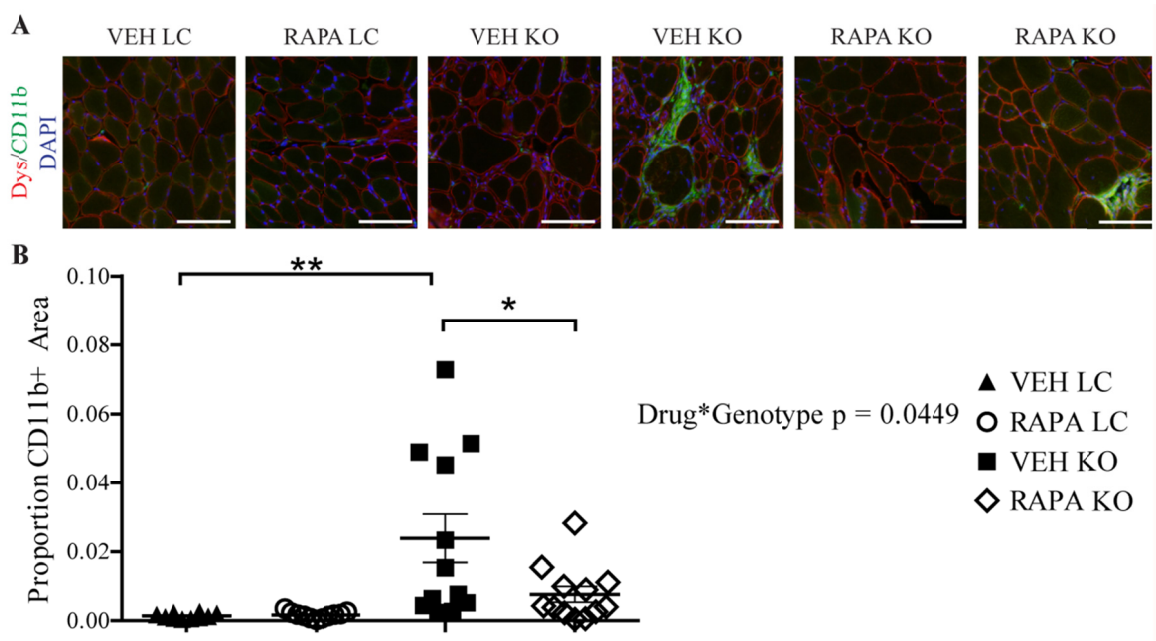

Figure 3.7 Four week daily RAPA treatment decreases immune cell infiltration in iliopsoas. (A) Images from transverse sections stained for macrophage marker CD11b (green), with dystrophin (red) and nuclear DAPI (blue) counterstains. Scale bar = 100µm. (B) Quantification of CD11b-positive areas in iliopsoas of daily study mice. Data are presented as the proportion green pixels per tissue/total pixels per tissue. Two-way ANOVA with Bonferroni's post-test; *, $p<0.05$; **, $p<0.01$. n=10 VEH LC, n=11 RAPA LC, n=12 VEH KO, n=12 RAPA KO.

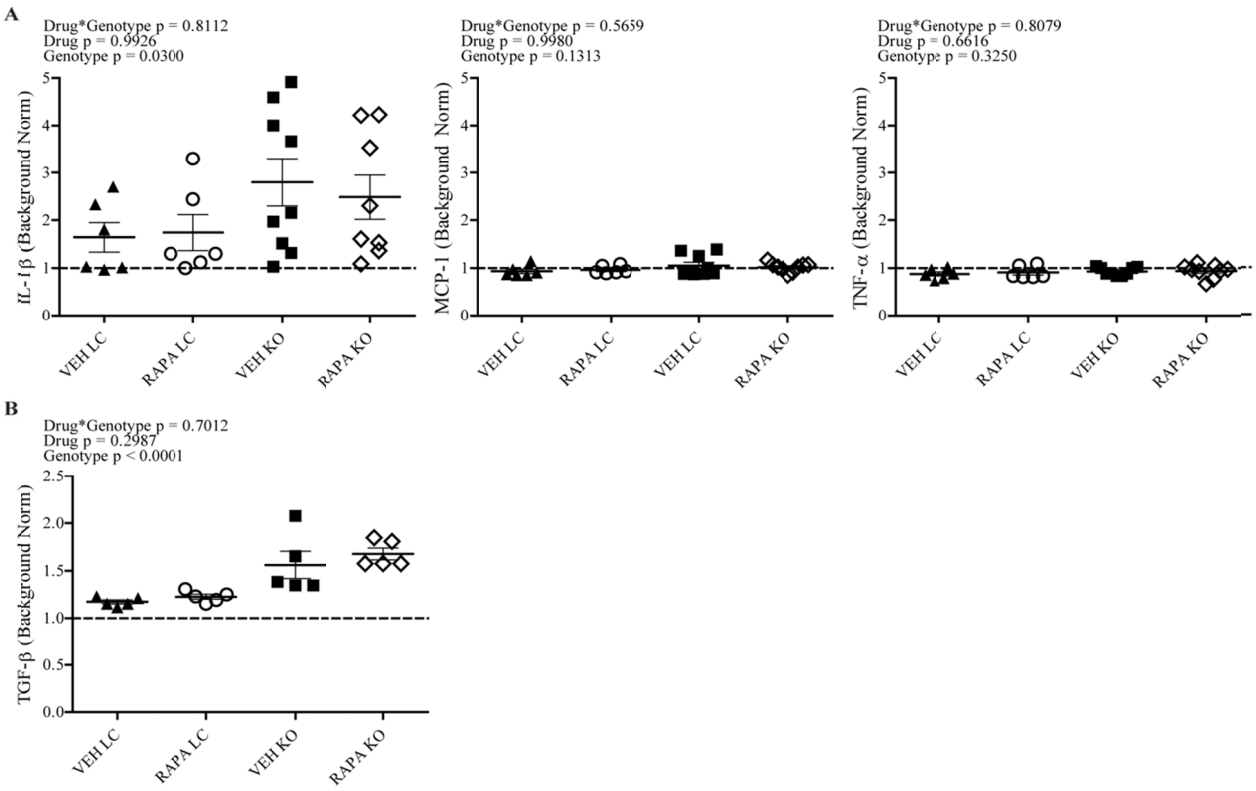

Figure 3.8 Inflammatory or fibrotic analytes from solubilized quadriceps muscle. (A) Fold-change over background values for pro-inflammatory cytokines (IL-1β, MCP-1, and TNF-α) tested via MILLIPLEX Map assay in quadriceps of daily RAPA study mice. (B) Fold-change over background values for TGF-β tested via MILLIPLEX Map assay in quadriceps muscle of daily RAPA study mice.

significantly increased in muscle of KO relative to LC study mice as determined by MILLIPLEX Map analysis; however, we did not detect any RAPA-mediated reduction in TGF-β (Figure 3.8B). However, extracellular matrix protein ColVI, which accumulates abnormally in dystrophic muscle (291,292), was increased in histological sections of iliopsoas muscle of VEH KO mice, demonstrating substantial fibrosis in 12 week old dystrophic muscle, but was significantly reduced in RAPA KO mice (Figure 3.9A, B). In fact, ColVI staining was not significantly different between RAPA LC and RAPA KO in the iliopsoas. Fibrosis is a key factor underlying mortality in muscular dystrophies because fibrotic accumulation in the diaphragm reduces its contractile ability and ultimately leads to respiratory failure. Importantly, we also observed a significant decrease in the fibrotic area of RAPA KO compared to VEH KO diaphragms (Figure 3.9A, B), demonstrating the therapeutic potential of RAPA treatment for dystroglycanopathies.

mTORC1 signaling correlates with levels of pathological markers in dystroglycanopathy muscle.

As mentioned previously, mTOR signaling has been linked to a number of muscle maintenance and disease processes, including regeneration and fibrosis. While 4-week RAPA treatment improved histopathological features in treated Myf5/*Fktn* KO mice, its specific site of action is unclear. In particular, mTORC1 could be hyper-activated in only a subset of cells within the muscle compartment. Furthermore, because of ongoing regeneration and muscle remodeling in dystrophic tissue, the normal equilibrium of various resident cell types within the muscle niche likely changes as the disease state progresses. In order to evaluate whether a subset of cells and/or cell types demonstrate

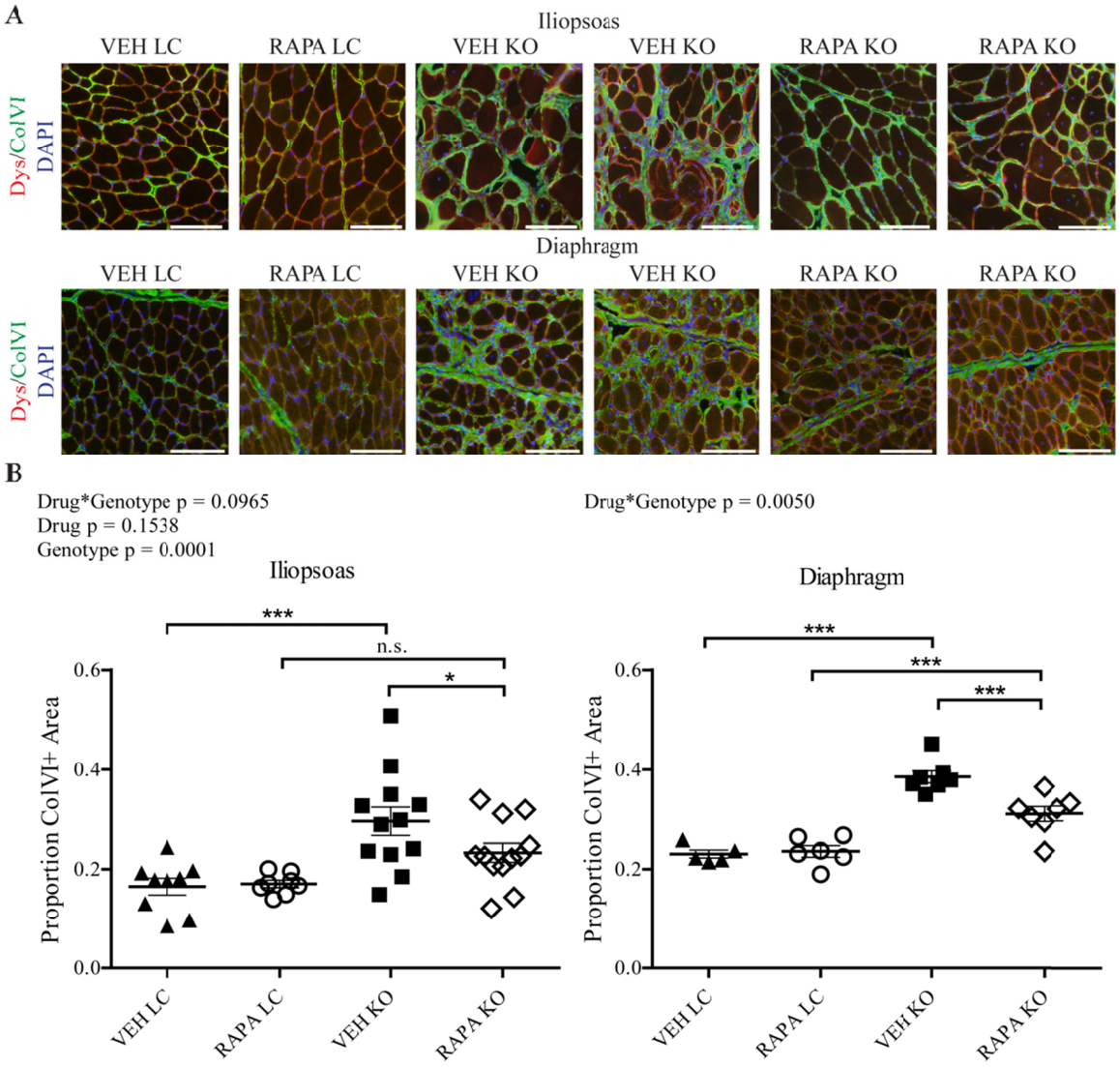

Figure 3.9 Fibrosis is reduced in iliopsoas and diaphragm of RAPA-treated Myf5/*Fktn* KO mice. (A) Representative images from iliopsoas (top) or diaphragm (bottom) of daily study mice stained with dystrophin/ColVI; nuclear DAPI counterstain shown in blue. Scale bar = 100µm (B) Quantification of muscle fibrosis, ColVI positive area, in iliopsoas (left) or diaphragm (right) muscles, detected by immunofluorescence and counted as positive (green) pixels per tissue/total pixels per tissue. Two-way ANOVA; *, $p<0.05$; ***, $p<0.001$. Ilio: n=9 VEH LC, n=8 RAPA LC, n=12 VEH KO, n=12 RAPA KO. Dia: n=5 VEH LC, n=6 RAPA LC, n=7 VEH KO, n=7 RAPA KO.

increased mTORC1 activity, we stained iliopsoas muscles from daily RAPA study mice with an antibody detecting phosphorylation of S6 ribosomal protein, which is dependent on the mTOR substrate S6-kinase for activation. While levels of pS6 were below detection level in LC mice, sections from KO mice revealed regions of robust staining (Figure 3.10A). pS6 was observed in both the muscle fibers and endomysial spaces of KO iliopsoas, demonstrating that mTORC1 activation is not limited to a single cell type. Activated S6 was also observed in RAPA KO iliopsoas, as expected, because muscles analyzed were approximately 18 hours to 2.5 days since the last VEH or RAPA dose for the muscle torque and treadmill RAPA studies, respectively. To delineate the potential locations of mTOR-mediated pathological processes, we correlated pS6 areas to markers of fibrosis (ColVI) or acute regeneration (eMHC). In VEH KO muscle, pS6 correlated weakly with eMHC levels (Pearson r=0.6169), but tracked closely with levels of ColVI (Pearson r=0.8236). In contrast, pS6 correlated more closely to eMHC (Spearman r=0.7676) than to ColVI (Pearson r=0.7066) in RAPA treated KO muscle (Figure 3.10B). Altogether, these results indicate a role for mTORC1 in both the regenerative and fibrotic processes of dystrophic muscle and suggest that RAPA may act to inhibit these signaling events in fibroblasts.

Daily RAPA treatment partially reduces elevated autophagic flux in Fktn-*deficient muscle.*

Recent work in mouse models has identified defective macroautophagy as a therapeutic target in dystrophic muscle (221,233); furthermore, pharmacologic or genetic reversal of this phenomenon, including by RAPA, appears to improve disease phenotype (220,232,293). To probe levels of autophagy in *Fktn*-deficient muscle, we analyzed

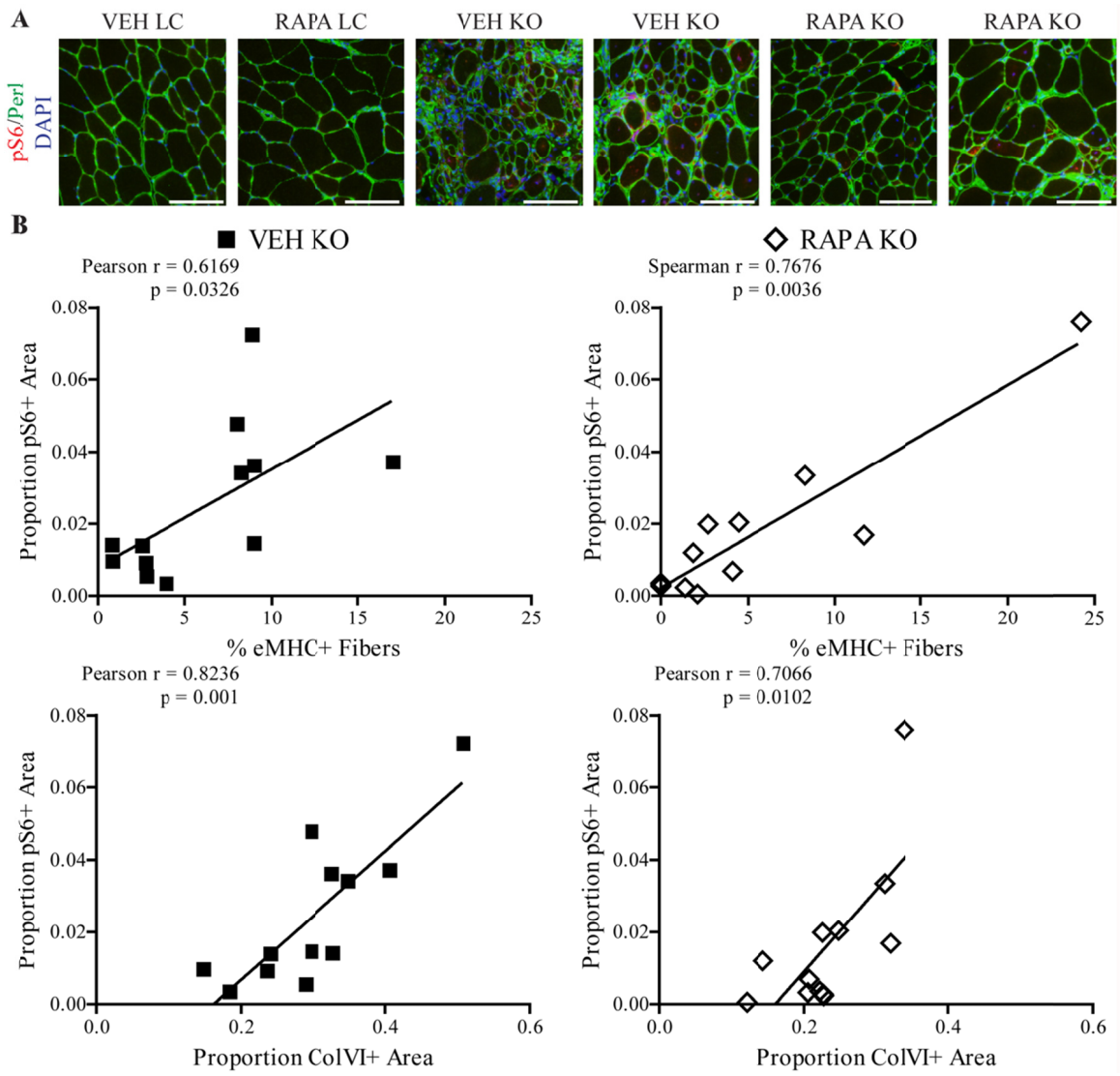

Figure 3.10 pS6 localizes to myofiber- and non-myofiber-specific niches in iliopsoas of Myf5/*Fktn* KO mice. (A) Images stained against phosphorylated S6 (S235/236) ribosomal protein (red) with basement membrane perlecan (green) and nuclear DAPI (blue) counterstains shown. Scale bar = 100μm. (B) Plots comparing pS6-positive areas to percentages of regenerating fibers (eMHC, top) or to fibrotic areas (ColVI, bottom) in iliopsoas of VEH (left) and RAPA (right) KO mice. Pearson r value shown for all groups except RAPA KO eMHC (Spearman r shown, D'Agostino & Pearson omnibus normality test failed).

expression of the autophagosome-associated proteins Beclin-1 and LC3B by western blot. We found a significant effect of genotype on relative quantities of the lipidated, autophagosome-partitioned form of LC3B (LC3B-II, lower band) (Figure 3.11A, B). In addition, there was an interaction of drug and genotype on Beclin-1 levels with RAPA promoting an increase in littermate, but a decrease in KO mice; Beclin-1 was significantly elevated in VEH KO compared to VEH LC mice, in post-test analysis (Figure 3.11A, B). Western blot analysis of the autophagy regulator Vps15 also demonstrated a genotype effect, but the increased level of this protein in KO muscle was unaffected by RAPA treatment (data not shown). These data provide evidence of increased autophagy in dystroglycanopathy muscle, in contrast to reports in other models of muscular dystrophy. However, because autophagy functions to target defective proteins and organelles for cellular removal (214,215), increased levels of Beclin-1 and LC3B-II in *Fktn*-deficient muscle likely point to clearance of tissue components following damage. For example, genes involved in mitochondrial biogenesis are upregulated following muscle injury as damaged organelles are replaced in the tissue (294). Furthermore, in *mdx* muscle, pharmacologic modulation of 5' adenosine monophosphate-activated protein kinase (AMPK) enhanced autophagy with an associated improvement of mitochondrial function and a coincident reduction of disease burden (220).

These data suggest a link between autophagy and mitochondrial remodeling in muscle. To determine whether RAPA treatment affects mitochondrial function, we assayed the activity of succinate dehydrogenase (SDH), a mitochondrial enzyme involved in oxidative phosphorylation at steps in both the citric acid cycle and the electron

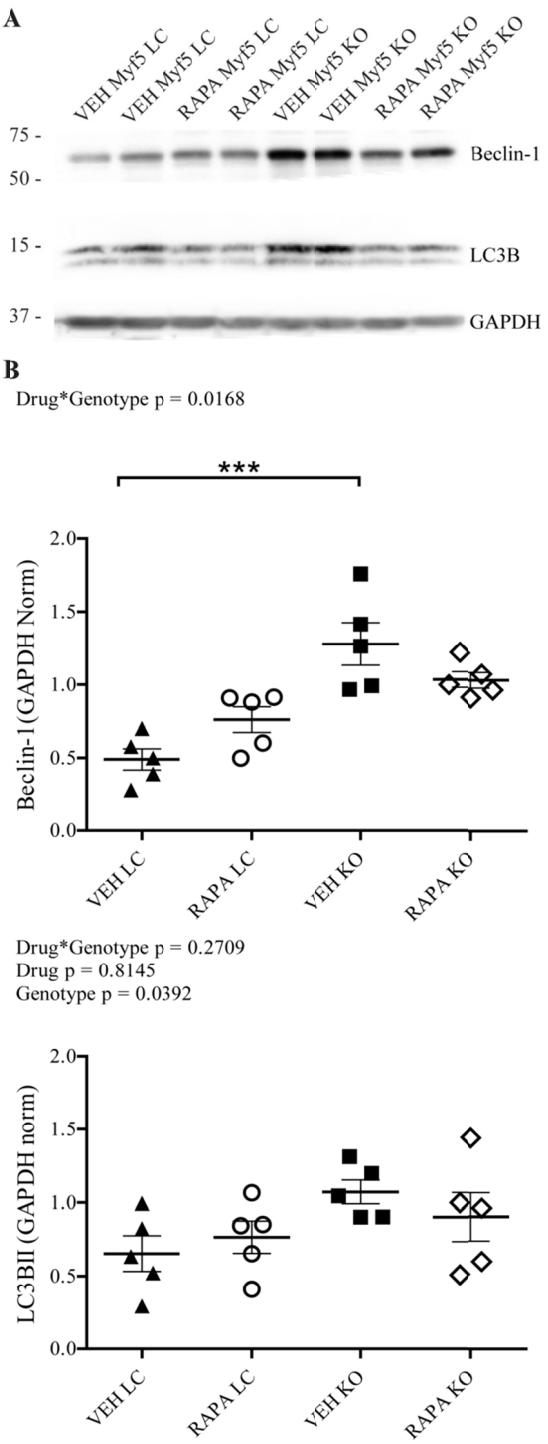

Figure 3.11 Autophagy proteins are upregulated in dystroglycanopathy muscle. (A) Western blot analysis showing levels of autophagy proteins Beclin-1 and LC3B. GAPDH was used as a loading control. (B) Densitometric analysis of Beclin-1 (top) and LC3B-II (lower band, bottom) protein levels, normalized to GAPDH loading control. Two-way ANOVA; ***, $p<0.001$.

transport chain. We observed lower SDH activity in KO compared to LC muscle when normalized to total tissue mass, but found no difference between RAPA and VEH KO mice. RAPA LC muscle tended to have more SDH activity than VEH LC muscle, but these differences were not statistically significant in the cohort tested (n=4 RAPA LC, n=3 VEH LC) (Figure 3.12). Thus, RAPA-mediated improvements to Myf5/*Fktn* KO muscle appear to occur independently of mitochondrial function and further highlight the divergence of fukutin- and dystrophin-deficient muscle with respect to autophagic phenotype. Altogether, our results point to a myoprotective effect of RAPA treatment that may delay the progression of disease in dystroglycanopathy tissue.

Discussion

Several muscular dystrophies arise from loss of the structural linkage between the extracellular matrix and the intracellular cytoskeleton (reviewed in (36,295)). While increased susceptibility of the sarcolemma to damage is a well-studied component of disease etiology, some signaling functions have also been ascribed to the DGC. Growth-receptor bound protein 2 (Grb2) has been shown to bind intracellularly to βDG, providing a possible link between the DGC and mTOR signaling through the extracellular signal-regulated kinase/ribosomal S6 kinase (ERK/RSK) pathway (205,207). Indeed, disruption of DG-laminin binding reduces ERK (206) and Akt activation and increases apoptosis in cultured myotubes (209). However, consistent with the data presented here, a direct connection between αDG glycosylation and mTOR activation has not been demonstrated. Still, accumulating evidence suggests a critical role for mTOR signaling in the development and maintenance of skeletal muscle (165,223,225,226,296).

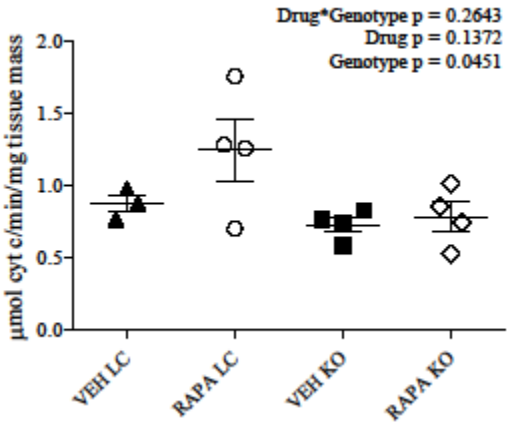

Figure 3.12 Mitochondrial function in TAs of Myf5/*Fktn* KO and LC mice. Tissue mass-normalized values of cytochrome C reduced *in vitro* by succinate dehydrogenase from homogenized TAs of VEH- or RAPA-treated LC and KO mice. Two-way ANOVA.

Abnormal age- and muscle-dependent mTOR activation has been observed previously in skeletal muscle of the *mdx* mouse, a mild model of dystrophin-deficient muscular dystrophy (221,231,297). Furthermore, simultaneous increases in mTOR phosphorylation and protein content have also been described in *mdx* diaphragm at 10 weeks (220). Here, we provide evidence of increased mTORC1 activation in aged *Fktn*-deficient muscle, a model of moderate to severe muscular dystrophy; however, changes in mTOR signaling were not intrinsic to the dystroglycan glycosylation defect as they did not arise until after the development of muscle pathology. Thus, activation of mTOR likely reflects the fibrotic progression that occurs during the dystrophic process. mTOR is indeed a known regulator of extracellular matrix protein synthesis in cultured fibroblasts, a process with apparent sensitivity to RAPA (298,299), and is activated in primary muscle fibroblasts in response to growth stimuli (286). It is therefore possible that the therapeutic benefit of RAPA treatment in dystroglycanopathy mice proceeds by impeding the development of endomysial fibrosis.

In agreement with our findings, mTORC1 inhibition has also shown therapeutic benefit in *mdx* mouse, although a consistent mechanism of action has not yet been established [e.g. (231,232)]. The outcomes reported in Figure 3.4 seem to support a RAPA-mediated delay of disease progression in dystroglycanopathy muscle. Functional phenotypes of LC and KO mice are expected to diverge with the advancement of muscle disease, as was the case for *in vivo* torque measurements: VEH LC, but not VEH KO mice demonstrated age-associated increases in torque following the 4-week dosing study; however, both RAPA LC and KO animals demonstrated an increase in torque at the conclusion of dosing. Analysis of downhill treadmill run distances between KO

treatment groups shows a similar finding as 4 of 7 RAPA-treated ran KO mice ran at least half the distance of their respective age- and treatment-matched controls, compared to a single instance in the VEH KO group. It is unclear why little to no improvement was observed in the remaining 3 RAPA KO mice, although dystrophic phenotypes of Myf5/*Fktn* KO mice have been reported to be variable (50). If RAPA treatment is capable of delaying disease progression, but incapable of reversing dystrophy, then mice with more severe muscle involvement at the commencement of the dosing schedule might have a correspondingly weaker response to the drug.

Recent mechanistic studies have focused on the role of autophagy in both normal and dystrophic muscle, with the finding that consistent Akt or mTORC1 activation inhibits autophagic processes in a way that is damaging to muscle tissue (300). Indeed, increasing evidence demonstrates that restoration or augmentation of autophagy can improve pathological features of muscle disease (220,222,232,233). Autophagy serves a key function in the clearance of damaged organelles from the cytosolic space, and accumulation of these dysfunctional cellular structures likely underpins the association between impaired autophagy and the dystrophic phenotype (216,233). Conversely, unchecked activation of the autophagy pathway is also detrimental to muscle and leads to atrophy or myopathy (301,302). Here, we report that proteins involved in autophagosome formation are upregulated in dystroglycanopathy muscle, suggesting that autophagy is not deficient in dystroglycanopathy muscle (Figure 3.11). However, we cannot distinguish between pathogenic deregulation of protein/organelle degradation pathways or an increase in cellular component recycling following repeated bouts of

myonecrosis. In either case, RAPA appears to partially relieve the altered autophagic phenotype of Myf5/*Fktn* KO mice.

Rapamycin (sirolimus) and related rapalogs (everolimus, temsirolimus) are FDA approved drugs for the treatment of tuberous sclerosis complex (TSC), lymphangioleiomyomatosis (sirolimus), renal transplant (sirolimus, everolimus), breast cancer, pancreatic cancer, subependymal giant astrocytoma (SEGA, everolimus), and renal cell carcinoma (everolimus, temsirolimus) (287). Importantly, sirolimus and everolimus are in use as single and combination drug therapy in pediatric populations for TSC, TSC-related SEGA, and for children 13 years and up with renal transplant (303-307). The 2 mg/kg RAPA dose used here, relatively low for mouse experiments, by allometric scaling is approximately equivalent to 5.7 mg/m^2 (308). In comparison, TSC and SEGA trials used doses as low as 1.5 or 3 mg/m^2 (sirolimus and everolimus, respectively) and as high as ~4 or 4.5 mg/m^2 (sirolimus, everolimus, respectively). In clinical trials evaluating sirolimus for renal transplant, a loading dose of 15 mg with a 5 mg maintenance dose (corresponding to 7.89 and 2.63 mg/m^2, respectively based on 1.9m^2 average male body area) was found to be safe. Thus, while the dose described in our study is at the higher range of dosage in pediatric patients, there is no evidence to support that this dose is too high to be considered clinically relevant. Potential adverse events, such as immunosuppression, metabolic changes, and hypertension, need to be considered; however, the clinical cohorts with adverse event reporting are predominately cancer or transplant patients, who consequently have significant comorbidities and combined therapies that may or may not be relevant to a dystroglycanopathy patient population (309). Notably, seven children, ranging in age from 4 to 16 years old received

rapamycin for intractable epilepsy due to tuberous sclerosis complex; daily treatment for 12 months was reported without significant side effects (304). While an absence of liver and kidney toxicity in the fourth week of daily treatment in this study cannot exclude potential adverse events with longer RAPA treatment schedules in dystroglycanopathy mice or patients, previous work found that long-term RAPA treatment (estimated 2.2mg/kg/day) increased lifespan of heterogeneous wild-type mice, with half of study mice receiving therapy for approximately 75 weeks (310). Therefore, while there is evidence that chronic RAPA treatment may be tolerable in mouse and human studies, caution is still warranted. Additional studies will be necessary to confirm the therapeutic value of long-term mTORC1 inhibition in dystroglycanopathy and to determine the optimal timing of treatment to ensure maximal tissue response.

Conclusions

We found evidence of elevated mTOR activation in later-stage dystroglycanopathy muscle of *Fktn*-deficient mice. Younger mice treated for 4 weeks with RAPA displayed a reduction in fibrosis and muscle damage, and had improved muscle function. We propose that RAPA may protect dystrophic muscle from damage to delay progression of disease and inhibit fibrotic remodeling. This suggests that mTORC1 signaling may be a viable therapeutic target for dystroglycanopathy-type muscular dystrophies, but further work is needed to define ideal treatment conditions.

CHAPTER 4

DISCUSSION AND CONCLUSIONS

Although it has been over 25 years since the discovery of the Duchenne muscular dystrophy gene, dystrophin-glycoprotein complex-related muscular dystrophies have remained without FDA-approved therapy. As is often the case in biomedical research, target identification has proven to be a significant challenge. However, the past few decades have seen an enormous advance in terms of the understanding of the molecular pathogeneses of these diseases, which have in turn opened new avenues for drug discovery. Because muscular dystrophies are characterized by a progressive loss of muscle mass, which corresponds histologically to a profound reduction of myofiber content within the muscle tissue, it appears that failed regeneration is central to the pathomechanism of disease. Proper muscle regeneration or repair following damage requires the coordination of several temporally regulated processes: the inflammatory response, activation of the muscle progenitor population followed by proliferation and fusion to form multi-nucleated myotubes, and finally maturation/differentiation of nascent myofibers. Each regenerative phase consists of specific events that proceed in sequence to ultimately yield new functional tissue; although much of this timeline has been described in detail, it is not entirely clear how it is altered in dystrophic muscle.

The role of the dystrophin-glycoprotein complex as a structural complex and the consequences of its defects in mature myofibers are well-established. However, a number of studies suggest that the dystrophin-glycoprotein complex likely has a unique

function in facilitating muscle regeneration. Early evidence in support of this was found in a mature-muscle specific dystroglycan KO mouse, in which dystroglycan expression remains intact in satellite cells and is consequently unaffected during regeneration (127). A comparison of this mouse to dystrophin-deficient *mdx* or δ-sarcoglycan mice, both of which have limited expression of dystrophin-glycoprotein complex components in regenerating muscle, revealed that preservation of dystroglycan throughout the steps of new myofiber formation dramatically improves its efficiency. Furthermore, deletion of dystroglycan in epiblasts at embryonic day 5 in mice (Mox2-cre/*Dag1* KO, MORE-dystroglycan null), which disrupts dystroglycan expression in all embryonic tissues, results in dramatically reduced muscle regeneration following a toxin challenge. Interestingly, aspects of this impaired regenerative phenotype are recapitulated in mice lacking dystroglycan specifically in satellite cells (tamoxifen-inducible Pax7-cre/*Dag1* KO, iPax7-dystroglycan), which demonstrated a delay in regeneration and produced significantly smaller muscle fibers following injury (127,311). This agrees with work from our laboratory, which showed that following toxin injury mice lacking glycosylation of α-dystroglycan in whole muscle (satellite cells and myofibers, Myf5-cre/*Fktn* KO) regenerated significantly smaller fibers than mice lacking the same only in mature muscle fibers (MCK-cre/*Fktn* KO) (50).

It has recently been reported that dystrophin and dystroglycan are transcribed at high levels in satellite cells, contrary to prevailing sentiment. In fact, it appears that a dystrophin-dystroglycan complex helps to regulate satellite cell polarity during asymmetric division, where a parent cell gives rise to one committed myogenic progenitor and one renewed satellite cell. Following injury, satellite cells lacking

dystrophin were activated but were not induced to proliferate, suggesting that satellite cells do not divide to the extent demanded by disease processes in dystrophin-deficient muscular dystrophies, ultimately tipping tissue balance in favor of non-regenerative processes (311). Similarly to satellite cells lacking dystrophin, satellite cells on individual myofibers from Large^{myd} mice have a significantly lower doubling rate than those on WT fibers. However, when removed from their native muscle fibers and expanded on laminin-coated plates, Large^{myd} satellite cells proliferate at a normal rate and show enhanced fusion relative to cells isolated from WT animals. This suggests that the intrinsic myogenic potential of satellite cells with aberrant α-dystroglycan glycosylation is uncompromised but is fundamentally dependent on certain aspects of their niche (182). It should be noted that comparison of results with cultured Large^{myd} satellite cells and analyses of *mdx* satellite cells grown on their native myofibers are difficult to interpret because satellite cells appear to express integrin, which may be able to functionally compensate for loss of dystrophin or dystroglycan on laminin-coated plates; still, the responsiveness of satellite cells to laminin likely reflects a role for glycosylated α-dystroglycan.

Although a delay in regeneration is seen with satellite-cell knockout of dystroglycan, mice lacking functional glycosylation of α-dystroglycan in whole muscle tissue or whole body (e.g. Large^{myd}) tend to show increased numbers of embryonic myosin heavy chain-expressing fibers (immature, regenerating) following injury, as do human Fukuyama congenital muscular dystrophy patients, which implies that generation of new myofibers is not impaired in these muscles, *per se* (50,133). However, accumulation of eMHC-positive fibers can indicate either ongoing muscle damage/high

frequency of damage events or a delay in the terminal differentiation of newly formed muscle fibers. While both MORE-dystroglycan and iPax7-dystroglycan KO mice demonstrate impairment of muscle regeneration, it is unclear to what extent these phenotypes overlap. Interestingly, evaluation of fukutin-deficient muscle revealed low abundance of mature muscle proteins along with malformation of NMJs (133,134). Innervation and stimulation of skeletal muscle signal for its maturation and regulate differentiation of myofibers and the expression of specific myosin heavy chain isoforms (reviewed in (165)). Because of this, it might be expected that regeneration profiles of mice lacking α-dystroglycan glycosylation in muscle ought to differ from those of whole-body α-dystroglycan glycosylation-deficient animals. Indeed, we found that 14 days after toxin challenge levels of eMHC-expressing fibers were elevated in the TA of whole-body inducible *Fktn*-KO (Tam-*Fktn* iKO) mice compared to saline-injected contralateral TAs, while eMHC fibers were equally abundant in toxin- or saline-treated TAs of Myf5/*Fktn* KO mice. It is therefore probable that α-dystroglycan glycosylation is important pre-synaptically at the NMJ and that in its absence NMJ morphology is abnormal, corresponding to a delay in maturation of newly formed myofibers. Characterization of mature fiber-types in TAs of Tam-*Fktn* iKO mice also revealed a significant increase in the proportion of type 2A fibers following injury, which is consistent with abnormal neuronal stimulation. Indeed, sustained low-frequency stimulation in rat TA muscle also leads to an increase in expression of MHC-2A, marking the transition from an overall glycolytic to oxidative phenotype (312,313). Our study found that NMJs were occupied (i.e. presynaptic and post-synaptic components of the NMJ colocalized), but did not evaluate the morphology of NMJs or firing patterns of MNs in Tam-*Fktn* iKO mice

following injury; therefore, while our findings and those of others implicate neuronal α-dystroglycan glycosylation in the process of muscle differentiation and fiber-type specification, its exact function remains unclear.

Regulation of the contractile and metabolic properties of muscle fibers is considered a potential therapeutic strategy for muscular dystrophy because slow, oxidative fibers appear to be preferentially spared from degeneration in dystrophic muscle. Much of this work has focused on PGC-1α or its upstream regulator sirtuin 1 (silent mating type information regulation 2 homolog, SIRT1), which control genes involved in mitochondrial biogenesis/oxidative phosphorylation, the neuromuscular junction program, and regulation of slow muscle fiber types. Induction of SIRT1 or PGC-1α in dystrophin-deficient skeletal muscles reduces disease pathology and improves fatigue resistance; these changes are accompanied by a switch from fast to slow fiber types in treated muscles (169-171,314). Because utrophin may be transcriptionally upregulated in slow fiber types and because PGC-1α positively influences expression of NMJ genes, including utrophin, modulation of this pathway offers a novel avenue for therapeutic compensation of dystrophin-deficiency by utrophin (170,315). Recent work has shown that genetic deletion of folliculin-interacting protein 1 (Fnip1) significantly increases the oxidative qualities in mouse muscle through induction of PGC-1α; when mice lacking Fnip1 were crossed into the *mdx* line, it greatly improved stability of the sarcolemma (316). However, while pharmacological SIRT1 inducers have been reported, none have been used in models of muscular dystrophy; furthermore, overexpression of PGC-1α has been accomplished to date, only by adenoviral-mediated or transgenic methodologies and not through a small molecule approach (317,318). Despite this,

simvastatin, a drug well-known for use in treating high cholesterol, has recently been shown to provide benefit in *mdx* muscle in part by promoting a slow, oxidative phenotype. Interestingly, these changes are independent of utrophin expression, indicating that the resilience of slow fiber types in dystrophic muscle is potentially not utrophin-reliant (222).

The slow myogenic program is also controlled by 5'-adenosine monophosphate activated protein kinase (AMPK), another regulator of PGC-1α. Initial studies using 30-day AMPK stimulation via activator 5-aminoimidazole-4-carboxamide-1-β-D-ribofuranoside (AICAR) found an increase in PGC-1α levels as well as an increase in oxidative capacity of treated *mdx* mice; these findings were further associated with an increase in sarcolemmal integrity owing to upregulation of utrophin-glycoprotein complex proteins (254). Interestingly, a later study found that improvements in physiological parameters of *mdx* diaphragms, including maximal force generation and a reduction of histopathological features, occur independently of metabolic plasticity or utrophin upregulation following administration of AICAR. Instead, it was reported that AICAR enhanced autophagy in *mdx* diaphragms, allowing for recycling of defective organellar structures, and, in particular, mitochondria abnormally susceptible to opening of the mitochondrial permeability transition pore (220). A number of mitochondrial disorders originate with oxidative stress, which has been reported in *mdx* mice and may be a key factor underlying muscle weakness in the model (297,319). Consistent with this, use of simvastatin in dystrophin-deficient mice reduced expression of NADPH oxidase 2 (NOX2), which correlated strongly with improved contractile force in the TA. Furthermore, it was determined that the reactive species H_2O_2 was reduced and

autophagy was enhanced in simvastatin treated mice, suggesting a link between oxidative stress and autophagy in dystrophin-deficient muscle (222).

A number of reports have confirmed that autophagy is defective in dystrophin-deficient muscle, and corrobating a finding first made in Col6a1$^{-/-}$ (lacking the α1 chain of collagen VI), a mouse model of Ulrich congenital muscular dystrophy. Dietary or pharmacologic approaches to boost autophagy in these models have been successful and have uncovered a concomitant amelioration of dystrophic features, suggesting that impaired autophagy is a major driver of muscular dystrophy (221,233). Genetic ablation of autophagy in skeletal muscle results in a myopathy with some features common to those described in *mdx* or Ullrich congenital muscular dystrophy mice, especially with respect to the accumulation of defective mitochondria (302,320). Together, these data highlight the requirement of normal autophagic signaling for skeletal muscle maintenance.

While autophagy seems clearly to be necessary in muscle, overactivation of this process is likewise detrimental and tends to result in atrophy (218). Although muscle hypertrophy (in the calf, for example) is sometimes seen in Duchenne muscular dystrophy, congenital dystroglycanopathies are more commonly associated with atrophy, including high proportions of atrophic muscle fibers (note, however, that milder limb-girdle muscular dystrophy, and in particular MDDGC5 typically presents with calf hypertrophy). Consistent with this atrophic phenotype, we found that muscles of Myf5/*Fktn* KO mice, which model more severe/early onset dystroglycanopathy, had higher levels of autophagy associated proteins Beclin-1 and LC3B-II. It should be noted that the hypertrophy/atrophy paradigm is insufficient to explain the finding of reduced

autophagy in Ullrich congenital muscular dystrophy and Duchenne muscular dystrophy mouse models because these observations were made in both muscles with predominantly atrophic (e.g. *mdx* diaphragm) and somewhat hypertrophic muscle fibers (e.g. *mdx* TA) muscles; however, standard-diet treated *mdx* mice had significantly higher levels of pathologically hypertrophic myofibers than their low-protein diet-fed counterparts (221). Furthermore, our results indicate only that basal autophagy levels are higher in dystroglycanopathy- than in wildtype-muscle and cannot definitively determine whether this signifies pathological activation of autophagy. Indeed, it is possible that the increase in expression of Beclin-1 and LC3-II in Myf5-*Fktn* KO mice reports, by proxy, on the turnover frequency of cellular structures. Necrotic/regenerative diseases are likely to feature substantial cycling of proteins and organelles as old dying cells are cleared and replaced, a process that is facilitated primarily through autophagy. The discrepancy between the phenotypes of Duchenne muscular dystrophy and dystroglycanopathy is interesting, though a clear explanation for this observation is still required. In the future, it will be important to determine 1) whether mitochondrial dysfunction is a feature of dystroglycanopathy muscle and 2) how the molecular mechanisms regulating autophagy, and therefore clearance of dysfunctional organelles, differ between dystroglycanopathy muscles and other dystrophic muscles.

A finding regularly reported in tandem with the autophagy defect in *mdx* muscle is an activation of the Akt/mTOR pathway, which has been confirmed in biopsies from Duchenne muscular dystrophy patients as well (e.g. (221)). Akt directly controls autophagy through modulation of the FOXO family of transcription factors, which induce expression of atrogenes; additionally, Akt is indirectly responsible for activation of

mTORC1, a nutrient sensitive protein kinase complex that regulates translation and is therefore apposed to autophagy in the control of cell growth (147,218,219,230,321,322). It therefore stands to reason that inhibition of Akt/mTOR signaling is a viable means of reversing some of the adverse features reported in dystrophic muscle. However, Akt may be required for a number of essential processes in muscle including myogenesis and regeneration (223,268,323), and recent studies have also suggested beneficial roles of Akt signaling in muscular dystrophy. For example, muscle-specific overexpression of a micro-RNA leading to activation of Akt significantly improved histology and function in *mdx-5cv* mice, which have more muscle dysfunction than *mdx* mice (104,224). Transgenic expression of Akt in *mdx* muscle also prevents force drop following eccentric contractions, indicating improved resistance to fatigue. It has also been suggested that overexpression of Akt in muscle results in an upregulation of the utrophin-glycoprotein in dystrophin-deficient muscle (268,324). In cultured myotubes, disruption of the α-dystroglycan-laminin interaction leads to a decrease in Akt signaling with an associated increase in apoptosis (209). It is therefore unclear whether Akt inhibition is a viable therapeutic strategy in dystrophic muscle; however, several lines of evidence indicate that targeting of its downstream effector mTOR may provide some benefit.

Inactivation of mTOR signaling through either nanoparticle delivery of the mTORC1 inhibitor rapamycin or maintenance of a diet low in amino acid content reportedly improves autophagy in *mdx* mice, consistent with the idea that activation of mTORC1 is central to defective autophagy in dystrophin-deficient muscle (221,232). Pharmacologic modulation of AMPK, which inhibits mTORC1, also alleviates pathological features of impaired autophagy (220). mTORC1 is capable of controlling

energy balance through direct modulation of autophagy. This process is mediated by Unc-51 like kinase (Ulk1), which initiates autophagy and contains phosphorylation sites for both mTORC1 and AMPK; phosphorylation of Ulk1 by mTORC1 prevents its interaction with AMPK, effectively inactivating it (325,326). Intriguingly, phosphorylation of Ulk1 by AMPK results in its translocation to mitochondria where it initiates mitophagy, the primary mechanism for degradation of defective mitochondria (327). This directly links the observations of mTOR activation and accumulation of defective mitochondria and suggests the mechanism by which mTOR inhibition may benefit dystrophin-deficient muscle, although some evidence suggests that this is a rapamycin-insensitive function (328).

Results from our laboratory and others suggest that mTOR inhibition may provide desirable effects in dystrophic muscle aside from restoration of autophagy. A study in using rapamycin in *mdx* mice found that 6-week treatment with the drug significantly reduced inflammation as measured by infiltration of CD4+ or CD8+ T-helper cells, which have been implicated in progression of dystrophic pathology (231,329). Our work shows evidence for a reduction in the levels of CD11b+ macrophages, which is consistent with the known anti-inflammatory properties of rapamycin. However, our results do not distinguish between immunosuppressant reduction of inflammation and a passive reduction due to a decrease in muscle damage. We report that levels of the pro-inflammatory cytokine interleukin-1β were elevated in Myf5/*Fktn* KO mice regardless of treatment with rapamycin, which seems to argue against direct immuno-modulation. In *mdx* muscle, rapamycin appears to reduce the number of necrotic fibers, which is comparable to our findings in dystroglycanopathy muscle (231). We noted a decrease in

serum levels of creatine kinase, a marker of muscle damage, in rapamycin treated mice following a downhill treadmill run protocol, which contrasts with the increase in CK seen in VEH Myf5/*Fktn* KO mice. Therefore, while we cannot definitively say whether rapamycin treatment directly reduces inflammation in dystrophic muscle, we do have evidence that it reduces damage to myofibers that is likely required for the initiation of an inflammatory response.

In addition to protection against muscle damage from lengthening contractions in dystroglycanopathy muscle, we also noticed that rapamycin treated Myf5/*Fktn* KO mice had significantly lower numbers of centrally nucleated (regenerated) fibers than KO mice receiving vehicle. Some studies have indicated that mTOR may be required for muscle regeneration and that rapamycin can substantially delay the regenerative time course following injury (282,330). Furthermore, it has been demonstrated that conditional loss of mTOR in satellite cells results in a decrease in their proliferation and differentiation rates (331). Despite these results, we found no difference in transient regeneration (e.g. eMHC-positive myofibers) between rapamycin- or vehicle-treated Myf5/*Fktn* KO mice; we therefore conclude that rapamycin is not impeding regeneration but rather decreasing the number of degenerative events in treated KO animals. Many of the studies probing mTOR function in muscle have relied upon genetic models, which seem to have more profound impacts on muscle than inhibition via rapamycin. While 2 month rapamycin treatment produced no detectable effects in muscle in one study, loss of mTORC1 signaling through raptor deletion specifically in mature mouse skeletal muscle causes muscular dystrophy (225). Complete genetic removal of mTOR in skeletal muscle results in an even more dramatic phenotype; interestingly, this appears to be partially

attributable to non-mTORC functions of mTOR. In particular, it has been shown that mTOR interacts with the transcription factor yin-yang 1 (YY1), which can bind to the muscle-specific dystrophin promoter in myoblasts and differentiated muscle. In accordance with this, dystrophin and dystrophin-glycoprotein complex expression was significantly reduced in muscles lacking mTOR, but not in those lacking raptor or rictor (226,332,333). Therefore, defects in the myogenic potential of satellite cells lacking mTOR could be dystrophin-related. Aside from this, we cannot rule out the possibility that rapamycin inhibits differentiation in Myf5/*Fktn* KO muscle, although if this were the case, we might expect accumulation of eMHC+ fibers over the course of 4 weeks of dosing rather than the roughly equivalent numbers observed in RAPA-treated or VEH-treated muscles. It is also important to consider that inhibition of myogenesis is more easily observed in an injury model than under physiological conditions in dystrophic muscle, where regeneration is unsynchronized and occurs on a smaller scale.

Typically, a failure in myogenesis or regeneration is associated with accumulation of fibrotic tissue in muscular dystrophy. Muscle progenitors and fibroblasts, which are responsible for synthesis of connective tissue, interact dynamically after injury; ablation of fibroblasts during early phases of regeneration results in premature differentiation and a long-term reduction in the size of myofibers. On the other hand, loss of satellite cells in muscle results in a complete failure of regeneration following injury including major fibrotic deposition (334). Synthesis of collagens in fibroblasts is potently stimulated by TGF-β1, which is released from alternatively activated macrophages and leads to transient upregulation of extracellular matrix components that serve as a scaffold for the formation of new muscle (reviewed in

(192,204)). It has been shown that pharmacologic depletion of macrophage populations in mice leads to reduced TGF-β expression and smaller muscle fibers following toxin injection, which supports a role for activated fibroblasts in the mediation of muscle regeneration. Furthermore, TGF-β appears to induce the expression of the anti-inflammatory molecule prostaglandin E_2 in cultured primary muscle progenitors or C2C12 myoblasts, suggesting that there may be a feedback mechanism by which these cells can repress inflammation and fibrosis after injury (335).

We found that TGF-β expression was increased in Myf5/*Fktn* KO mice but unaffected by rapamycin; however, rapamycin treatment significantly reduced the levels of fibrosis in iliopsoas and diaphragm muscles of dystroglycanopathy mice. These results likely indicate that rapamycin-mediated inhibition of fibrosis lies downstream of the initial pro-fibrotic signal. Consistent with this, mTOR is activated in primary muscle fibroblasts induced to proliferate with the TGF-β family member myostatin and inhibited by rapamycin, which simultaneously reduced collagen production and fibroblast proliferation (286). In cultured fibroblasts, genetic deletion of Akt1 or inhibition of mTORC1 with rapamycin significantly reduced expression of collagen isoforms, further supporting a role for mTOR signaling in fibrosis (299). We observed that mTORC1 is activated in late-stage fibrotic dystrophic muscle and not in pre-dystrophic muscle that is deficient in α-dystroglycan glycosylation. Furthermore, total levels of Akt and S6 protein correlate with the extent of fibrosis potentially suggesting the existence a subpopulation of cells with a higher demand for mTOR signaling. In iliopsoas of younger Myf5/*Fktn* KO mice, phosphorylated S6, which is downstream of mTORC1, was localized to both muscle fibers and interstitial areas and its levels correlated strongly with proportions of

fibrosis. It is therefore possible rapamycin inhibits fibrosis in dystrophic muscle through inhibition of fibroblast proliferation or synthesis.

While we anticipate that a reduction in fibrosis and an associated preservation of myofiber content should improve dystrophic muscle function, muscle weakness precedes extensive fibrosis in some animal models of muscular dystrophy (e.g. (50,336)). Conversely, the *mdx-5cv* mouse is weaker than the *mdx* mouse despite that their muscles are equally fibrotic (104). Treatment of *mdx* mice with rapamycin-loaded nanoparticles resulted in a rapid improvement in grip strength without reducing muscle fibrosis. In that study, mice were dosed twice weekly for 4 weeks at approximately 0.002mg/mouse, which is significantly lower than our daily 2mg/kg treatment (approximately 0.05mg/mouse at 20 g, 28 compared to 8 doses) (232). These results seem to suggest that the functional improvements observed in Myf5/*Fktn* mice dosed with rapamycin for 4 weeks cannot be attributed solely to a decreased fibrosis. Furthermore, they may indicate that rapamycin dose-dependently affects dystrophic muscle function and fibrosis; that is, low-dose rapamycin may improve function while higher doses are required to produce the histological improvements we report. However, we also performed a 4 week drug trial with rapamycin administered at 2mg/kg 3 times weekly and observed no functional improvement although it should be noted that we did not take *in situ* torque measurements, which is a substantially more sensitive method for evaluating muscle function than the forelimb grip strength test. Despite this, we found an apparent reduction in endomysial fibrosis of iliopsoas of treated mice without a change in numbers of regenerated fibers nor any protection from exercise-induced damage (not shown). These results suggest that rapamycin treatment dose-dependently preserves myofibers in

dystroglycanopathy muscle, but also illustrates that there are likely fibroblast-independent actions of rapamycin in dystrophic muscle.

In *mdx* mice, these actions are reported to be linked to autophagy, but in Myf5/*Fktn* KO mice autophagy is not overtly impaired. It should be noted that while we observed a significant genotype-linked increase in LC3B-II, the effect was marginal relative to the rise in Beclin-1 levels in Myf5/Fktn KO mice. As Beclin-1 is involved in the earlier nucleation of budding phagophores and LC3B appears later in autophagosome formation, we cannot rule out the possibility that autophagy is defective at a point following Beclin-1 activity in dystroglycanopathy muscle (337). Further experiments are therefore required to definitively establish that autophagy is indeed elevated in Myf5/Fktn KO animals. Rapamycin treatment appears to produce a modest increase in autophagy, as measured by Beclin-1 protein levels, in LC mice but decreases it in KO mice which, consistent with our other data, may indicate decreased myofiber turnover. However, the mechanism by which rapamycin prevents damage in dystroglycanopathy muscle remains unknown.

Rapamycin acts through a binding interaction with 12 kDa FK-506 binding protein (FKBP12); the rapamycin-FKBP12 complex is then able to bind to mTORC1 but not mTORC2 and apparently blocks substrate access to the mTOR catalytic domain (230). Interestingly, mice haplodeficient for FKBP12 have improved resistance to fatigue and an increase in type I muscle fibers. Very low dose rapamycin (10μg/kg) given intraperitoneally every other day for 6 weeks also increased diaphragm endurance in mice, while modest increases in type I fibers were observed following 2 weeks of this dosing regimen. Diaphragms isolated and incubated with 1nM, but not 10nM, rapamycin

also demonstrated decreased force deficits following consecutive contractions, indicating dose dependence of this effect that may likewise extend to the alterations in muscle fiber type (338). Indeed, while higher doses of rapamycin do inhibit Akt- or functional overload-induced muscle hypertrophy, they have no apparent effect on fiber types (212,339). It is therefore unlikely that an increase in myofiber stability is mediated through a change in fiber type following daily oral rapamycin treatment. These results also highlight that all beneficial effects of rapamycin may not scale with higher doses. However, given that dystrophic muscle often contains pronounced inflammatory and fibrotic phenotypes that may be ameliorated by rapamycin treatment, we expect that stronger inhibition of mTORC1 activity should correspond to relatively greater improvements in muscle health. It is also important to consider that dynamic interplay between the inflammatory, regenerative, and matrix synthesis responses likely contributes to successful repair events after muscle damage. Rapamycin treatment may help to restore the proper balance between these processes, ultimately improving muscle regeneration in a way that is not solely related to the myogenic potential of muscle precursor cells (Figure 4.1).

Our findings merit a more rigorous preclinical evaluation of mTORC1 inhibition for dystroglycanopathy. Although it is true that higher dose rapamycin treatment does not guarantee improved efficacy, we contend that since daily, but not 3 times/week, rapamycin treatment improves functional parameters in Myf5/*Fktn* KO mice our study is likely at the lower end of the effective dosing spectrum. Encouragingly, we did not observe kidney or liver toxicity following daily rapamycin treatment, which suggests that it may be safe to proceed to greater doses. However, as noted in the previous chapter, the

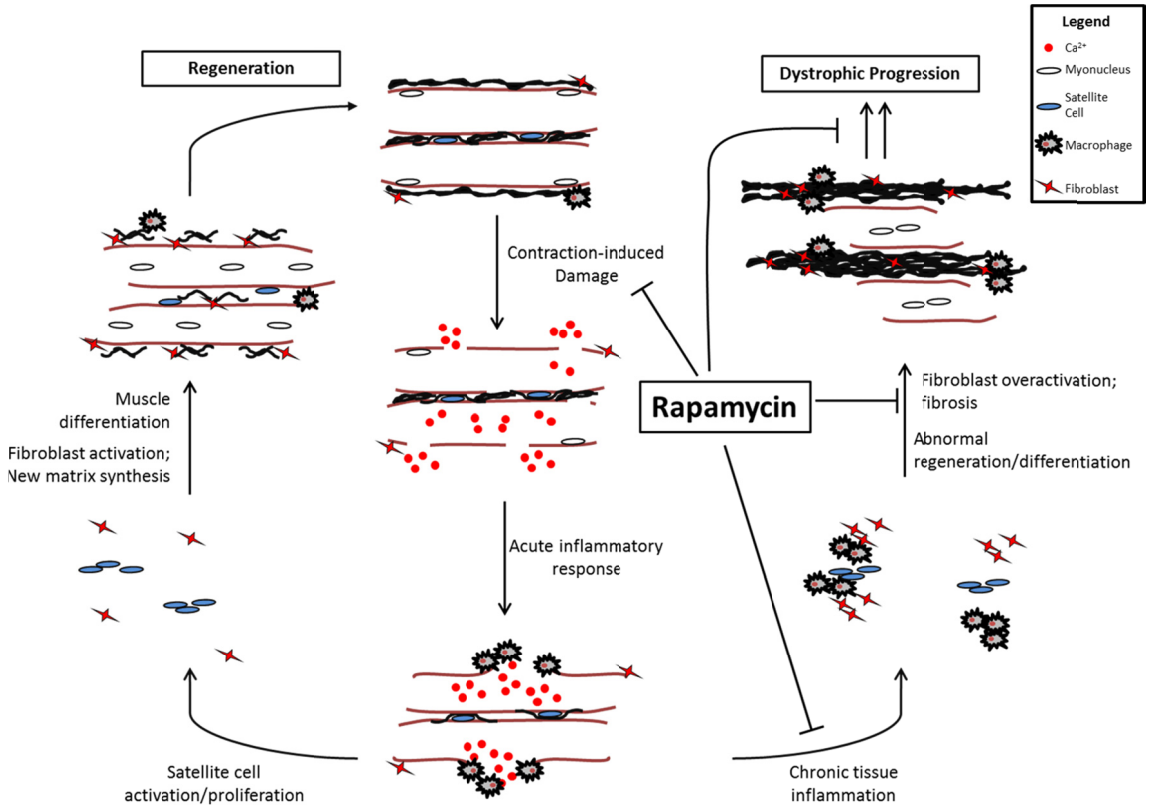

Figure 4.1 Roles for rapamycin in dystrophic muscle. The sarcolemma is damaged during muscle contraction, allowing Ca^{2+} (red dots) to flow into the cell and resulting in necrosis. Cellular debris is cleared via macrophages (gray) in an acute inflammatory response to injury. (Left) Satellite cells proliferate and mature during muscle regeneration. Later, they fuse and differentiate into mature myofibers, while fibroblasts (red stars) are activated to synthesize new extracellular matrix components. Myonuclei reside in the center of new muscle fibers following regeneration, and later migrate to the cell periphery. (Right) In dystrophic muscle, inflammation persists through repeated cycles of myofiber degeneration, resulting in misregulation of signals required for proper regeneration. This can lead to overactivation of fibroblasts, which causes excessive deposition of matrix proteins. Rapamycin may increase muscle fiber stability and reduce contraction induced damage, act as an anti-inflammatory, or inhibit mTOR-mediated matrix synthesis, ultimately delaying disease progression.

dose used here is near the limit used clinically (after applying allometric scaling). Therefore, it may be desirable to utilize mTORC1 inhibitors with enhanced pharmacological properties, especially in light of the poor aqueous solubility and bioavailability of rapamycin. A number of rapamycin derivative compounds, termed "rapalogs," have been developed in an effort to improve mTORC1 targeting *in vivo*. Among these, two (everolimus and temsirolimus) are now approved for clinical use. Temsirolimus is administered intravenously and is essentially a water-soluble rapamycin prodrug that is metabolized to sirolimus, while everolimus can be taken orally and does not require metabolism for activation. Both offer a distinct improvement in terms of bioavailability when compared to rapamycin, which is primarily eliminated in fecal matter (340,341). Notably, development of mTOR inhibitors has taken a turn in recent years, due to the identification of the rapamycin-insensitive mTORC2 upstream of Akt as well as the discovery that mTORC1 inhibition can lead to feedback activation of Akt. The vast majority of clinical trials utilizing mTOR inhibitors are aimed at treating cancers in which activation of Akt is a central determinant of malignancy. Thus, substantial efforts have been made to synthesize mTOR kinase inhibitors that target both mTORC1 and mTORC2, or, alternatively, ATP-competitive kinase inhibitors with dual specificity for TORCs and phosphoinositide3-kinases, and therefore block both upstream inputs to Akt (342,343) (Table 4.1). Importantly for our work, the effects of Akt inhibition are less clear in muscular dystrophy than are those of mTORC1 inhibition. Consequently, we expect that newer rapalogs rather than second-generation kinase inhibitors may provide the best opportunity for therapeutic benefit in muscular dystrophy patients; furthermore, because it is available orally and has been used successfully in pediatric populations,

Table 4.1 Selected mTOR Inhibitors

Drug	Clinical Use	Target
Rapamycin (Sirolimus, Rapamune)	Organ rejection (Approved)	mTORC1
Everolimus (RAD001, Afinitor)	Advanced renal cell carcinoma (Approved); Subependymal giant astrocytoma (Approved)	mTORC1
Temsirolimus (CCI-779, Torisel)	Advanced renal cell carcinoma (Approved)	mTORC1
Ridaforolimus (Taltorvic)	Metastatic soft tissue sarcoma; Bone Sarcoma (Phase III)	mTORC1
CC-223	Multiple myeloma; Diffuse large B-cell lymphoma; Glioblastoma; Hepatocellular carcinoma; Non-small cell lung cancer; hormone+ breast cancer (Phase I/II)	mTORC1/2
Sapanisertib (INK-128)	Non-small cell lung carcinoma; Non-hematologic malignancy; Hepatocellular carcinoma; Glioblastoma; Advanced solid malignancies; thyroid cancer (Phase I/II)	mTORC1/2
Apitolisib (GDC-0980)	Renal cell carcinoma; breast cancer; Non-Hodgkin's lymphoma; Solid cancers; Endometrial carcinoma; Prostate cancer (Phase I/II)	PI3K/mTOR
XL765	Glioblastoma; Non-small cell lung cancer; breast cancer (Phase I/II)	PI3K/mTOR
Dactolisib (NVP-BEZ235)	Transitional cell carcinoma*; Castration-resistant prostate cancer*; Pancreatic neuroendocrine tumors*; Acute lymphoblastic leukemia; Breast cancer; Malignant solid tumor (Phase I/II)	PI3K/mTOR

everolimus is likely to be the most successful compound for further preclinical evaluation.

The need for new therapeutics to treat muscular dystrophy is as urgent now as it has ever been. Unsuccessful clinical trials for promising drug candidates have underscored the challenge of actually bringing drugs to market for these diseases. The work presented here offers evidence in favor of the use of the mTORC1 inhibitor rapamycin for the treatment of dystroglycanopathy. This strategy offers the apparent advantage of inhibiting certain disease processes that may be common to several dystrophin-glycoprotein complex-related muscular dystrophies, although it should be cautioned that some essential physiological functions are ascribed to mTOR signaling in muscle and that proper determination of optimum dose and treatment schedules will require care. Furthermore, our dosing study was initiated in 8 week old Myf5/*Fktn* KO mice, which are typically situated midway in the dystrophic process (i.e. active degeneration and regeneration). It is not unknown whether rapamycin or a related drug is capable of reversing later-stage disease features, nor is it clear whether treatment beginning at an even earlier stage would be more effective. These considerations are important because severe dystroglycanopathies are congenital, meaning that muscle weakness presents at or just after birth. Ultimately, translation of the findings presented here into therapeutics for muscular dystrophy would require analysis of the effective timeline of mTORC1 inhibition, especially with regards to the period during which it is capable of enhancing the function of dystrophic muscle, and an evaluation of its ability to extend lifespan in a lethal muscular dystrophy model (e.g. Myf5/*Fktn* KO mice). Our analysis has also been limited with respect to determination of the effects of rapamycin

on different muscle types although the iliopsoas, the primary muscle assessed here, is one of the most severely affected in the model used and therefore lends the promise of an effect in others; it will also be of use to verify the effect found here in another dystroglycanopathy model (to ensure that it is not fukutin-specific) and to more systematically evaluate rapamycin in models of other dystrophin-glycoprotein complex-related muscular dystrophies. In summation, the results of this work set the stage for additional analysis of rapamycin or rapalogs in models of muscular dystrophy, and, potentially, human muscular dystrophy patients.

REFERENCES

1. Parsons, E. P., Bradley, D. M., and Clarke, A. J. (2003) Newborn screening for Duchenne muscular dystrophy. *Arch Dis Child* **88**, 91-92

2. Emery, A. E. (1991) Population frequencies of inherited neuromuscular diseases--a world survey. *Neuromuscular disorders : NMD* **1**, 19-29

3. Davies, K. E., Pearson, P. L., Harper, P. S., Murray, J. M., O'Brien, T., Sarfarazi, M., and Williamson, R. (1983) Linkage analysis of two cloned DNA sequences flanking the Duchenne muscular dystrophy locus on the short arm of the human X chromosome. *Nucleic acids research* **11**, 2303-2312

4. Murray, J. M., Davies, K. E., Harper, P. S., Meredith, L., Mueller, C. R., and Williamson, R. (1982) Linkage relationship of a cloned DNA sequence on the short arm of the X chromosome to Duchenne muscular dystrophy. *Nature* **300**, 69-71

5. Hoffman, E. P., Brown, R. H., Jr., and Kunkel, L. M. (1987) Dystrophin: the protein product of the Duchenne muscular dystrophy locus. *Cell* **51**, 919-928

6. Zubrzycka-Gaarn, E. E., Bulman, D. E., Karpati, G., Burghes, A. H., Belfall, B., Klamut, H. J., Talbot, J., Hodges, R. S., Ray, P. N., and Worton, R. G. (1988) The Duchenne muscular dystrophy gene product is localized in sarcolemma of human skeletal muscle. *Nature* **333**, 466-469

7. Campbell, K. P., and Kahl, S. D. (1989) Association of dystrophin and an integral membrane glycoprotein. *Nature* **338**, 259-262

8. Ervasti, J. M., and Campbell, K. P. (1993) A role for the dystrophin-glycoprotein complex as a transmembrane linker between laminin and actin. *The Journal of cell biology* **122**, 809-823

9. Rybakova, I. N., Amann, K. J., and Ervasti, J. M. (1996) A new model for the interaction of dystrophin with F-actin. *The Journal of cell biology* **135**, 661-672

10. Rybakova, I. N., Patel, J. R., and Ervasti, J. M. (2000) The dystrophin complex forms a mechanically strong link between the sarcolemma and costameric actin. *The Journal of cell biology* **150**, 1209-1214

11. Ervasti, J. M., and Campbell, K. P. (1991) Membrane organization of the dystrophin-glycoprotein complex. *Cell* **66**, 1121-1131

12. Ibraghimov-Beskrovnaya, O., Ervasti, J. M., Leveille, C. J., Slaughter, C. A., Sernett, S. W., and Campbell, K. P. (1992) Primary structure of dystrophin-associated glycoproteins linking dystrophin to the extracellular matrix. *Nature* **355**, 696-702

13. Holt, K. H., Crosbie, R. H., Venzke, D. P., and Campbell, K. P. (2000) Biosynthesis of dystroglycan: processing of a precursor propeptide. *FEBS letters* **468**, 79-83

14. Crosbie, R. H., Heighway, J., Venzke, D. P., Lee, J. C., and Campbell, K. P. (1997) Sarcospan, the 25-kDa transmembrane component of the dystrophin-glycoprotein complex. *The Journal of biological chemistry* **272**, 31221-31224

15. Suzuki, A., Yoshida, M., and Ozawa, E. (1995) Mammalian alpha 1- and beta 1-syntrophin bind to the alternative splice-prone region of the dystrophin COOH terminus. *The Journal of cell biology* **128**, 373-381

16. Peng, H. B., Ali, A. A., Daggett, D. F., Rauvala, H., Hassell, J. R., and Smalheiser, N. R. (1998) The relationship between perlecan and dystroglycan and its implication in the formation of the neuromuscular junction. *Cell adhesion and communication* **5**, 475-489

17. Gee, S. H., Montanaro, F., Lindenbaum, M. H., and Carbonetto, S. (1994) Dystroglycan-alpha, a dystrophin-associated glycoprotein, is a functional agrin receptor. *Cell* **77**, 675-686

18. Sugiyama, J., Bowen, D. C., and Hall, Z. W. (1994) Dystroglycan binds nerve and muscle agrin. *Neuron* **13**, 103-115

19. Campanelli, J. T., Roberds, S. L., Campbell, K. P., and Scheller, R. H. (1994) A role for dystrophin-associated glycoproteins and utrophin in agrin-induced AChR clustering. *Cell* **77**, 663-674

20. Talts, J. F., Andac, Z., Gohring, W., Brancaccio, A., and Timpl, R. (1999) Binding of the G domains of laminin alpha1 and alpha2 chains and perlecan to heparin, sulfatides, alpha-dystroglycan and several extracellular matrix proteins. *The EMBO journal* **18**, 863-870

21. Sugita, S., Saito, F., Tang, J., Satz, J., Campbell, K., and Sudhof, T. C. (2001) A stoichiometric complex of neurexins and dystroglycan in brain. *The Journal of cell biology* **154**, 435-445

22. Kanagawa, M., Omori, Y., Sato, S., Kobayashi, K., Miyagoe-Suzuki, Y., Takeda, S., Endo, T., Furukawa, T., and Toda, T. (2010) Post-translational maturation of dystroglycan is necessary for pikachurin binding and ribbon synaptic localization. *The Journal of biological chemistry* **285**, 31208-31216

23. Flanigan, K. M., Dunn, D. M., von Niederhausern, A., Soltanzadeh, P., Gappmaier, E., Howard, M. T., Sampson, J. B., Mendell, J. R., Wall, C., King, W. M., Pestronk, A., Florence, J. M., Connolly, A. M., Mathews, K. D., Stephan, C. M., Laubenthal, K. S., Wong, B. L., Morehart, P. J., Meyer, A., Finkel, R. S., Bonnemann, C. G., Medne, L., Day, J. W., Dalton, J. C., Margolis, M. K., Hinton, V. J., United Dystrophinopathy Project, C., and Weiss, R. B. (2009) Mutational spectrum of DMD mutations in dystrophinopathy patients: application of modern diagnostic techniques to a large cohort. *Hum Mutat* **30**, 1657-1666

24. Deburgrave, N., Daoud, F., Llense, S., Barbot, J. C., Recan, D., Peccate, C., Burghes, A. H., Beroud, C., Garcia, L., Kaplan, J. C., Chelly, J., and Leturcq, F. (2007) Protein- and mRNA-based phenotype-genotype correlations in DMD/BMD with point mutations and molecular basis for BMD with nonsense and frameshift mutations in the DMD gene. *Hum Mutat* **28**, 183-195

25. Koenig, M., Beggs, A. H., Moyer, M., Scherpf, S., Heindrich, K., Bettecken, T., Meng, G., Muller, C. R., Lindlof, M., Kaariainen, H., de la Chapellet, A., Kiuru, A., Savontaus, M. L., Gilgenkrantz, H., Recan, D., Chelly, J., Kaplan, J. C., Covone, A. E., Archidiacono, N., Romeo, G., Liechti-Gailati, S., Schneider, V., Braga, S., Moser, H., Darras, B. T., Murphy, P., Francke, U., Chen, J. D., Morgan, G., Denton, M., Greenberg, C. R., Wrogemann, K., Blonden, L. A., van Paassen, M. B., van Ommen, G. J., and Kunkel, L. M. (1989) The molecular basis for Duchenne versus Becker muscular dystrophy: correlation of severity with type of deletion. *American journal of human genetics* **45**, 498-506

26. Sadoulet-Puccio, H. M., and Kunkel, L. M. (1996) Dystrophin and its isoforms. *Brain Pathol* **6**, 25-35

27. Culligan, K. G., Mackey, A. J., Finn, D. M., Maguire, P. B., and Ohlendieck, K. (1998) Role of dystrophin isoforms and associated proteins in muscular dystrophy (review). *Int J Mol Med* **2**, 639-648

28. Blake, D. J., Hawkes, R., Benson, M. A., and Beesley, P. W. (1999) Different dystrophin-like complexes are expressed in neurons and glia. *The Journal of cell biology* **147**, 645-658

29. Blake, D. J., Weir, A., Newey, S. E., and Davies, K. E. (2002) Function and genetics of dystrophin and dystrophin-related proteins in muscle. *Physiological reviews* **82**, 291-329

30. Felisari, G., Martinelli Boneschi, F., Bardoni, A., Sironi, M., Comi, G. P., Robotti, M., Turconi, A. C., Lai, M., Corrao, G., and Bresolin, N. (2000) Loss of Dp140 dystrophin isoform and intellectual impairment in Duchenne dystrophy. *Neurology* **55**, 559-564

31. Magri, F., Govoni, A., D'Angelo, M. G., Del Bo, R., Ghezzi, S., Sandra, G., Turconi, A. C., Sciacco, M., Ciscato, P., Bordoni, A., Tedeschi, S., Fortunato, F., Lucchini, V., Bonato, S., Lamperti, C., Coviello, D., Torrente, Y., Corti, S., Moggio, M., Bresolin, N., and Comi, G. P. (2011) Genotype and phenotype characterization in a large dystrophinopathic cohort with extended follow-up. *J Neurol* **258**, 1610-1623

32. Tarakci, H., and Berger, J. (2016) The sarcoglycan complex in skeletal muscle. *Front Biosci (Landmark Ed)* **21**, 744-756

33. Hack, A. A., Groh, M. E., and McNally, E. M. (2000) Sarcoglycans in muscular dystrophy. *Microscopy research and technique* **48**, 167-180

34. Kameya, S., Miyagoe, Y., Nonaka, I., Ikemoto, T., Endo, M., Hanaoka, K., Nabeshima, Y., and Takeda, S. (1999) alpha1-syntrophin gene disruption results in the absence of neuronal-type nitric-oxide synthase at the sarcolemma but does not induce muscle degeneration. *The Journal of biological chemistry* **274**, 2193-2200

35. Jones, K. J., Compton, A. G., Yang, N., Mills, M. A., Peters, M. F., Mowat, D., Kunkel, L. M., Froehner, S. C., and North, K. N. (2003) Deficiency of the syntrophins and alpha-dystrobrevin in patients with inherited myopathy. *Neuromuscular disorders : NMD* **13**, 456-467

36. Durbeej, M., and Campbell, K. P. (2002) Muscular dystrophies involving the dystrophin-glycoprotein complex: an overview of current mouse models. *Current opinion in genetics & development* **12**, 349-361

37. Metzinger, L., Blake, D. J., Squier, M. V., Anderson, L. V., Deconinck, A. E., Nawrotzki, R., Hilton-Jones, D., and Davies, K. E. (1997) Dystrobrevin deficiency at the sarcolemma of patients with muscular dystrophy. *Human molecular genetics* **6**, 1185-1191

38. Grady, R. M., Grange, R. W., Lau, K. S., Maimone, M. M., Nichol, M. C., Stull, J. T., and Sanes, J. R. (1999) Role for alpha-dystrobrevin in the pathogenesis of dystrophin-dependent muscular dystrophies. *Nature cell biology* **1**, 215-220

39. Nakamori, M., and Takahashi, M. P. (2011) The role of alpha-dystrobrevin in striated muscle. *Int J Mol Sci* **12**, 1660-1671

40. Lebakken, C. S., Venzke, D. P., Hrstka, R. F., Consolino, C. M., Faulkner, J. A., Williamson, R. A., and Campbell, K. P. (2000) Sarcospan-deficient mice maintain normal muscle function. *Molecular and cellular biology* **20**, 1669-1677

41. Peter, A. K., Marshall, J. L., and Crosbie, R. H. (2008) Sarcospan reduces dystrophic pathology: stabilization of the utrophin-glycoprotein complex. *The Journal of cell biology* **183**, 419-427

42. Marshall, J. L., Chou, E., Oh, J., Kwok, A., Burkin, D. J., and Crosbie-Watson, R. H. (2012) Dystrophin and utrophin expression require sarcospan: loss of alpha7 integrin exacerbates a newly discovered muscle phenotype in sarcospan-null mice. *Human molecular genetics* **21**, 4378-4393

43. Hara, Y., Balci-Hayta, B., Yoshida-Moriguchi, T., Kanagawa, M., Beltran-Valero de Bernabe, D., Gundesli, H., Willer, T., Satz, J. S., Crawford, R. W., Burden, S. J., Kunz, S., Oldstone, M. B., Accardi, A., Talim, B., Muntoni, F., Topaloglu, H., Dincer, P., and Campbell, K. P. (2011) A dystroglycan mutation associated with limb-girdle muscular dystrophy. *The New England journal of medicine* **364**, 939-946

44. Geis, T., Marquard, K., Rodl, T., Reihle, C., Schirmer, S., von Kalle, T., Bornemann, A., Hehr, U., and Blankenburg, M. (2013) Homozygous dystroglycan mutation associated with a novel muscle-eye-brain disease-like phenotype with multicystic leucodystrophy. *Neurogenetics* **14**, 205-213

45. Yoshida-Moriguchi, T., and Campbell, K. P. (2015) Matriglycan: a novel polysaccharide that links dystroglycan to the basement membrane. *Glycobiology* **25**, 702-713

46. Beltran-Valero de Bernabe, D., Currier, S., Steinbrecher, A., Celli, J., van Beusekom, E., van der Zwaag, B., Kayserili, H., Merlini, L., Chitayat, D., Dobyns, W. B., Cormand, B., Lehesjoki, A. E., Cruces, J., Voit, T., Walsh, C. A., van Bokhoven, H., and Brunner, H. G. (2002) Mutations in the O-mannosyltransferase gene POMT1 give rise to the severe neuronal migration disorder Walker-Warburg syndrome. *American journal of human genetics* **71**, 1033-1043

47. van Reeuwijk, J., Janssen, M., van den Elzen, C., Beltran-Valero de Bernabe, D., Sabatelli, P., Merlini, L., Boon, M., Scheffer, H., Brockington, M., Muntoni, F., Huynen, M. A., Verrips, A., Walsh, C. A., Barth, P. G., Brunner, H. G., and van Bokhoven, H. (2005) POMT2 mutations cause alpha-dystroglycan hypoglycosylation and Walker-Warburg syndrome. *Journal of medical genetics* **42**, 907-912

48. Hara, Y., Kanagawa, M., Kunz, S., Yoshida-Moriguchi, T., Satz, J. S., Kobayashi, Y. M., Zhu, Z., Burden, S. J., Oldstone, M. B., and Campbell, K. P. (2011) Like-acetylglucosaminyltransferase (LARGE)-dependent modification of dystroglycan at Thr-317/319 is required for laminin binding and arenavirus infection. *Proceedings of the National Academy of Sciences of the United States of America* **108**, 17426-17431

49. Yoshida-Moriguchi, T., Willer, T., Anderson, M. E., Venzke, D., Whyte, T., Muntoni, F., Lee, H., Nelson, S. F., Yu, L., and Campbell, K. P. (2013) SGK196 is a glycosylation-specific O-mannose kinase required for dystroglycan function. *Science* **341**, 896-899

50. Beedle, A. M., Turner, A. J., Saito, Y., Lueck, J. D., Foltz, S. J., Fortunato, M. J., Nienaber, P. M., and Campbell, K. P. (2012) Mouse fukutin deletion impairs dystroglycan processing and recapitulates muscular dystrophy. *The Journal of clinical investigation* **122**, 3330-3342

51. Kuga, A., Kanagawa, M., Sudo, A., Chan, Y. M., Tajiri, M., Manya, H., Kikkawa, Y., Nomizu, M., Kobayashi, K., Endo, T., Lu, Q. L., Wada, Y., and Toda, T. (2012) Absence of post-phosphoryl modification in dystroglycanopathy mouse models and wild-type tissues expressing non-laminin binding form of alpha-dystroglycan. *The Journal of biological chemistry* **287**, 9560-9567

52. Kanagawa, M., Kobayashi, K., Tajiri, M., Manya, H., Kuga, A., Yamaguchi, Y., Akasaka-Manya, K., Furukawa, J. I., Mizuno, M., Kawakami, H., Shinohara, Y., Wada, Y., Endo, T., and Toda, T. (2016) Identification of a Post-translational Modification with Ribitol-Phosphate and Its Defect in Muscular Dystrophy. *Cell Rep*

53. Willer, T., Inamori, K., Venzke, D., Harvey, C., Morgensen, G., Hara, Y., Beltran Valero de Bernabe, D., Yu, L., Wright, K. M., and Campbell, K. P. (2014) The glucuronyltransferase B4GAT1 is required for initiation of LARGE-mediated alpha-dystroglycan functional glycosylation. *eLife* **3**

54. Praissman, J. L., Live, D. H., Wang, S., Ramiah, A., Chinoy, Z. S., Boons, G. J., Moremen, K. W., and Wells, L. (2014) B4GAT1 is the priming enzyme for the LARGE-dependent functional glycosylation of alpha-dystroglycan. *eLife* **3**

55. Praissman, J. L., Willer, T., Sheikh, M. O., Toi, A., Chitayat, D., Lin, Y. Y., Lee, H., Stalnaker, S. H., Wang, S., Prabhakar, P. K., Nelson, S. F., Stemple, D. L., Moore, S. A., Moremen, K. W., Campbell, K. P., and Wells, L. (2016) The functional O-mannose glycan on alpha-dystroglycan contains a phospho-ribitol primed for matriglycan addition. *eLife* **5**

56. Inamori, K., Yoshida-Moriguchi, T., Hara, Y., Anderson, M. E., Yu, L., and Campbell, K. P. (2012) Dystroglycan function requires xylosyl- and glucuronyltransferase activities of LARGE. *Science* **335**, 93-96

57. Goddeeris, M. M., Wu, B., Venzke, D., Yoshida-Moriguchi, T., Saito, F., Matsumura, K., Moore, S. A., and Campbell, K. P. (2013) LARGE glycans on dystroglycan function as a tunable matrix scaffold to prevent dystrophy. *Nature* **503**, 136-140

58. Vuillaumier-Barrot, S., Bouchet-Seraphin, C., Chelbi, M., Devisme, L., Quentin, S., Gazal, S., Laquerriere, A., Fallet-Bianco, C., Loget, P., Odent, S., Carles, D., Bazin, A., Aziza, J., Clemenson, A., Guimiot, F., Bonniere, M., Monnot, S., Bole-Feysot, C., Bernard, J. P., Loeuillet, L., Gonzales, M., Socha, K., Grandchamp, B., Attie-Bitach, T., Encha-Razavi, F., and Seta, N. (2012) Identification of mutations in TMEM5 and ISPD as a cause of severe cobblestone lissencephaly. *American journal of human genetics* **91**, 1135-1143

59. Willer, T., Lee, H., Lommel, M., Yoshida-Moriguchi, T., de Bernabe, D. B., Venzke, D., Cirak, S., Schachter, H., Vajsar, J., Voit, T., Muntoni, F., Loder, A. S., Dobyns, W. B., Winder, T. L., Strahl, S., Mathews, K. D., Nelson, S. F., Moore, S. A., and Campbell, K. P. (2012) ISPD loss-of-function mutations disrupt dystroglycan O-mannosylation and cause Walker-Warburg syndrome. *Nature genetics* **44**, 575-580

60. Riemersma, M., Froese, D. S., van Tol, W., Engelke, U. F., Kopec, J., van Scherpenzeel, M., Ashikov, A., Krojer, T., von Delft, F., Tessari, M., Buczkowska, A., Swiezewska, E., Jae, L. T., Brummelkamp, T. R., Manya, H., Endo, T., van Bokhoven, H., Yue, W. W., and Lefeber, D. J. (2015) Human ISPD Is a Cytidyltransferase Required for Dystroglycan O-Mannosylation. *Chem Biol* **22**, 1643-1652

61. Lefeber, D. J., Schonberger, J., Morava, E., Guillard, M., Huyben, K. M., Verrijp, K., Grafakou, O., Evangeliou, A., Preijers, F. W., Manta, P., Yildiz, J., Grunewald, S., Spilioti, M., van den Elzen, C., Klein, D., Hess, D., Ashida, H., Hofsteenge, J., Maeda, Y., van den Heuvel, L., Lammens, M., Lehle, L., and Wevers, R. A. (2009) Deficiency of Dol-P-Man synthase subunit DPM3 bridges the congenital disorders of glycosylation with the dystroglycanopathies. *American journal of human genetics* **85**, 76-86

62. Barone, R., Aiello, C., Race, V., Morava, E., Foulquier, F., Riemersma, M., Passarelli, C., Concolino, D., Carella, M., Santorelli, F., Vleugels, W., Mercuri, E., Garozzo, D., Sturiale, L., Messina, S., Jaeken, J., Fiumara, A., Wevers, R. A., Bertini, E., Matthijs, G., and Lefeber, D. J. (2012) DPM2-CDG: a muscular dystrophy-dystroglycanopathy syndrome with severe epilepsy. *Annals of neurology* **72**, 550-558

63. Yang, A. C., Ng, B. G., Moore, S. A., Rush, J., Waechter, C. J., Raymond, K. M., Willer, T., Campbell, K. P., Freeze, H. H., and Mehta, L. (2013) Congenital disorder of glycosylation due to DPM1 mutations presenting with dystroglycanopathy-type congenital muscular dystrophy. *Molecular genetics and metabolism* **110**, 345-351

64. Carss, K. J., Stevens, E., Foley, A. R., Cirak, S., Riemersma, M., Torelli, S., Hoischen, A., Willer, T., van Scherpenzeel, M., Moore, S. A., Messina, S., Bertini, E., Bonnemann, C. G., Abdenur, J. E., Grosmann, C. M., Kesari, A.,

Punetha, J., Quinlivan, R., Waddell, L. B., Young, H. K., Wraige, E., Yau, S., Brodd, L., Feng, L., Sewry, C., MacArthur, D. G., North, K. N., Hoffman, E., Stemple, D. L., Hurles, M. E., van Bokhoven, H., Campbell, K. P., Lefeber, D. J., Consortium, U. K., Lin, Y. Y., and Muntoni, F. (2013) Mutations in GDP-mannose pyrophosphorylase B cause congenital and limb-girdle muscular dystrophies associated with hypoglycosylation of alpha-dystroglycan. *American journal of human genetics* **93**, 29-41

65. Combs, A. C., and Ervasti, J. M. (2005) Enhanced laminin binding by alpha-dystroglycan after enzymatic deglycosylation. *The Biochemical journal* **390**, 303-309

66. Manya, H., Sakai, K., Kobayashi, K., Taniguchi, K., Kawakita, M., Toda, T., and Endo, T. (2003) Loss-of-function of an N-acetylglucosaminyltransferase, POMGnT1, in muscle-eye-brain disease. *Biochemical and biophysical research communications* **306**, 93-97

67. Chiba, A., Matsumura, K., Yamada, H., Inazu, T., Shimizu, T., Kusunoki, S., Kanazawa, I., Kobata, A., and Endo, T. (1997) Structures of sialylated O-linked oligosaccharides of bovine peripheral nerve alpha-dystroglycan. The role of a novel O-mannosyl-type oligosaccharide in the binding of alpha-dystroglycan with laminin. *The Journal of biological chemistry* **272**, 2156-2162

68. Liu, J., Yang, Y., Li, X., Zhang, P., Qi, Y., and Hu, H. (2010) Cellular and molecular characterization of abnormal brain development in protein o-mannose N-acetylglucosaminyltransferase 1 knockout mice. *Methods Enzymol* **479**, 353-366

69. Yoshida, A., Kobayashi, K., Manya, H., Taniguchi, K., Kano, H., Mizuno, M., Inazu, T., Mitsuhashi, H., Takahashi, S., Takeuchi, M., Herrmann, R., Straub, V., Talim, B., Voit, T., Topaloglu, H., Toda, T., and Endo, T. (2001) Muscular dystrophy and neuronal migration disorder caused by mutations in a glycosyltransferase, POMGnT1. *Dev Cell* **1**, 717-724

70. Xiong, H., Kobayashi, K., Tachikawa, M., Manya, H., Takeda, S., Chiyonobu, T., Fujikake, N., Wang, F., Nishimoto, A., Morris, G. E., Nagai, Y., Kanagawa, M., Endo, T., and Toda, T. (2006) Molecular interaction between fukutin and POMGnT1 in the glycosylation pathway of alpha-dystroglycan. *Biochemical and biophysical research communications* **350**, 935-941

71. Godfrey, C., Clement, E., Mein, R., Brockington, M., Smith, J., Talim, B., Straub, V., Robb, S., Quinlivan, R., Feng, L., Jimenez-Mallebrera, C., Mercuri, E., Manzur, A. Y., Kinali, M., Torelli, S., Brown, S. C., Sewry, C. A., Bushby, K., Topaloglu, H., North, K., Abbs, S., and Muntoni, F. (2007) Refining genotype phenotype correlations in muscular dystrophies with defective glycosylation of dystroglycan. *Brain* **130**, 2725-2735

72. van Reeuwijk, J., Brunner, H. G., and van Bokhoven, H. (2005) Glyc-O-genetics of Walker-Warburg syndrome. *Clin Genet* **67**, 281-289

73. Fukuyama, Y., Osawa, M., and Suzuki, H. (1981) Congenital progressive muscular dystrophy of the Fukuyama type - clinical, genetic and pathological considerations. *Brain Dev* **3**, 1-29

74. Kobayashi, K., Nakahori, Y., Miyake, M., Matsumura, K., Kondo-Iida, E., Nomura, Y., Segawa, M., Yoshioka, M., Saito, K., Osawa, M., Hamano, K., Sakakihara, Y., Nonaka, I., Nakagome, Y., Kanazawa, I., Nakamura, Y., Tokunaga, K., and Toda, T. (1998) An ancient retrotransposal insertion causes Fukuyama-type congenital muscular dystrophy. *Nature* **394**, 388-392

75. Cormand, B., Pihko, H., Bayes, M., Valanne, L., Santavuori, P., Talim, B., Gershoni-Baruch, R., Ahmad, A., van Bokhoven, H., Brunner, H. G., Voit, T., Topaloglu, H., Dobyns, W. B., and Lehesjoki, A. E. (2001) Clinical and genetic distinction between Walker-Warburg syndrome and muscle-eye-brain disease. *Neurology* **56**, 1059-1069

76. MUSCULAR DYSTROPHY-DYSTROGLYCANOPATHY (LIMB-GIRDLE), TYPE C, 1; MDDGC1.

77. Brockington, M., Blake, D. J., Prandini, P., Brown, S. C., Torelli, S., Benson, M. A., Ponting, C. P., Estournet, B., Romero, N. B., Mercuri, E., Voit, T., Sewry, C. A., Guicheney, P., and Muntoni, F. (2001) Mutations in the fukutin-related protein gene (FKRP) cause a form of congenital muscular dystrophy with secondary laminin alpha2 deficiency and abnormal glycosylation of alpha-dystroglycan. *American journal of human genetics* **69**, 1198-1209

78. Manzini, M. C., Tambunan, D. E., Hill, R. S., Yu, T. W., Maynard, T. M., Heinzen, E. L., Shianna, K. V., Stevens, C. R., Partlow, J. N., Barry, B. J., Rodriguez, J., Gupta, V. A., Al-Qudah, A. K., Eyaid, W. M., Friedman, J. M., Salih, M. A., Clark, R., Moroni, I., Mora, M., Beggs, A. H., Gabriel, S. B., and Walsh, C. A. (2012) Exome sequencing and functional validation in zebrafish identify GTDC2 mutations as a cause of Walker-Warburg syndrome. *American journal of human genetics* **91**, 541-547

79. Longman, C., Brockington, M., Torelli, S., Jimenez-Mallebrera, C., Kennedy, C., Khalil, N., Feng, L., Saran, R. K., Voit, T., Merlini, L., Sewry, C. A., Brown, S. C., and Muntoni, F. (2003) Mutations in the human LARGE gene cause MDC1D, a novel form of congenital muscular dystrophy with severe mental retardation and abnormal glycosylation of alpha-dystroglycan. *Human molecular genetics* **12**, 2853-2861

80. Stevens, E., Carss, K. J., Cirak, S., Foley, A. R., Torelli, S., Willer, T., Tambunan, D. E., Yau, S., Brodd, L., Sewry, C. A., Feng, L., Haliloglu, G., Orhan, D.,

Dobyns, W. B., Enns, G. M., Manning, M., Krause, A., Salih, M. A., Walsh, C. A., Hurles, M., Campbell, K. P., Manzini, M. C., Consortium, U. K., Stemple, D., Lin, Y. Y., and Muntoni, F. (2013) Mutations in B3GALNT2 cause congenital muscular dystrophy and hypoglycosylation of alpha-dystroglycan. *American journal of human genetics* **92**, 354-365

81. Buysse, K., Riemersma, M., Powell, G., van Reeuwijk, J., Chitayat, D., Roscioli, T., Kamsteeg, E. J., van den Elzen, C., van Beusekom, E., Blaser, S., Babul-Hirji, R., Halliday, W., Wright, G. J., Stemple, D. L., Lin, Y. Y., Lefeber, D. J., and van Bokhoven, H. (2013) Missense mutations in beta-1,3-N-acetylglucosaminyltransferase 1 (B3GNT1) cause Walker-Warburg syndrome. *Human molecular genetics* **22**, 1746-1754

82. Di Costanzo, S., Balasubramanian, A., Pond, H. L., Rozkalne, A., Pantaleoni, C., Saredi, S., Gupta, V. A., Sunu, C. M., Yu, T. W., Kang, P. B., Salih, M. A., Mora, M., Gussoni, E., Walsh, C. A., and Manzini, M. C. (2014) POMK mutations disrupt muscle development leading to a spectrum of neuromuscular presentations. *Human molecular genetics* **23**, 5781-5792

83. Jae, L. T., Raaben, M., Riemersma, M., van Beusekom, E., Blomen, V. A., Velds, A., Kerkhoven, R. M., Carette, J. E., Topaloglu, H., Meinecke, P., Wessels, M. W., Lefeber, D. J., Whelan, S. P., van Bokhoven, H., and Brummelkamp, T. R. (2013) Deciphering the glycosylome of dystroglycanopathies using haploid screens for lassa virus entry. *Science* **340**, 479-483

84. Lefeber, D. J., de Brouwer, A. P., Morava, E., Riemersma, M., Schuurs-Hoeijmakers, J. H., Absmanner, B., Verrijp, K., van den Akker, W. M., Huijben, K., Steenbergen, G., van Reeuwijk, J., Jozwiak, A., Zucker, N., Lorber, A., Lammens, M., Knopf, C., van Bokhoven, H., Grunewald, S., Lehle, L., Kapusta, L., Mandel, H., and Wevers, R. A. (2011) Autosomal recessive dilated cardiomyopathy due to DOLK mutations results from abnormal dystroglycan O-mannosylation. *PLoS Genet* **7**, e1002427

85. Sparks, S., Quijano-Roy, S., Harper, A., Rutkowski, A., Gordon, E., Hoffman, E. P., and Pegoraro, E. (2012) Congenital Muscular Dystrophy Overview. in *GeneReviews(R)* (Pagon, R. A., Adam, M. P., Ardinger, H. H., Wallace, S. E., Amemiya, A., Bean, L. J. H., Bird, T. D., Fong, C. T., Mefford, H. C., Smith, R. J. H., and Stephens, K. eds.), Seattle (WA). pp

86. Brenman, J. E., Chao, D. S., Xia, H., Aldape, K., and Bredt, D. S. (1995) Nitric oxide synthase complexed with dystrophin and absent from skeletal muscle sarcolemma in Duchenne muscular dystrophy. *Cell* **82**, 743-752

87. Thomas, G. D., and Victor, R. G. (1998) Nitric oxide mediates contraction-induced attenuation of sympathetic vasoconstriction in rat skeletal muscle. *The Journal of physiology* **506 (Pt 3)**, 817-826

88. Lau, K. S., Grange, R. W., Chang, W. J., Kamm, K. E., Sarelius, I., and Stull, J. T. (1998) Skeletal muscle contractions stimulate cGMP formation and attenuate vascular smooth muscle myosin phosphorylation via nitric oxide. *FEBS letters* **431**, 71-74

89. Kobayashi, Y. M., Rader, E. P., Crawford, R. W., Iyengar, N. K., Thedens, D. R., Faulkner, J. A., Parikh, S. V., Weiss, R. M., Chamberlain, J. S., Moore, S. A., and Campbell, K. P. (2008) Sarcolemma-localized nNOS is required to maintain activity after mild exercise. *Nature* **456**, 511-515

90. Grady, R. M., Zhou, H., Cunningham, J. M., Henry, M. D., Campbell, K. P., and Sanes, J. R. (2000) Maturation and maintenance of the neuromuscular synapse: genetic evidence for roles of the dystrophin--glycoprotein complex. *Neuron* **25**, 279-293

91. Duclos, F., Straub, V., Moore, S. A., Venzke, D. P., Hrstka, R. F., Crosbie, R. H., Durbeej, M., Lebakken, C. S., Ettinger, A. J., van der Meulen, J., Holt, K. H., Lim, L. E., Sanes, J. R., Davidson, B. L., Faulkner, J. A., Williamson, R., and Campbell, K. P. (1998) Progressive muscular dystrophy in alpha-sarcoglycan-deficient mice. *The Journal of cell biology* **142**, 1461-1471

92. Hack, A. A., Ly, C. T., Jiang, F., Clendenin, C. J., Sigrist, K. S., Wollmann, R. L., and McNally, E. M. (1998) Gamma-sarcoglycan deficiency leads to muscle membrane defects and apoptosis independent of dystrophin. *The Journal of cell biology* **142**, 1279-1287

93. Araishi, K., Sasaoka, T., Imamura, M., Noguchi, S., Hama, H., Wakabayashi, E., Yoshida, M., Hori, T., and Ozawa, E. (1999) Loss of the sarcoglycan complex and sarcospan leads to muscular dystrophy in beta-sarcoglycan-deficient mice. *Human molecular genetics* **8**, 1589-1598

94. Coral-Vazquez, R., Cohn, R. D., Moore, S. A., Hill, J. A., Weiss, R. M., Davisson, R. L., Straub, V., Barresi, R., Bansal, D., Hrstka, R. F., Williamson, R., and Campbell, K. P. (1999) Disruption of the sarcoglycan-sarcospan complex in vascular smooth muscle: a novel mechanism for cardiomyopathy and muscular dystrophy. *Cell* **98**, 465-474

95. Hack, A. A., Cordier, L., Shoturma, D. I., Lam, M. Y., Sweeney, H. L., and McNally, E. M. (1999) Muscle degeneration without mechanical injury in sarcoglycan deficiency. *Proceedings of the National Academy of Sciences of the United States of America* **96**, 10723-10728

96. Chen, J., Shi, W., Zhang, Y., Sokol, R., Cai, H., Lun, M., Moore, B. F., Farber, M. J., Stepanchick, J. S., Bonnemann, C. G., and Chan, Y. M. (2006) Identification of functional domains in sarcoglycans essential for their interaction and plasma membrane targeting. *Exp Cell Res* **312**, 1610-1625

97. Sicinski, P., Geng, Y., Ryder-Cook, A. S., Barnard, E. A., Darlison, M. G., and Barnard, P. J. (1989) The molecular basis of muscular dystrophy in the mdx mouse: a point mutation. *Science* **244**, 1578-1580

98. Chamberlain, J. S., Metzger, J., Reyes, M., Townsend, D., and Faulkner, J. A. (2007) Dystrophin-deficient mdx mice display a reduced life span and are susceptible to spontaneous rhabdomyosarcoma. *FASEB journal : official publication of the Federation of American Societies for Experimental Biology* **21**, 2195-2204

99. Helliwell, T. R., Man, N. T., Morris, G. E., and Davies, K. E. (1992) The dystrophin-related protein, utrophin, is expressed on the sarcolemma of regenerating human skeletal muscle fibres in dystrophies and inflammatory myopathies. *Neuromuscular disorders : NMD* **2**, 177-184

100. Tinsley, J. M., Potter, A. C., Phelps, S. R., Fisher, R., Trickett, J. I., and Davies, K. E. (1996) Amelioration of the dystrophic phenotype of mdx mice using a truncated utrophin transgene. *Nature* **384**, 349-353

101. Deconinck, N., Tinsley, J., De Backer, F., Fisher, R., Kahn, D., Phelps, S., Davies, K., and Gillis, J. M. (1997) Expression of truncated utrophin leads to major functional improvements in dystrophin-deficient muscles of mice. *Nature medicine* **3**, 1216-1221

102. Deconinck, A. E., Rafael, J. A., Skinner, J. A., Brown, S. C., Potter, A. C., Metzinger, L., Watt, D. J., Dickson, J. G., Tinsley, J. M., and Davies, K. E. (1997) Utrophin-dystrophin-deficient mice as a model for Duchenne muscular dystrophy. *Cell* **90**, 717-727

103. Chapman, V. M., Miller, D. R., Armstrong, D., and Caskey, C. T. (1989) Recovery of induced mutations for X chromosome-linked muscular dystrophy in mice. *Proceedings of the National Academy of Sciences of the United States of America* **86**, 1292-1296

104. Beastrom, N., Lu, H., Macke, A., Canan, B. D., Johnson, E. K., Penton, C. M., Kaspar, B. K., Rodino-Klapac, L. R., Zhou, L., Janssen, P. M., and Montanaro, F. (2011) mdx((5)cv) mice manifest more severe muscle dysfunction and diaphragm force deficits than do mdx Mice. *The American journal of pathology* **179**, 2464-2474

105. Fukada, S., Morikawa, D., Yamamoto, Y., Yoshida, T., Sumie, N., Yamaguchi, M., Ito, T., Miyagoe-Suzuki, Y., Takeda, S., Tsujikawa, K., and Yamamoto, H. (2010) Genetic background affects properties of satellite cells and mdx phenotypes. *The American journal of pathology* **176**, 2414-2424

106. Coley, W. D., Bogdanik, L., Vila, M. C., Yu, Q., Van Der Meulen, J. H., Rayavarapu, S., Novak, J. S., Nearing, M., Quinn, J. L., Saunders, A., Dolan, C., Andrews, W., Lammert, C., Austin, A., Partridge, T. A., Cox, G. A., Lutz, C., and Nagaraju, K. (2016) Effect of genetic background on the dystrophic phenotype in mdx mice. *Human molecular genetics* **25**, 130-145

107. Bassett, D. I., and Currie, P. D. (2003) The zebrafish as a model for muscular dystrophy and congenital myopathy. *Human molecular genetics* **12 Spec No 2**, R265-270

108. Guyon, J. R., Goswami, J., Jun, S. J., Thorne, M., Howell, M., Pusack, T., Kawahara, G., Steffen, L. S., Galdzicki, M., and Kunkel, L. M. (2009) Genetic isolation and characterization of a splicing mutant of zebrafish dystrophin. *Human molecular genetics* **18**, 202-211

109. Cooper, B. J., Winand, N. J., Stedman, H., Valentine, B. A., Hoffman, E. P., Kunkel, L. M., Scott, M. O., Fischbeck, K. H., Kornegay, J. N., Avery, R. J., and et al. (1988) The homologue of the Duchenne locus is defective in X-linked muscular dystrophy of dogs. *Nature* **334**, 154-156

110. Schatzberg, S. J., Olby, N. J., Breen, M., Anderson, L. V., Langford, C. F., Dickens, H. F., Wilton, S. D., Zeiss, C. J., Binns, M. M., Kornegay, J. N., Morris, G. E., and Sharp, N. J. (1999) Molecular analysis of a spontaneous dystrophin 'knockout' dog. *Neuromuscular disorders : NMD* **9**, 289-295

111. Shimatsu, Y., Katagiri, K., Furuta, T., Nakura, M., Tanioka, Y., Yuasa, K., Tomohiro, M., Kornegay, J. N., Nonaka, I., and Takeda, S. (2003) Canine X-linked muscular dystrophy in Japan (CXMDJ). *Exp Anim* **52**, 93-97

112. Nonneman, D. J., Brown-Brandl, T., Jones, S. A., Wiedmann, R. T., and Rohrer, G. A. (2012) A defect in dystrophin causes a novel porcine stress syndrome. *BMC Genomics* **13**, 233

113. Klymiuk, N., Blutke, A., Graf, A., Krause, S., Burkhardt, K., Wuensch, A., Krebs, S., Kessler, B., Zakhartchenko, V., Kurome, M., Kemter, E., Nagashima, H., Schoser, B., Herbach, N., Blum, H., Wanke, R., Aartsma-Rus, A., Thirion, C., Lochmuller, H., Walter, M. C., and Wolf, E. (2013) Dystrophin-deficient pigs provide new insights into the hierarchy of physiological derangements of dystrophic muscle. *Human molecular genetics* **22**, 4368-4382

114. Hollinger, K., Yang, C. X., Montz, R. E., Nonneman, D., Ross, J. W., and Selsby, J. T. (2014) Dystrophin insufficiency causes selective muscle histopathology and loss of dystrophin-glycoprotein complex assembly in pig skeletal muscle. *FASEB journal : official publication of the Federation of American Societies for Experimental Biology* **28**, 1600-1609

115. Collins, C. A., and Morgan, J. E. (2003) Duchenne's muscular dystrophy: animal models used to investigate pathogenesis and develop therapeutic strategies. *Int J Exp Pathol* **84**, 165-172

116. Fan, Z., Wang, J., Ahn, M., Shiloh-Malawsky, Y., Chahin, N., Elmore, S., Bagnell, C. R., Jr., Wilber, K., An, H., Lin, W., Zhu, H., Styner, M., and Kornegay, J. N. (2014) Characteristics of magnetic resonance imaging biomarkers in a natural history study of golden retriever muscular dystrophy. *Neuromuscular disorders : NMD* **24**, 178-191

117. Thibaud, J. L., Azzabou, N., Barthelemy, I., Fleury, S., Cabrol, L., Blot, S., and Carlier, P. G. (2012) Comprehensive longitudinal characterization of canine muscular dystrophy by serial NMR imaging of GRMD dogs. *Neuromuscular disorders : NMD* **22 Suppl 2**, S85-99

118. Zucconi, E., Valadares, M. C., Vieira, N. M., Bueno, C. R., Jr., Secco, M., Jazedje, T., da Silva, H. C., Vainzof, M., and Zatz, M. (2010) Ringo: discordance between the molecular and clinical manifestation in a golden retriever muscular dystrophy dog. *Neuromuscular disorders : NMD* **20**, 64-70

119. Vieira, N. M., Elvers, I., Alexander, M. S., Moreira, Y. B., Eran, A., Gomes, J. P., Marshall, J. L., Karlsson, E. K., Verjovski-Almeida, S., Lindblad-Toh, K., Kunkel, L. M., and Zatz, M. (2015) Jagged 1 Rescues the Duchenne Muscular Dystrophy Phenotype. *Cell* **163**, 1204-1213

120. Willer, T., Prados, B., Falcon-Perez, J. M., Renner-Muller, I., Przemeck, G. K., Lommel, M., Coloma, A., Valero, M. C., de Angelis, M. H., Tanner, W., Wolf, E., Strahl, S., and Cruces, J. (2004) Targeted disruption of the Walker-Warburg syndrome gene Pomt1 in mouse results in embryonic lethality. *Proceedings of the National Academy of Sciences of the United States of America* **101**, 14126-14131

121. Hu, H., Li, J., Gagen, C. S., Gray, N. W., Zhang, Z., Qi, Y., and Zhang, P. (2011) Conditional knockout of protein O-mannosyltransferase 2 reveals tissue-specific roles of O-mannosyl glycosylation in brain development. *J Comp Neurol* **519**, 1320-1337

122. Chan, Y. M., Keramaris-Vrantsis, E., Lidov, H. G., Norton, J. H., Zinchenko, N., Gruber, H. E., Thresher, R., Blake, D. J., Ashar, J., Rosenfeld, J., and Lu, Q. L. (2010) Fukutin-related protein is essential for mouse muscle, brain and eye development and mutation recapitulates the wide clinical spectrums of dystroglycanopathies. *Human molecular genetics* **19**, 3995-4006

123. Kurahashi, H., Taniguchi, M., Meno, C., Taniguchi, Y., Takeda, S., Horie, M., Otani, H., and Toda, T. (2005) Basement membrane fragility underlies embryonic lethality in fukutin-null mice. *Neurobiol Dis* **19**, 208-217

124. Williamson, R. A., Henry, M. D., Daniels, K. J., Hrstka, R. F., Lee, J. C., Sunada, Y., Ibraghimov-Beskrovnaya, O., and Campbell, K. P. (1997) Dystroglycan is essential for early embryonic development: disruption of Reichert's membrane in Dag1-null mice. *Human molecular genetics* **6**, 831-841

125. Sauer, B. (1998) Inducible gene targeting in mice using the Cre/lox system. *Methods* **14**, 381-392

126. Moore, S. A., Saito, F., Chen, J., Michele, D. E., Henry, M. D., Messing, A., Cohn, R. D., Ross-Barta, S. E., Westra, S., Williamson, R. A., Hoshi, T., and Campbell, K. P. (2002) Deletion of brain dystroglycan recapitulates aspects of congenital muscular dystrophy. *Nature* **418**, 422-425

127. Cohn, R. D., Henry, M. D., Michele, D. E., Barresi, R., Saito, F., Moore, S. A., Flanagan, J. D., Skwarchuk, M. W., Robbins, M. E., Mendell, J. R., Williamson, R. A., and Campbell, K. P. (2002) Disruption of DAG1 in differentiated skeletal muscle reveals a role for dystroglycan in muscle regeneration. *Cell* **110**, 639-648

128. Saito, F., Moore, S. A., Barresi, R., Henry, M. D., Messing, A., Ross-Barta, S. E., Cohn, R. D., Williamson, R. A., Sluka, K. A., Sherman, D. L., Brophy, P. J., Schmelzer, J. D., Low, P. A., Wrabetz, L., Feltri, M. L., and Campbell, K. P. (2003) Unique role of dystroglycan in peripheral nerve myelination, nodal structure, and sodium channel stabilization. *Neuron* **38**, 747-758

129. Satz, J. S., Barresi, R., Durbeej, M., Willer, T., Turner, A., Moore, S. A., and Campbell, K. P. (2008) Brain and eye malformations resembling Walker-Warburg syndrome are recapitulated in mice by dystroglycan deletion in the epiblast. *J Neurosci* **28**, 10567-10575

130. Lane, P. W., Beamer, T. C., and Myers, D. D. (1976) Myodystrophy, a new myopathy on chromosome 8 of the mouse. *The Journal of heredity* **67**, 135-138

131. Grewal, P. K., Holzfeind, P. J., Bittner, R. E., and Hewitt, J. E. (2001) Mutant glycosyltransferase and altered glycosylation of alpha-dystroglycan in the myodystrophy mouse. *Nature genetics* **28**, 151-154

132. Michele, D. E., Barresi, R., Kanagawa, M., Saito, F., Cohn, R. D., Satz, J. S., Dollar, J., Nishino, I., Kelley, R. I., Somer, H., Straub, V., Mathews, K. D., Moore, S. A., and Campbell, K. P. (2002) Post-translational disruption of dystroglycan-ligand interactions in congenital muscular dystrophies. *Nature* **418**, 417-422

133. Taniguchi, M., Kurahashi, H., Noguchi, S., Fukudome, T., Okinaga, T., Tsukahara, T., Tajima, Y., Ozono, K., Nishino, I., Nonaka, I., and Toda, T. (2006) Aberrant neuromuscular junctions and delayed terminal muscle fiber maturation in alpha-dystroglycanopathies. *Human molecular genetics* **15**, 1279-1289

134. Herbst, R., Iskratsch, T., Unger, E., and Bittner, R. E. (2009) Aberrant development of neuromuscular junctions in glycosylation-defective Large(myd) mice. *Neuromuscular disorders : NMD* **19**, 366-378

135. Jacobson, C., Montanaro, F., Lindenbaum, M., Carbonetto, S., and Ferns, M. (1998) alpha-Dystroglycan functions in acetylcholine receptor aggregation but is not a coreceptor for agrin-MuSK signaling. *J Neurosci* **18**, 6340-6348

136. Jacobson, C., Cote, P. D., Rossi, S. G., Rotundo, R. L., and Carbonetto, S. (2001) The dystroglycan complex is necessary for stabilization of acetylcholine receptor clusters at neuromuscular junctions and formation of the synaptic basement membrane. *The Journal of cell biology* **152**, 435-450

137. Gumerson, J. D., Davis, C. S., Kabaeva, Z. T., Hayes, J. M., Brooks, S. V., and Michele, D. E. (2013) Muscle-specific expression of LARGE restores neuromuscular transmission deficits in dystrophic LARGE(myd) mice. *Human molecular genetics* **22**, 757-768

138. Comim, C. M., Schactae, A. L., Soares, J. A., Ventura, L., Freiberger, V., Mina, F., Dominguini, D., Vainzof, M., and Quevedo, J. (2016) Behavioral Responses in Animal Model of Congenital Muscular Dystrophy 1D. *Mol Neurobiol* **53**, 402-407

139. Frosk, P., Greenberg, C. R., Tennese, A. A., Lamont, R., Nylen, E., Hirst, C., Frappier, D., Roslin, N. M., Zaik, M., Bushby, K., Straub, V., Zatz, M., de Paula, F., Morgan, K., Fujiwara, T. M., and Wrogemann, K. (2005) The most common mutation in FKRP causing limb girdle muscular dystrophy type 2I (LGMD2I) may have occurred only once and is present in Hutterites and other populations. *Hum Mutat* **25**, 38-44

140. Kanagawa, M., Nishimoto, A., Chiyonobu, T., Takeda, S., Miyagoe-Suzuki, Y., Wang, F., Fujikake, N., Taniguchi, M., Lu, Z., Tachikawa, M., Nagai, Y., Tashiro, F., Miyazaki, J., Tajima, Y., Takeda, S., Endo, T., Kobayashi, K., Campbell, K. P., and Toda, T. (2009) Residual laminin-binding activity and enhanced dystroglycan glycosylation by LARGE in novel model mice to dystroglycanopathy. *Human molecular genetics* **18**, 621-631

141. Ackroyd, M. R., Skordis, L., Kaluarachchi, M., Godwin, J., Prior, S., Fidanboylu, M., Piercy, R. J., Muntoni, F., and Brown, S. C. (2009) Reduced expression of fukutin related protein in mice results in a model for fukutin related protein associated muscular dystrophies. *Brain* **132**, 439-451

142. Blaeser, A., Keramaris, E., Chan, Y. M., Sparks, S., Cowley, D., Xiao, X., and Lu, Q. L. (2013) Mouse models of fukutin-related protein mutations show a wide range of disease phenotypes. *Hum Genet* **132**, 923-934

143. Lommel, M., Cirak, S., Willer, T., Hermann, R., Uyanik, G., van Bokhoven, H., Korner, C., Voit, T., Baric, I., Hehr, U., and Strahl, S. (2010) Correlation of enzyme activity and clinical phenotype in POMT1-associated dystroglycanopathies. *Neurology* **74**, 157-164

144. Stevens, E., Torelli, S., Feng, L., Phadke, R., Walter, M. C., Schneiderat, P., Eddaoudi, A., Sewry, C. A., and Muntoni, F. (2013) Flow cytometry for the analysis of alpha-dystroglycan glycosylation in fibroblasts from patients with dystroglycanopathies. *PloS one* **8**, e68958

145. Jimenez-Mallebrera, C., Torelli, S., Feng, L., Kim, J., Godfrey, C., Clement, E., Mein, R., Abbs, S., Brown, S. C., Campbell, K. P., Kroger, S., Talim, B., Topaloglu, H., Quinlivan, R., Roper, H., Childs, A. M., Kinali, M., Sewry, C. A., and Muntoni, F. (2009) A comparative study of alpha-dystroglycan glycosylation in dystroglycanopathies suggests that the hypoglycosylation of alpha-dystroglycan does not consistently correlate with clinical severity. *Brain Pathol* **19**, 596-611

146. Kanagawa, M., Yu, C. C., Ito, C., Fukada, S., Hozoji-Inada, M., Chiyo, T., Kuga, A., Matsuo, M., Sato, K., Yamaguchi, M., Ito, T., Ohtsuka, Y., Katanosaka, Y., Miyagoe-Suzuki, Y., Naruse, K., Kobayashi, K., Okada, T., Takeda, S., and Toda, T. (2013) Impaired viability of muscle precursor cells in muscular dystrophy with glycosylation defects and amelioration of its severe phenotype by limited gene expression. *Human molecular genetics* **22**, 3003-3015

147. Braun, T., and Gautel, M. (2011) Transcriptional mechanisms regulating skeletal muscle differentiation, growth and homeostasis. *Nature reviews. Molecular cell biology* **12**, 349-361

148. Wright, W. E., Sassoon, D. A., and Lin, V. K. (1989) Myogenin, a factor regulating myogenesis, has a domain homologous to MyoD. *Cell* **56**, 607-617

149. Edmondson, D. G., and Olson, E. N. (1989) A gene with homology to the myc similarity region of MyoD1 is expressed during myogenesis and is sufficient to activate the muscle differentiation program. *Genes & development* **3**, 628-640

150. Braun, T., Rudnicki, M. A., Arnold, H. H., and Jaenisch, R. (1992) Targeted inactivation of the muscle regulatory gene Myf-5 results in abnormal rib development and perinatal death. *Cell* **71**, 369-382

151. Rudnicki, M. A., Braun, T., Hinuma, S., and Jaenisch, R. (1992) Inactivation of MyoD in mice leads to up-regulation of the myogenic HLH gene Myf-5 and results in apparently normal muscle development. *Cell* **71**, 383-390

152. Rudnicki, M. A., Schnegelsberg, P. N., Stead, R. H., Braun, T., Arnold, H. H., and Jaenisch, R. (1993) MyoD or Myf-5 is required for the formation of skeletal muscle. *Cell* **75**, 1351-1359

153. Hasty, P., Bradley, A., Morris, J. H., Edmondson, D. G., Venuti, J. M., Olson, E. N., and Klein, W. H. (1993) Muscle deficiency and neonatal death in mice with a targeted mutation in the myogenin gene. *Nature* **364**, 501-506

154. Nabeshima, Y., Hanaoka, K., Hayasaka, M., Esumi, E., Li, S., Nonaka, I., and Nabeshima, Y. (1993) Myogenin gene disruption results in perinatal lethality because of severe muscle defect. *Nature* **364**, 532-535

155. Montarras, D., Chelly, J., Bober, E., Arnold, H., Ott, M. O., Gros, F., and Pinset, C. (1991) Developmental patterns in the expression of Myf5, MyoD, myogenin, and MRF4 during myogenesis. *New Biol* **3**, 592-600

156. Kassar-Duchossoy, L., Gayraud-Morel, B., Gomes, D., Rocancourt, D., Buckingham, M., Shinin, V., and Tajbakhsh, S. (2004) Mrf4 determines skeletal muscle identity in Myf5:Myod double-mutant mice. *Nature* **431**, 466-471

157. Mauro, A. (1961) Satellite cell of skeletal muscle fibers. *J Biophys Biochem Cytol* **9**, 493-495

158. Sabourin, L. A., Girgis-Gabardo, A., Seale, P., Asakura, A., and Rudnicki, M. A. (1999) Reduced differentiation potential of primary MyoD-/- myogenic cells derived from adult skeletal muscle. *The Journal of cell biology* **144**, 631-643

159. Ustanina, S., Carvajal, J., Rigby, P., and Braun, T. (2007) The myogenic factor Myf5 supports efficient skeletal muscle regeneration by enabling transient myoblast amplification. *Stem cells* **25**, 2006-2016

160. Zammit, P. S., Golding, J. P., Nagata, Y., Hudon, V., Partridge, T. A., and Beauchamp, J. R. (2004) Muscle satellite cells adopt divergent fates: a mechanism for self-renewal? *The Journal of cell biology* **166**, 347-357

161. Troy, A., Cadwallader, A. B., Fedorov, Y., Tyner, K., Tanaka, K. K., and Olwin, B. B. (2012) Coordination of satellite cell activation and self-renewal by Par-complex-dependent asymmetric activation of p38alpha/beta MAPK. *Cell Stem Cell* **11**, 541-553

162. Riuzzi, F., Sorci, G., Sagheddu, R., and Donato, R. (2012) HMGB1-RAGE regulates muscle satellite cell homeostasis through p38-MAPK- and myogenin-dependent repression of Pax7 transcription. *Journal of cell science* **125**, 1440-1454

163. Schiaffino, S., Hanzlikova, V., and Pierobon, S. (1970) Relations between structure and function in rat skeletal muscle fibers. *The Journal of cell biology* **47**, 107-119

164. Caiozzo, V. J., Baker, M. J., Huang, K., Chou, H., Wu, Y. Z., and Baldwin, K. M. (2003) Single-fiber myosin heavy chain polymorphism: how many patterns and what proportions? *American journal of physiology. Regulatory, integrative and comparative physiology* **285**, R570-580

165. Schiaffino, S., and Reggiani, C. (2011) Fiber types in mammalian skeletal muscles. *Physiological reviews* **91**, 1447-1531

166. Peter, J. B., Barnard, R. J., Edgerton, V. R., Gillespie, C. A., and Stempel, K. E. (1972) Metabolic profiles of three fiber types of skeletal muscle in guinea pigs and rabbits. *Biochemistry* **11**, 2627-2633

167. Burke, R. E., Levine, D. N., and Zajac, F. E., 3rd. (1971) Mammalian motor units: physiological-histochemical correlation in three types in cat gastrocnemius. *Science* **174**, 709-712

168. Miura, S., Kai, Y., Ono, M., and Ezaki, O. (2003) Overexpression of peroxisome proliferator-activated receptor gamma coactivator-1alpha down-regulates GLUT4 mRNA in skeletal muscles. *The Journal of biological chemistry* **278**, 31385-31390

169. Lin, J., Wu, H., Tarr, P. T., Zhang, C. Y., Wu, Z., Boss, O., Michael, L. F., Puigserver, P., Isotani, E., Olson, E. N., Lowell, B. B., Bassel-Duby, R., and Spiegelman, B. M. (2002) Transcriptional co-activator PGC-1 alpha drives the formation of slow-twitch muscle fibres. *Nature* **418**, 797-801

170. Handschin, C., Kobayashi, Y. M., Chin, S., Seale, P., Campbell, K. P., and Spiegelman, B. M. (2007) PGC-1alpha regulates the neuromuscular junction program and ameliorates Duchenne muscular dystrophy. *Genes & development* **21**, 770-783

171. Selsby, J. T., Morine, K. J., Pendrak, K., Barton, E. R., and Sweeney, H. L. (2012) Rescue of dystrophic skeletal muscle by PGC-1alpha involves a fast to slow fiber type shift in the mdx mouse. *PloS one* **7**, e30063

172. Gumerson, J. D., Kabaeva, Z. T., Davis, C. S., Faulkner, J. A., and Michele, D. E. (2010) Soleus muscle in glycosylation-deficient muscular dystrophy is protected from contraction-induced injury. *American journal of physiology. Cell physiology* **299**, C1430-1440

173. Fink, R. H., Stephenson, D. G., and Williams, D. A. (1990) Physiological properties of skinned fibres from normal and dystrophic (Duchenne) human muscle activated by Ca2+ and Sr2+. *The Journal of physiology* **420**, 337-353

174. Wang, J. F., Forst, J., Schroder, S., and Schroder, J. M. (1999) Correlation of muscle fiber type measurements with clinical and molecular genetic data in Duchenne muscular dystrophy. *Neuromuscular disorders : NMD* **9**, 150-158

175. Mercuri, E., and Muntoni, F. (2013) Muscular dystrophies. *Lancet* **381**, 845-860

176. Cohn, R. D., and Campbell, K. P. (2000) Molecular basis of muscular dystrophies. *Muscle & nerve* **23**, 1456-1471

177. Petrof, B. J., Shrager, J. B., Stedman, H. H., Kelly, A. M., and Sweeney, H. L. (1993) Dystrophin protects the sarcolemma from stresses developed during muscle contraction. *Proceedings of the National Academy of Sciences of the United States of America* **90**, 3710-3714

178. Han, R., Kanagawa, M., Yoshida-Moriguchi, T., Rader, E. P., Ng, R. A., Michele, D. E., Muirhead, D. E., Kunz, S., Moore, S. A., Iannaccone, S. T., Miyake, K., McNeil, P. L., Mayer, U., Oldstone, M. B., Faulkner, J. A., and Campbell, K. P. (2009) Basal lamina strengthens cell membrane integrity via the laminin G domain-binding motif of alpha-dystroglycan. *Proceedings of the National Academy of Sciences of the United States of America* **106**, 12573-12579

179. Liu, J., Aoki, M., Illa, I., Wu, C., Fardeau, M., Angelini, C., Serrano, C., Urtizberea, J. A., Hentati, F., Hamida, M. B., Bohlega, S., Culper, E. J., Amato, A. A., Bossie, K., Oeltjen, J., Bejaoui, K., McKenna-Yasek, D., Hosler, B. A., Schurr, E., Arahata, K., de Jong, P. J., and Brown, R. H., Jr. (1998) Dysferlin, a novel skeletal muscle gene, is mutated in Miyoshi myopathy and limb girdle muscular dystrophy. *Nature genetics* **20**, 31-36

180. Bashir, R., Britton, S., Strachan, T., Keers, S., Vafiadaki, E., Lako, M., Richard, I., Marchand, S., Bourg, N., Argov, Z., Sadeh, M., Mahjneh, I., Marconi, G., Passos-Bueno, M. R., Moreira Ede, S., Zatz, M., Beckmann, J. S., and Bushby, K. (1998) A gene related to Caenorhabditis elegans spermatogenesis factor fer-1 is mutated in limb-girdle muscular dystrophy type 2B. *Nature genetics* **20**, 37-42

181. Han, R., and Campbell, K. P. (2007) Dysferlin and muscle membrane repair. *Curr Opin Cell Biol* **19**, 409-416

182. Ross, J., Benn, A., Jonuschies, J., Boldrin, L., Muntoni, F., Hewitt, J. E., Brown, S. C., and Morgan, J. E. (2012) Defects in glycosylation impair satellite stem cell function and niche composition in the muscles of the dystrophic Large(myd) mouse. *Stem cells* **30**, 2330-2341

183. Kim, J., Hopkinson, M., Kavishwar, M., Fernandez-Fuente, M., and Brown, S. C. (2015) Prenatal muscle development in a mouse model for the secondary dystroglycanopathies. *Skeletal muscle* **6**, 3

184. Charge, S. B., and Rudnicki, M. A. (2004) Cellular and molecular regulation of muscle regeneration. *Physiological reviews* **84**, 209-238

185. Le Grand, F., and Rudnicki, M. A. (2007) Skeletal muscle satellite cells and adult myogenesis. *Curr Opin Cell Biol* **19**, 628-633

186. Tidball, J. G., and Villalta, S. A. (2010) Regulatory interactions between muscle and the immune system during muscle regeneration. *American journal of physiology. Regulatory, integrative and comparative physiology* **298**, R1173-1187

187. Mosser, D. M., and Edwards, J. P. (2008) Exploring the full spectrum of macrophage activation. *Nat Rev Immunol* **8**, 958-969

188. Wang, H., Melton, D. W., Porter, L., Sarwar, Z. U., McManus, L. M., and Shireman, P. K. (2014) Altered macrophage phenotype transition impairs skeletal muscle regeneration. *The American journal of pathology* **184**, 1167-1184

189. Arnold, L., Henry, A., Poron, F., Baba-Amer, Y., van Rooijen, N., Plonquet, A., Gherardi, R. K., and Chazaud, B. (2007) Inflammatory monocytes recruited after skeletal muscle injury switch into antiinflammatory macrophages to support myogenesis. *J Exp Med* **204**, 1057-1069

190. Saclier, M., Yacoub-Youssef, H., Mackey, A. L., Arnold, L., Ardjoune, H., Magnan, M., Sailhan, F., Chelly, J., Pavlath, G. K., Mounier, R., Kjaer, M., and Chazaud, B. (2013) Differentially activated macrophages orchestrate myogenic precursor cell fate during human skeletal muscle regeneration. *Stem cells* **31**, 384-396

191. Porter, J. D., Khanna, S., Kaminski, H. J., Rao, J. S., Merriam, A. P., Richmonds, C. R., Leahy, P., Li, J., Guo, W., and Andrade, F. H. (2002) A chronic inflammatory response dominates the skeletal muscle molecular signature in dystrophin-deficient mdx mice. *Human molecular genetics* **11**, 263-272

192. Mann, C. J., Perdiguero, E., Kharraz, Y., Aguilar, S., Pessina, P., Serrano, A. L., and Munoz-Canoves, P. (2011) Aberrant repair and fibrosis development in skeletal muscle. *Skeletal muscle* **1**, 21

193. Villalta, S. A., Nguyen, H. X., Deng, B., Gotoh, T., and Tidball, J. G. (2009) Shifts in macrophage phenotypes and macrophage competition for arginine metabolism affect the severity of muscle pathology in muscular dystrophy. *Human molecular genetics* **18**, 482-496

194. Nguyen, H. X., and Tidball, J. G. (2003) Interactions between neutrophils and macrophages promote macrophage killing of rat muscle cells in vitro. *The Journal of physiology* **547**, 125-132

195. Nguyen, H. X., and Tidball, J. G. (2003) Expression of a muscle-specific, nitric oxide synthase transgene prevents muscle membrane injury and reduces muscle inflammation during modified muscle use in mice. *The Journal of physiology* **550**, 347-356

196. Kuang, S., Gillespie, M. A., and Rudnicki, M. A. (2008) Niche regulation of muscle satellite cell self-renewal and differentiation. *Cell Stem Cell* **2**, 22-31

197. Thomas, K., Engler, A. J., and Meyer, G. A. (2015) Extracellular matrix regulation in the muscle satellite cell niche. *Connect Tissue Res* **56**, 1-8

198. Joe, A. W., Yi, L., Natarajan, A., Le Grand, F., So, L., Wang, J., Rudnicki, M. A., and Rossi, F. M. (2010) Muscle injury activates resident fibro/adipogenic progenitors that facilitate myogenesis. *Nature cell biology* **12**, 153-163

199. Uezumi, A., Fukada, S., Yamamoto, N., Takeda, S., and Tsuchida, K. (2010) Mesenchymal progenitors distinct from satellite cells contribute to ectopic fat cell formation in skeletal muscle. *Nature cell biology* **12**, 143-152

200. Chen, Y. W., Nagaraju, K., Bakay, M., McIntyre, O., Rawat, R., Shi, R., and Hoffman, E. P. (2005) Early onset of inflammation and later involvement of TGFbeta in Duchenne muscular dystrophy. *Neurology* **65**, 826-834

201. Bedair, H., Liu, T. T., Kaar, J. L., Badlani, S., Russell, A. J., Li, Y., and Huard, J. (2007) Matrix metalloproteinase-1 therapy improves muscle healing. *Journal of applied physiology* **102**, 2338-2345

202. Chen, X., and Li, Y. (2009) Role of matrix metalloproteinases in skeletal muscle: migration, differentiation, regeneration and fibrosis. *Cell Adh Migr* **3**, 337-341

203. Wang, W., Pan, H., Murray, K., Jefferson, B. S., and Li, Y. (2009) Matrix metalloproteinase-1 promotes muscle cell migration and differentiation. *The American journal of pathology* **174**, 541-549

204. Wynn, T. A. (2008) Cellular and molecular mechanisms of fibrosis. *J Pathol* **214**, 199-210

205. Yang, B., Jung, D., Motto, D., Meyer, J., Koretzky, G., and Campbell, K. P. (1995) SH3 domain-mediated interaction of dystroglycan and Grb2. *The Journal of biological chemistry* **270**, 11711-11714

206. Rojek, J. M., Moraz, M. L., Pythoud, C., Rothenberger, S., Van der Goot, F. G., Campbell, K. P., and Kunz, S. (2012) Binding of Lassa virus perturbs extracellular matrix-induced signal transduction via dystroglycan. *Cellular microbiology* **14**, 1122-1134

207. Spence, H. J., Dhillon, A. S., James, M., and Winder, S. J. (2004) Dystroglycan, a scaffold for the ERK-MAP kinase cascade. *EMBO reports* **5**, 484-489

208. Garbincius, J. F., and Michele, D. E. (2015) Dystrophin-glycoprotein complex regulates muscle nitric oxide production through mechanoregulation of AMPK signaling. *Proceedings of the National Academy of Sciences of the United States of America* **112**, 13663-13668

209. Langenbach, K. J., and Rando, T. A. (2002) Inhibition of dystroglycan binding to laminin disrupts the PI3K/AKT pathway and survival signaling in muscle cells. *Muscle & nerve* **26**, 644-653

210. Dogra, C., Changotra, H., Wergedal, J. E., and Kumar, A. (2006) Regulation of phosphatidylinositol 3-kinase (PI3K)/Akt and nuclear factor-kappa B signaling pathways in dystrophin-deficient skeletal muscle in response to mechanical stretch. *Journal of cellular physiology* **208**, 575-585

211. Bhatnagar, S., and Kumar, A. (2010) Therapeutic targeting of signaling pathways in muscular dystrophy. *J Mol Med (Berl)* **88**, 155-166

212. Bodine, S. C., Stitt, T. N., Gonzalez, M., Kline, W. O., Stover, G. L., Bauerlein, R., Zlotchenko, E., Scrimgeour, A., Lawrence, J. C., Glass, D. J., and Yancopoulos, G. D. (2001) Akt/mTOR pathway is a crucial regulator of skeletal muscle hypertrophy and can prevent muscle atrophy in vivo. *Nature cell biology* **3**, 1014-1019

213. Rommel, C., Bodine, S. C., Clarke, B. A., Rossman, R., Nunez, L., Stitt, T. N., Yancopoulos, G. D., and Glass, D. J. (2001) Mediation of IGF-1-induced skeletal myotube hypertrophy by PI(3)K/Akt/mTOR and PI(3)K/Akt/GSK3 pathways. *Nature cell biology* **3**, 1009-1013

214. Levine, B., and Kroemer, G. (2008) Autophagy in the pathogenesis of disease. *Cell* **132**, 27-42

215. Mizushima, N., Levine, B., Cuervo, A. M., and Klionsky, D. J. (2008) Autophagy fights disease through cellular self-digestion. *Nature* **451**, 1069-1075

216. Mizushima, N., and Komatsu, M. (2011) Autophagy: renovation of cells and tissues. *Cell* **147**, 728-741

217. Wang, R. C., Wei, Y., An, Z., Zou, Z., Xiao, G., Bhagat, G., White, M., Reichelt, J., and Levine, B. (2012) Akt-mediated regulation of autophagy and tumorigenesis through Beclin 1 phosphorylation. *Science* **338**, 956-959

218. Mammucari, C., Milan, G., Romanello, V., Masiero, E., Rudolf, R., Del Piccolo, P., Burden, S. J., Di Lisi, R., Sandri, C., Zhao, J., Goldberg, A. L., Schiaffino, S., and Sandri, M. (2007) FoxO3 controls autophagy in skeletal muscle in vivo. *Cell metabolism* **6**, 458-471

219. Tzivion, G., Dobson, M., and Ramakrishnan, G. (2011) FoxO transcription factors; Regulation by AKT and 14-3-3 proteins. *Biochimica et biophysica acta* **1813**, 1938-1945

220. Pauly, M., Daussin, F., Burelle, Y., Li, T., Godin, R., Fauconnier, J., Koechlin-Ramonatxo, C., Hugon, G., Lacampagne, A., Coisy-Quivy, M., Liang, F., Hussain, S., Matecki, S., and Petrof, B. J. (2012) AMPK activation stimulates autophagy and ameliorates muscular dystrophy in the mdx mouse diaphragm. *The American journal of pathology* **181**, 583-592

221. De Palma, C., Morisi, F., Cheli, S., Pambianco, S., Cappello, V., Vezzoli, M., Rovere-Querini, P., Moggio, M., Ripolone, M., Francolini, M., Sandri, M., and Clementi, E. (2012) Autophagy as a new therapeutic target in Duchenne muscular dystrophy. *Cell death & disease* **3**, e418

222. Whitehead, N. P., Kim, M. J., Bible, K. L., Adams, M. E., and Froehner, S. C. (2015) A new therapeutic effect of simvastatin revealed by functional improvement in muscular dystrophy. *Proceedings of the National Academy of Sciences of the United States of America* **112**, 12864-12869

223. Kim, M. H., Kay, D. I., Rudra, R. T., Chen, B. M., Hsu, N., Izumiya, Y., Martinez, L., Spencer, M. J., Walsh, K., Grinnell, A. D., and Crosbie, R. H. (2011) Myogenic Akt signaling attenuates muscular degeneration, promotes myofiber regeneration and improves muscle function in dystrophin-deficient mdx mice. *Human molecular genetics* **20**, 1324-1338

224. Alexander, M. S., Casar, J. C., Motohashi, N., Vieira, N. M., Eisenberg, I., Marshall, J. L., Gasperini, M. J., Lek, A., Myers, J. A., Estrella, E. A., Kang, P. B., Shapiro, F., Rahimov, F., Kawahara, G., Widrick, J. J., and Kunkel, L. M. (2014) MicroRNA-486-dependent modulation of DOCK3/PTEN/AKT signaling pathways improves muscular dystrophy-associated symptoms. *The Journal of clinical investigation* **124**, 2651-2667

225. Bentzinger, C. F., Romanino, K., Cloetta, D., Lin, S., Mascarenhas, J. B., Oliveri, F., Xia, J., Casanova, E., Costa, C. F., Brink, M., Zorzato, F., Hall, M. N., and Ruegg, M. A. (2008) Skeletal muscle-specific ablation of raptor, but not of rictor,

causes metabolic changes and results in muscle dystrophy. *Cell metabolism* **8**, 411-424

226. Risson, V., Mazelin, L., Roceri, M., Sanchez, H., Moncollin, V., Corneloup, C., Richard-Bulteau, H., Vignaud, A., Baas, D., Defour, A., Freyssenet, D., Tanti, J. F., Le-Marchand-Brustel, Y., Ferrier, B., Conjard-Duplany, A., Romanino, K., Bauche, S., Hantai, D., Mueller, M., Kozma, S. C., Thomas, G., Ruegg, M. A., Ferry, A., Pende, M., Bigard, X., Koulmann, N., Schaeffer, L., and Gangloff, Y. G. (2009) Muscle inactivation of mTOR causes metabolic and dystrophin defects leading to severe myopathy. *The Journal of cell biology* **187**, 859-874

227. Yamada, E., Bastie, C. C., Koga, H., Wang, Y., Cuervo, A. M., and Pessin, J. E. (2012) Mouse skeletal muscle fiber-type-specific macroautophagy and muscle wasting are regulated by a Fyn/STAT3/Vps34 signaling pathway. *Cell Rep* **1**, 557-569

228. Wang, Y., and Pessin, J. E. (2013) Mechanisms for fiber-type specificity of skeletal muscle atrophy. *Curr Opin Clin Nutr Metab Care* **16**, 243-250

229. Gurpur, P. B., Liu, J., Burkin, D. J., and Kaufman, S. J. (2009) Valproic acid activates the PI3K/Akt/mTOR pathway in muscle and ameliorates pathology in a mouse model of Duchenne muscular dystrophy. *The American journal of pathology* **174**, 999-1008

230. Shimobayashi, M., and Hall, M. N. (2014) Making new contacts: the mTOR network in metabolism and signalling crosstalk. *Nature reviews. Molecular cell biology* **15**, 155-162

231. Eghtesad, S., Jhunjhunwala, S., Little, S. R., and Clemens, P. R. (2011) Rapamycin ameliorates dystrophic phenotype in mdx mouse skeletal muscle. *Molecular medicine* **17**, 917-924

232. Bibee, K. P., Cheng, Y. J., Ching, J. K., Marsh, J. N., Li, A. J., Keeling, R. M., Connolly, A. M., Golumbek, P. T., Myerson, J. W., Hu, G., Chen, J., Shannon, W. D., Lanza, G. M., Weihl, C. C., and Wickline, S. A. (2014) Rapamycin nanoparticles target defective autophagy in muscular dystrophy to enhance both strength and cardiac function. *FASEB journal : official publication of the Federation of American Societies for Experimental Biology* **28**, 2047-2061

233. Grumati, P., Coletto, L., Sabatelli, P., Cescon, M., Angelin, A., Bertaggia, E., Blaauw, B., Urciuolo, A., Tiepolo, T., Merlini, L., Maraldi, N. M., Bernardi, P., Sandri, M., and Bonaldo, P. (2010) Autophagy is defective in collagen VI muscular dystrophies, and its reactivation rescues myofiber degeneration. *Nature medicine* **16**, 1313-1320

234. Ohlendieck, K., Ervasti, J. M., Snook, J. B., and Campbell, K. P. (1991) Dystrophin-glycoprotein complex is highly enriched in isolated skeletal muscle sarcolemma. *The Journal of cell biology* **112**, 135-148

235. Sealock, R., and Froehner, S. C. (1994) Dystrophin-associated proteins and synapse formation: is alpha-dystroglycan the agrin receptor? *Cell* **77**, 617-619

236. Kanagawa, M., Michele, D. E., Satz, J. S., Barresi, R., Kusano, H., Sasaki, T., Timpl, R., Henry, M. D., and Campbell, K. P. (2005) Disruption of perlecan binding and matrix assembly by post-translational or genetic disruption of dystroglycan function. *FEBS letters* **579**, 4792-4796

237. Reissner, C., Stahn, J., Breuer, D., Klose, M., Pohlentz, G., Mormann, M., and Missler, M. (2014) Dystroglycan binding to alpha-neurexin competes with neurexophilin-1 and neuroligin in the brain. *The Journal of biological chemistry* **289**, 27585-27603

238. Constantin, B. (2014) Dystrophin complex functions as a scaffold for signalling proteins. *Biochimica et biophysica acta* **1838**, 635-642

239. Nigro, V., and Piluso, G. (2014) Spectrum of muscular dystrophies associated with sarcolemmal-protein genetic defects. *Biochimica et biophysica acta*

240. Live, D., Wells, L., and Boons, G. J. (2013) Dissecting the molecular basis of the role of the O-mannosylation pathway in disease: alpha-dystroglycan and forms of muscular dystrophy. *Chembiochem : a European journal of chemical biology* **14**, 2392-2402

241. Butler-Browne, G. S., and Whalen, R. G. (1984) Myosin isozyme transitions occurring during the postnatal development of the rat soleus muscle. *Developmental biology* **102**, 324-334

242. Chang, N. C., and Rudnicki, M. A. (2014) Satellite cells: the architects of skeletal muscle. *Current topics in developmental biology* **107**, 161-181

243. Damiani, E., Angelini, C., Pelosi, M., Sacchetto, R., Bortoloso, E., and Margreth, A. (1996) Skeletal muscle sarcoplasmic reticulum phenotype in myotonic dystrophy. *Neuromuscular disorders : NMD* **6**, 33-47

244. Trollet, C., Anvar, S. Y., Venema, A., Hargreaves, I. P., Foster, K., Vignaud, A., Ferry, A., Negroni, E., Hourde, C., Baraibar, M. A., t Hoen, P. A., Davies, J. E., Rubinsztein, D. C., Heales, S. J., Mouly, V., van der Maarel, S. M., Butler-Browne, G., Raz, V., and Dickson, G. (2010) Molecular and phenotypic characterization of a mouse model of oculopharyngeal muscular dystrophy reveals severe muscular atrophy restricted to fast glycolytic fibres. *Human molecular genetics* **19**, 2191-2207

245. Sancisi, V., Germinario, E., Esposito, A., Morini, E., Peron, S., Moggio, M., Tomelleri, G., Danieli-Betto, D., and Tupler, R. (2014) Altered Tnnt3 characterizes selective weakness of fast fibers in mice overexpressing FSHD region gene 1 (FRG1). *American journal of physiology. Regulatory, integrative and comparative physiology* **306**, R124-137

246. Beedle, A. M., Nienaber, P. M., and Campbell, K. P. (2007) Fukutin-related protein associates with the sarcolemmal dystrophin-glycoprotein complex. *The Journal of biological chemistry* **282**, 16713-16717

247. Fortunato, M. J., Ball, C. E., Hollinger, K., Patel, N. B., Modi, J. N., Rajasekaran, V., Nonneman, D. J., Ross, J. W., Kennedy, E. J., Selsby, J. T., and Beedle, A. M. (2014) Development of rabbit monoclonal antibodies for detection of alpha-dystroglycan in normal and dystrophic tissue. *PloS one* **9**, e97567

248. Kanagawa, M., Lu, Z., Ito, C., Matsuda, C., Miyake, K., and Toda, T. (2014) Contribution of dysferlin deficiency to skeletal muscle pathology in asymptomatic and severe dystroglycanopathy models: generation of a new model for Fukuyama congenital muscular dystrophy. *PloS one* **9**, e106721

249. Kabaeva, Z., Meekhof, K. E., and Michele, D. E. (2011) Sarcolemma instability during mechanical activity in Largemyd cardiac myocytes with loss of dystroglycan extracellular matrix receptor function. *Human molecular genetics* **20**, 3346-3355

250. Hannon, K., Smith, C. K., 2nd, Bales, K. R., and Santerre, R. F. (1992) Temporal and quantitative analysis of myogenic regulatory and growth factor gene expression in the developing mouse embryo. *Developmental biology* **151**, 137-144

251. Ott, M. O., Bober, E., Lyons, G., Arnold, H., and Buckingham, M. (1991) Early expression of the myogenic regulatory gene, myf-5, in precursor cells of skeletal muscle in the mouse embryo. *Development* **111**, 1097-1107

252. Bassez, G., Chapoy, E., Bastuji-Garin, S., Radvanyi-Hoffman, H., Authier, F. J., Pellissier, J. F., Eymard, B., and Gherardi, R. K. (2008) Type 2 myotonic dystrophy can be predicted by the combination of type 2 muscle fiber central nucleation and scattered atrophy. *Journal of neuropathology and experimental neurology* **67**, 319-325

253. Blanco, G., Pritchard, C., Underhill, P., Breeds, S., Townsend, K. M., Greenfield, A., and Brown, S. D. (2004) Molecular phenotyping of the mouse ky mutant reveals UCP1 upregulation at the neuromuscular junctions of dystrophic soleus muscle. *Neuromuscular disorders : NMD* **14**, 217-228

254. Ljubicic, V., Miura, P., Burt, M., Boudreault, L., Khogali, S., Lunde, J. A., Renaud, J. M., and Jasmin, B. J. (2011) Chronic AMPK activation evokes the slow, oxidative myogenic program and triggers beneficial adaptations in mdx mouse skeletal muscle. *Human molecular genetics* **20**, 3478-3493

255. Angelini, C., and Tasca, E. (2012) Fatigue in muscular dystrophies. *Neuromuscular disorders : NMD* **22 Suppl 3**, S214-220

256. Smith, I. C., Huang, J., Quadrilatero, J., Tupling, A. R., and Vandenboom, R. (2010) Posttetanic potentiation in mdx muscle. *Journal of muscle research and cell motility* **31**, 267-277

257. Lee, W. H., Abe, S., Kim, H. J., Usami, A., Honda, A., Sakiyama, K., and Ide, Y. (2006) Characteristics of muscle fibers reconstituted in the regeneration process of masseter muscle in an mdx mouse model of muscular dystrophy. *Journal of muscle research and cell motility* **27**, 235-240

258. Nonaka, I., Sugita, H., Takada, K., and Kumagai, K. (1982) Muscle histochemistry in congenital muscular dystrophy with central nervous system involvement. *Muscle & nerve* **5**, 102-106

259. Luz, M. A., Marques, M. J., and Santo Neto, H. (2002) Impaired regeneration of dystrophin-deficient muscle fibers is caused by exhaustion of myogenic cells. *Brazilian journal of medical and biological research = Revista brasileira de pesquisas medicas e biologicas / Sociedade Brasileira de Biofisica ... [et al.]* **35**, 691-695

260. Heslop, L., Morgan, J. E., and Partridge, T. A. (2000) Evidence for a myogenic stem cell that is exhausted in dystrophic muscle. *Journal of cell science* **113 (Pt 12)**, 2299-2308

261. Pette, D., and Staron, R. S. (2000) Myosin isoforms, muscle fiber types, and transitions. *Microscopy research and technique* **50**, 500-509

262. Esser, K., Nelson, T., Lupa-Kimball, V., and Blough, E. (1999) The CACC box and myocyte enhancer factor-2 sites within the myosin light chain 2 slow promoter cooperate in regulating nerve-specific transcription in skeletal muscle. *The Journal of biological chemistry* **274**, 12095-12102

263. Dusterhoft, S., and Pette, D. (1993) Satellite Cells from Slow Rat Muscle Express Slow Myosin under Appropriate Culture Conditions. *Differentiation* **53**, 25-33

264. Rosenblatt, J. D., Parry, D. J., and Partridge, T. A. (1996) Phenotype of adult mouse muscle myoblasts reflects their fiber type of origin. *Differentiation* **60**, 39-45

265. Endo, T. (2015) Glycobiology of alpha-dystroglycan and muscular dystrophy. *Journal of biochemistry* **157**, 1-12

266. Cote, P. D., Moukhles, H., Lindenbaum, M., and Carbonetto, S. (1999) Chimaeric mice deficient in dystroglycans develop muscular dystrophy and have disrupted myoneural synapses. *Nature genetics* **23**, 338-342

267. Foltz, S. J., Modi, J. N., Melick, G. A., Abousaud, M. I., Luan, J., Fortunato, M. J., and Beedle, A. M. (2016) Abnormal Skeletal Muscle Regeneration plus Mild Alterations in Mature Fiber Type Specification in Fktn-Deficient Dystroglycanopathy Muscular Dystrophy Mice. *PloS one* **11**, e0147049

268. Marshall, J. L., Holmberg, J., Chou, E., Ocampo, A. C., Oh, J., Lee, J., Peter, A. K., Martin, P. T., and Crosbie-Watson, R. H. (2012) Sarcospan-dependent Akt activation is required for utrophin expression and muscle regeneration. *The Journal of cell biology* **197**, 1009-1027

269. Sarbassov, D. D., Guertin, D. A., Ali, S. M., and Sabatini, D. M. (2005) Phosphorylation and regulation of Akt/PKB by the rictor-mTOR complex. *Science* **307**, 1098-1101

270. Ramos, F. J., Chen, S. C., Garelick, M. G., Dai, D. F., Liao, C. Y., Schreiber, K. H., MacKay, V. L., An, E. H., Strong, R., Ladiges, W. C., Rabinovitch, P. S., Kaeberlein, M., and Kennedy, B. K. (2012) Rapamycin reverses elevated mTORC1 signaling in lamin A/C-deficient mice, rescues cardiac and skeletal muscle function, and extends survival. *Science translational medicine* **4**, 144ra103

271. Pereboev, A. V., Ahmed, N., thi Man, N., and Morris, G. E. (2001) Epitopes in the interacting regions of beta-dystroglycan (PPxY motif) and dystrophin (WW domain). *Biochimica et biophysica acta* **1527**, 54-60

272. Call, J. A., Warren, G. L., Verma, M., and Lowe, D. A. (2013) Acute failure of action potential conduction in mdx muscle reveals new mechanism of contraction-induced force loss. *The Journal of physiology* **591**, 3765-3776

273. Call, J. A., McKeehen, J. N., Novotny, S. A., and Lowe, D. A. (2010) Progressive resistance voluntary wheel running in the mdx mouse. *Muscle & nerve* **42**, 871-880

274. Cooperstein, S. J., Lazarow, A., and Kurfess, N. J. (1950) A microspectrophotometric method for the determination of succinic dehydrogenase. *The Journal of biological chemistry* **186**, 129-139

275. Schindelin, J., Arganda-Carreras, I., Frise, E., Kaynig, V., Longair, M., Pietzsch, T., Preibisch, S., Rueden, C., Saalfeld, S., Schmid, B., Tinevez, J. Y., White, D.

J., Hartenstein, V., Eliceiri, K., Tomancak, P., and Cardona, A. (2012) Fiji: an open-source platform for biological-image analysis. *Nature methods* **9**, 676-682

276. Dean, R. B., and Dixon, W. J. (1951) Simplified Statistics for Small Numbers of Observations. *Anal Chem* **23**, 636-638

277. Rorabacher, D. B. (1991) Statistical Treatment for Rejection of Deviant Values - Critical-Values of Dixon Q Parameter and Related Subrange Ratios at the 95-Percent Confidence Level. *Anal Chem* **63**, 139-146

278. Bhatnagar, S., Panguluri, S. K., Gupta, S. K., Dahiya, S., Lundy, R. F., and Kumar, A. (2010) Tumor necrosis factor-alpha regulates distinct molecular pathways and gene networks in cultured skeletal muscle cells. *PloS one* **5**, e13262

279. Chiang, G. G., and Abraham, R. T. (2005) Phosphorylation of mammalian target of rapamycin (mTOR) at Ser-2448 is mediated by p70S6 kinase. *The Journal of biological chemistry* **280**, 25485-25490

280. Holz, M. K., and Blenis, J. (2005) Identification of S6 kinase 1 as a novel mammalian target of rapamycin (mTOR)-phosphorylating kinase. *The Journal of biological chemistry* **280**, 26089-26093

281. Zhang, P., Liang, X., Shan, T., Jiang, Q., Deng, C., Zheng, R., and Kuang, S. (2015) mTOR is necessary for proper satellite cell activity and skeletal muscle regeneration. *Biochemical and biophysical research communications* **463**, 102-108

282. Ge, Y., Wu, A. L., Warnes, C., Liu, J., Zhang, C., Kawasome, H., Terada, N., Boppart, M. D., Schoenherr, C. J., and Chen, J. (2009) mTOR regulates skeletal muscle regeneration in vivo through kinase-dependent and kinase-independent mechanisms. *American journal of physiology. Cell physiology* **297**, C1434-1444

283. Goodman, C. A., Frey, J. W., Mabrey, D. M., Jacobs, B. L., Lincoln, H. C., You, J. S., and Hornberger, T. A. (2011) The role of skeletal muscle mTOR in the regulation of mechanical load-induced growth. *The Journal of physiology* **589**, 5485-5501

284. Majmundar, A. J., Skuli, N., Mesquita, R. C., Kim, M. N., Yodh, A. G., Nguyen-McCarty, M., and Simon, M. C. (2012) O(2) regulates skeletal muscle progenitor differentiation through phosphatidylinositol 3-kinase/AKT signaling. *Molecular and cellular biology* **32**, 36-49

285. Gui, Y. S., Wang, L., Tian, X., Li, X., Ma, A., Zhou, W., Zeng, N., Zhang, J., Cai, B., Zhang, H., Chen, J. Y., and Xu, K. F. (2015) mTOR Overactivation and Compromised Autophagy in the Pathogenesis of Pulmonary Fibrosis. *PloS one* **10**, e0138625

286. Li, Z. B., Kollias, H. D., and Wagner, K. R. (2008) Myostatin directly regulates skeletal muscle fibrosis. *The Journal of biological chemistry* **283**, 19371-19378

287. FDALabel: Full-Text Search of Drug Labeling.

288. Gorassini, M., Eken, T., Bennett, D. J., Kiehn, O., and Hultborn, H. (2000) Activity of hindlimb motor units during locomotion in the conscious rat. *Journal of neurophysiology* **83**, 2002-2011

289. McNally, E. M., and Pytel, P. (2007) Muscle diseases: the muscular dystrophies. *Annual review of pathology* **2**, 87-109

290. Leenen, P. J., de Bruijn, M. F., Voerman, J. S., Campbell, P. A., and van Ewijk, W. (1994) Markers of mouse macrophage development detected by monoclonal antibodies. *Journal of immunological methods* **174**, 5-19

291. Zanotti, S., Saredi, S., Ruggieri, A., Fabbri, M., Blasevich, F., Romaggi, S., Morandi, L., and Mora, M. (2007) Altered extracellular matrix transcript expression and protein modulation in primary Duchenne muscular dystrophy myotubes. *Matrix biology : journal of the International Society for Matrix Biology* **26**, 615-624

292. de Greef, J. C., Hamlyn, R., Jensen, B. S., O'Campo Landa, R., Levy, J. R., Kobuke, K., and Campbell, K. P. (2016) Collagen VI deficiency reduces muscle pathology, but does not improve muscle function, in the gamma-sarcoglycan-null mouse. *Human molecular genetics* **25**, 1357-1369

293. Hollinger, K., Gardan-Salmon, D., Santana, C., Rice, D., Snella, E., and Selsby, J. T. (2013) Rescue of dystrophic skeletal muscle by PGC-1alpha involves restored expression of dystrophin-associated protein complex components and satellite cell signaling. *American journal of physiology. Regulatory, integrative and comparative physiology* **305**, R13-23

294. Wagatsuma, A., Kotake, N., and Yamada, S. (2011) Muscle regeneration occurs to coincide with mitochondrial biogenesis. *Molecular and cellular biochemistry* **349**, 139-147

295. Sciandra, F., Bozzi, M., Bianchi, M., Pavoni, E., Giardina, B., and Brancaccio, A. (2003) Dystroglycan and muscular dystrophies related to the dystrophin-glycoprotein complex. *Annali dell'Istituto superiore di sanita* **39**, 173-181

296. Peng, X. D., Xu, P. Z., Chen, M. L., Hahn-Windgassen, A., Skeen, J., Jacobs, J., Sundararajan, D., Chen, W. S., Crawford, S. E., Coleman, K. G., and Hay, N. (2003) Dwarfism, impaired skin development, skeletal muscle atrophy, delayed bone development, and impeded adipogenesis in mice lacking Akt1 and Akt2. *Genes & development* **17**, 1352-1365

297. Pal, R., Palmieri, M., Loehr, J. A., Li, S., Abo-Zahrah, R., Monroe, T. O., Thakur, P. B., Sardiello, M., and Rodney, G. G. (2014) Src-dependent impairment of autophagy by oxidative stress in a mouse model of Duchenne muscular dystrophy. *Nature communications* **5**, 4425

298. Shegogue, D., and Trojanowska, M. (2004) Mammalian target of rapamycin positively regulates collagen type I production via a phosphatidylinositol 3-kinase-independent pathway. *The Journal of biological chemistry* **279**, 23166-23175

299. Goc, A., Choudhary, M., Byzova, T. V., and Somanath, P. R. (2011) TGFbeta- and bleomycin-induced extracellular matrix synthesis is mediated through Akt and mammalian target of rapamycin (mTOR). *Journal of cellular physiology* **226**, 3004-3013

300. Castets, P., Lin, S., Rion, N., Di Fulvio, S., Romanino, K., Guridi, M., Frank, S., Tintignac, L. A., Sinnreich, M., and Ruegg, M. A. (2013) Sustained activation of mTORC1 in skeletal muscle inhibits constitutive and starvation-induced autophagy and causes a severe, late-onset myopathy. *Cell metabolism* **17**, 731-744

301. Malicdan, M. C., Noguchi, S., Nonaka, I., Saftig, P., and Nishino, I. (2008) Lysosomal myopathies: an excessive build-up in autophagosomes is too much to handle. *Neuromuscular disorders : NMD* **18**, 521-529

302. Masiero, E., and Sandri, M. (2010) Autophagy inhibition induces atrophy and myopathy in adult skeletal muscles. *Autophagy* **6**, 307-309

303. Cardamone, M., Flanagan, D., Mowat, D., Kennedy, S. E., Chopra, M., and Lawson, J. A. (2014) Mammalian target of rapamycin inhibitors for intractable epilepsy and subependymal giant cell astrocytomas in tuberous sclerosis complex. *The Journal of pediatrics* **164**, 1195-1200

304. Canpolat, M., Per, H., Gumus, H., Yikilmaz, A., Unal, E., Patiroglu, T., Cinar, L., Kurtsoy, A., and Kumandas, S. (2014) Rapamycin has a beneficial effect on controlling epilepsy in children with tuberous sclerosis complex: results of 7 children from a cohort of 86. *Child's nervous system : ChNS : official journal of the International Society for Pediatric Neurosurgery* **30**, 227-240

305. Franz, D. N., Leonard, J., Tudor, C., Chuck, G., Care, M., Sethuraman, G., Dinopoulos, A., Thomas, G., and Crone, K. R. (2006) Rapamycin causes regression of astrocytomas in tuberous sclerosis complex. *Annals of neurology* **59**, 490-498

306. Krueger, D. A., Care, M. M., Holland, K., Agricola, K., Tudor, C., Mangeshkar, P., Wilson, K. A., Byars, A., Sahmoud, T., and Franz, D. N. (2010) Everolimus

for subependymal giant-cell astrocytomas in tuberous sclerosis. *The New England journal of medicine* **363**, 1801-1811

307. Peng, Z. F., Yang, L., Wang, T. T., Han, P., Liu, Z. H., and Wei, Q. (2014) Efficacy and safety of sirolimus for renal angiomyolipoma in patients with tuberous sclerosis complex or sporadic lymphangioleiomyomatosis: a systematic review. *The Journal of urology* **192**, 1424-1430

308. Reagan-Shaw, S., Nihal, M., and Ahmad, N. (2008) Dose translation from animal to human studies revisited. *FASEB journal : official publication of the Federation of American Societies for Experimental Biology* **22**, 659-661

309. Kaplan, B., Qazi, Y., and Wellen, J. R. (2014) Strategies for the management of adverse events associated with mTOR inhibitors. *Transplantation reviews* **28**, 126-133

310. Harrison, D. E., Strong, R., Sharp, Z. D., Nelson, J. F., Astle, C. M., Flurkey, K., Nadon, N. L., Wilkinson, J. E., Frenkel, K., Carter, C. S., Pahor, M., Javors, M. A., Fernandez, E., and Miller, R. A. (2009) Rapamycin fed late in life extends lifespan in genetically heterogeneous mice. *Nature* **460**, 392-395

311. Dumont, N. A., Wang, Y. X., von Maltzahn, J., Pasut, A., Bentzinger, C. F., Brun, C. E., and Rudnicki, M. A. (2015) Dystrophin expression in muscle stem cells regulates their polarity and asymmetric division. *Nature medicine* **21**, 1455-1463

312. Ausoni, S., Gorza, L., Schiaffino, S., Gundersen, K., and Lomo, T. (1990) Expression of myosin heavy chain isoforms in stimulated fast and slow rat muscles. *J Neurosci* **10**, 153-160

313. Termin, A., Staron, R. S., and Pette, D. (1989) Changes in myosin heavy chain isoforms during chronic low-frequency stimulation of rat fast hindlimb muscles. A single-fiber study. *Eur J Biochem* **186**, 749-754

314. Chalkiadaki, A., Igarashi, M., Nasamu, A. S., Knezevic, J., and Guarente, L. (2014) Muscle-specific SIRT1 gain-of-function increases slow-twitch fibers and ameliorates pathophysiology in a mouse model of duchenne muscular dystrophy. *PLoS Genet* **10**, e1004490

315. Chakkalakal, J. V., Stocksley, M. A., Harrison, M. A., Angus, L. M., Deschenes-Furry, J., St-Pierre, S., Megeney, L. A., Chin, E. R., Michel, R. N., and Jasmin, B. J. (2003) Expression of utrophin A mRNA correlates with the oxidative capacity of skeletal muscle fiber types and is regulated by calcineurin/NFAT signaling. *Proceedings of the National Academy of Sciences of the United States of America* **100**, 7791-7796

316. Reyes, N. L., Banks, G. B., Tsang, M., Margineantu, D., Gu, H., Djukovic, D., Chan, J., Torres, M., Liggitt, H. D., Hirenallur, S. D., Hockenbery, D. M., Raftery, D., and Iritani, B. M. (2015) Fnip1 regulates skeletal muscle fiber type specification, fatigue resistance, and susceptibility to muscular dystrophy. *Proceedings of the National Academy of Sciences of the United States of America* **112**, 424-429

317. Milne, J. C., Lambert, P. D., Schenk, S., Carney, D. P., Smith, J. J., Gagne, D. J., Jin, L., Boss, O., Perni, R. B., Vu, C. B., Bemis, J. E., Xie, R., Disch, J. S., Ng, P. Y., Nunes, J. J., Lynch, A. V., Yang, H., Galonek, H., Israelian, K., Choy, W., Iffland, A., Lavu, S., Medvedik, O., Sinclair, D. A., Olefsky, J. M., Jirousek, M. R., Elliott, P. J., and Westphal, C. H. (2007) Small molecule activators of SIRT1 as therapeutics for the treatment of type 2 diabetes. *Nature* **450**, 712-716

318. Ljubicic, V., Burt, M., Lunde, J. A., and Jasmin, B. J. (2014) Resveratrol induces expression of the slow, oxidative phenotype in mdx mouse muscle together with enhanced activity of the SIRT1-PGC-1alpha axis. *American journal of physiology. Cell physiology* **307**, C66-82

319. Whitehead, N. P., Yeung, E. W., Froehner, S. C., and Allen, D. G. (2010) Skeletal muscle NADPH oxidase is increased and triggers stretch-induced damage in the mdx mouse. *PloS one* **5**, e15354

320. Masiero, E., Agatea, L., Mammucari, C., Blaauw, B., Loro, E., Komatsu, M., Metzger, D., Reggiani, C., Schiaffino, S., and Sandri, M. (2009) Autophagy is required to maintain muscle mass. *Cell metabolism* **10**, 507-515

321. Inoki, K., Li, Y., Zhu, T., Wu, J., and Guan, K. L. (2002) TSC2 is phosphorylated and inhibited by Akt and suppresses mTOR signalling. *Nature cell biology* **4**, 648-657

322. Inoki, K., Zhu, T., and Guan, K. L. (2003) TSC2 mediates cellular energy response to control cell growth and survival. *Cell* **115**, 577-590

323. Motohashi, N., Alexander, M. S., Shimizu-Motohashi, Y., Myers, J. A., Kawahara, G., and Kunkel, L. M. (2013) Regulation of IRS1/Akt insulin signaling by microRNA-128a during myogenesis. *Journal of cell science* **126**, 2678-2691

324. Blaauw, B., Mammucari, C., Toniolo, L., Agatea, L., Abraham, R., Sandri, M., Reggiani, C., and Schiaffino, S. (2008) Akt activation prevents the force drop induced by eccentric contractions in dystrophin-deficient skeletal muscle. *Human molecular genetics* **17**, 3686-3696

325. Kim, J., Kundu, M., Viollet, B., and Guan, K. L. (2011) AMPK and mTOR regulate autophagy through direct phosphorylation of Ulk1. *Nature cell biology* **13**, 132-141

326. Sanchez, A. M., Csibi, A., Raibon, A., Cornille, K., Gay, S., Bernardi, H., and Candau, R. (2012) AMPK promotes skeletal muscle autophagy through activation of forkhead FoxO3a and interaction with Ulk1. *Journal of cellular biochemistry* **113**, 695-710

327. Wu, W., Tian, W., Hu, Z., Chen, G., Huang, L., Li, W., Zhang, X., Xue, P., Zhou, C., Liu, L., Zhu, Y., Zhang, X., Li, L., Zhang, L., Sui, S., Zhao, B., and Feng, D. (2014) ULK1 translocates to mitochondria and phosphorylates FUNDC1 to regulate mitophagy. *EMBO reports* **15**, 566-575

328. Kang, S. A., Pacold, M. E., Cervantes, C. L., Lim, D., Lou, H. J., Ottina, K., Gray, N. S., Turk, B. E., Yaffe, M. B., and Sabatini, D. M. (2013) mTORC1 phosphorylation sites encode their sensitivity to starvation and rapamycin. *Science* **341**, 1236566

329. Spencer, M. J., Montecino-Rodriguez, E., Dorshkind, K., and Tidball, J. G. (2001) Helper (CD4(+)) and cytotoxic (CD8(+)) T cells promote the pathology of dystrophin-deficient muscle. *Clin Immunol* **98**, 235-243

330. Erbay, E., and Chen, J. (2001) The mammalian target of rapamycin regulates C2C12 myogenesis via a kinase-independent mechanism. *The Journal of biological chemistry* **276**, 36079-36082

331. Zhang, P. P., Liang, X. R., Shan, T. Z., Jiang, Q. Y., Deng, C. Y., Zheng, R., and Kuang, S. H. (2015) mTOR is necessary for proper satellite cell activity and skeletal muscle regeneration. *Biochemical and biophysical research communications* **463**, 102-108

332. Galvagni, F., Cartocci, E., and Oliviero, S. (1998) The dystrophin promoter is negatively regulated by YY1 in undifferentiated muscle cells. *The Journal of biological chemistry* **273**, 33708-33713

333. Cunningham, J. T., Rodgers, J. T., Arlow, D. H., Vazquez, F., Mootha, V. K., and Puigserver, P. (2007) mTOR controls mitochondrial oxidative function through a YY1-PGC-1alpha transcriptional complex. *Nature* **450**, 736-740

334. Murphy, M. M., Lawson, J. A., Mathew, S. J., Hutcheson, D. A., and Kardon, G. (2011) Satellite cells, connective tissue fibroblasts and their interactions are crucial for muscle regeneration. *Development* **138**, 3625-3637

335. Shen, W., Li, Y., Zhu, J., Schwendener, R., and Huard, J. (2008) Interaction between macrophages, TGF-beta1, and the COX-2 pathway during the

inflammatory phase of skeletal muscle healing after injury. *Journal of cellular physiology* **214**, 405-412

336. Muntoni, F., Mateddu, A., Marchei, F., Clerk, A., and Serra, G. (1993) Muscular weakness in the mdx mouse. *J Neurol Sci* **120**, 71-77

337. Kaur, J., and Debnath, J. (2015) Autophagy at the crossroads of catabolism and anabolism. *Nature reviews. Molecular cell biology* **16**, 461-472

338. Lee, C. S., Georgiou, D. K., Dagnino-Acosta, A., Xu, J., Ismailov, II, Knoblauch, M., Monroe, T. O., Ji, R., Hanna, A. D., Joshi, A. D., Long, C., Oakes, J., Tran, T., Corona, B. T., Lorca, S., Ingalls, C. P., Narkar, V. A., Lanner, J. T., Bayle, J. H., Durham, W. J., and Hamilton, S. L. (2014) Ligands for FKBP12 increase Ca2+ influx and protein synthesis to improve skeletal muscle function. *The Journal of biological chemistry* **289**, 25556-25570

339. Pallafacchina, G., Calabria, E., Serrano, A. L., Kalhovde, J. M., and Schiaffino, S. (2002) A protein kinase B-dependent and rapamycin-sensitive pathway controls skeletal muscle growth but not fiber type specification. *Proceedings of the National Academy of Sciences of the United States of America* **99**, 9213-9218

340. Faivre, S., Kroemer, G., and Raymond, E. (2006) Current development of mTOR inhibitors as anticancer agents. *Nat Rev Drug Discov* **5**, 671-688

341. Vignot, S., Faivre, S., Aguirre, D., and Raymond, E. (2005) mTOR-targeted therapy of cancer with rapamycin derivatives. *Ann Oncol* **16**, 525-537

342. Wander, S. A., Hennessy, B. T., and Slingerland, J. M. (2011) Next-generation mTOR inhibitors in clinical oncology: how pathway complexity informs therapeutic strategy. *The Journal of clinical investigation* **121**, 1231-1241

343. Malley, C. O., and Pidgeon, G. P. (2016) The mTOR pathway in obesity driven gastrointestinal cancers: Potential targets and clinical trials. *BBA Clin* **5**, 29-40